The influence of the vulcanization system on the ozone stability of rubber compounds

Mgr. Bohdan-Volodymyr Berezhnyy

Master's Thesis
2025



Tomas Bata University in Zlín
Faculty of Technology

Tomas Bata University in Zlín
Faculty of Technology
Department of Polymer Engineering

Academic year: 2024/2025

ASSIGNMENT OF DIPLOMA THESIS

(project, art work, art performance)

Name and surname:	**Bohdan-Volodymyr Berezhnyy**
Personal number:	**T22066**
Study programme:	**N0722A130002 Polymer Engineering**
Type of Study:	**Full-time**
Work topic:	**The Influence of the Vulcanization System on the Ozone Stability of Rubber**
Work topic in English:	**The Influence of the Vulcanization System on the Ozone Stability of Rubber**

Theses guidelines

Theoretical part
Ozone stability of rubber compounds
Vulcanization systems for rubber compounds
Practical part
Preparation of rubber compounds
Ozone ageing of rubber compounds
Results and Discussion, Conclusions

Form processing of diploma thesis: **printed/electronic**
Language of elaboration: **English**

Recommended resources:

Treib, C; Loos, K; Johlitz, M; Lion, A: Ozone ageing: experimental methods on pristine and protected natural rubber. Continuum Mechanics and Thermodynamics, 34(6), 1563-1577
Kruzelak, J; Sykora, R; Hudec, I: Sulphur and peroxide vulcanisation of rubber compounds – overview. Chemical papers, 2016, 70(12), 1533-1555
Li, LF; Bai, YN; Lei, M; Liu, L: Progress in Rubber Vulcanization Accelerator. Progress in Chemistry, 2015, 27 (10), 1500-1508
& another licensed resources (book, journals, etc.)

Supervisors of diploma thesis: **Ing. Martin Stěnička, Ph.D.**
Centre of Polymer Systems

Date of assignment of diploma thesis: **January 2, 2025**
Submission deadline of diploma thesis: **May 9, 2025**

L.S.

prof. Ing. Roman Čermák, Ph.D. m.p.
Dean

Ing. Jana Navrátilová, Ph.D. m.p.
Head of Department

In Zlín March 3, 2025

MASTER'S THESIS AUTHOR'S DECLARATION

I take cognizance of the fact that

- by submitting my Master's thesis, I give consent to the publication of my thesis in accordance with the Act No. 111/1998 Coll., as amended, regardless of the result of the thesis defence;
- the Master's thesis will be stored in electronic form in the university information system and will be available for consultation;
- one copy of the Master's thesis in hard copy form will be kept and stored by Tomas Bata University in Zlín;
- my Master's thesis is fully subject to the Act No. 121/2000 Coll. on Copyright, on Rights Related to Copyright and on Amendment to Certain Acts (Copyright Act), as amended, particularly to Section 35 Paragraph 3;
- according to Section 60 Paragraph 1 of the Copyright Act, Tomas Bata University in Zlín has the right to conclude a licence agreement on the utilization of a school work as is specified in Section 12 Paragraph 4 of the Copyright Act;
- according to Section 60 Paragraphs 2 and 3, I may utilize my school work – Master's thesis – or grant a licence to utilize it only with the prior written consent of Tomas Bata University in Zlín, which in such a case is entitled to require me to pay a reasonable contribution in order to cover the costs incurred by Tomas Bata University in Zlín for the preparation of the work (up to their full amount);
- if software provided by Tomas Bata University in Zlín or other entities was used for the preparation of the Master's thesis only for learning or research purposes (i.e. for non-commercial use), the conclusions of the Master's thesis cannot be used for commercial purposes;
- if the output of the Master's thesis is any type of software product, the source codes and/or files of which the project is comprised are also considered part of the thesis; failure to submit this part may result in a failure to defend the thesis.

I declare that

- I have worked on my Master's thesis independently and properly cited the literature used; in case of publication of the conclusions, I shall be listed as co-author;
- the submitted hard copy version of the Master's thesis and the electronic version uploaded to the IS/STAG are identical in content.

In Zlín on ....

author's signature

ABSTRAKT

Cílem diplomové práce bylo sledovat ozonovou stabilitu pryže na bázi přírodního kaučuku optimalizací vulkanizačního systému. Byly použity tři běžně používané typy urychlovačů TBBS, MBTS a TMTD v širokém rozsahu koncentrací. Teoretická část pojednává o přírodním kaučuku, skladbě směsí s důrazem na vulkanizační systémy, vlastní přípravě směsí a samozřejmě odolností vůči ozonu. Praktická část práce se zabývá výrobou směsí a zkušebních těles a provedením vlastního stárnutí v ozonu a následného srovnání vybraných mechanických vlastností (zkouška tvrdosti a zkouška v tahu). Ozonové zkoušky byly provedeny za následujících podmínek: koncentrace ozonu 50 pphm, teplota 40 °C a relativní vlhkost 50 % po dobu celkem 96 h. Degradace vzorků byla hodnocena pomocí digitálního mikroskopu a následnou analýzou vzniknuté povrchové plochy v softwaru Matlab. Bylo prokázáno, že vhodnou volbou vulkanizačního systému se dají kontrolovat nejen mechanické vlastnosti, ale i dokáže zmírnit následky působení ozonů na kaučukové výrobky.

Klíčová slova: přírodní kaučuk, pryžové směsi, vulkanizační systémy, vulkanizační činidla, akcelerátory, ozonové stárnutí, ozonová stabilita

ABSTRACT

An objective of Master's Thesis was to monitor the ozone stability of rubber compounds on the basis of natural rubber by optimizing the vulcanization system. Three commonly used accelerators – TBBS, MBTS, and TMTD – were utilized in a wide range of concentrations. The theoretical part discusses natural rubber, the composition formulation with an emphasis on vulcanization systems, the preparation of the mixtures, and of course, resistance to ozone. The practical part of the thesis focuses on the production of mixtures and test specimens, the execution of an actual ozone aging, and the subsequent comparison of selected mechanical properties (hardness test and tensile test). Ozone tests were carried out under the following conditions: ozone concentration of 50 pphm, temperature of 40 °C, and relative humidity of 50 % for a total duration of 96 h. The degradation of the samples was evaluated using a digital microscope and subsequent analysis of the appeared surface area in Matlab software. It was demonstrated that by choosing an appropriate vulcanization system, it is possible not only to control mechanical properties, but also to mitigate the effects of ozone exposure on natural rubber products.

Keywords: natural rubber, rubber compounds, vulcanization systems, vulcanizing agents, accelerators, ozone aging, ozone stability

ACKNOWLEDGMENTS

First and foremost, I acknowledge our Almighty God, Jesus Christ of Nazareth, who has granted me an opportunity to write this scientific work. Without his strength and everyday support, this work would not be even started.

I would like to express my deepest gratitude to my supervisor, Martin Stěnička, Ph.D., for his patience, understanding, and guidance throughout numerous consultations. My sincere thanks also go to one of his colleagues, who first introduced me to a rubber field in a laboratory, and has to remain anonymous. Special thanks go to Ondřej Peter, without whose assistance this work would be incomplete. I also had the pleasure of working with Kateřina Hájková, who helped me in the laboratory.

In addition, I am profoundly grateful for invaluable advices from my friend and former supervisor, Prof. Oleksandr Grytsenko, from my alma mater university. His suggestions played a crucial role in shaping this thesis.

Lastly, I would like to mention my loving parents, who always believe in me.

This work is dedicated to my grandmother Hanna Berezhna, who opened me an exciting world of chemistry

MOTTO

"Trust in the Lord with all thine heart; and lean not unto thine own understanding. In all thy ways acknowledge him, and he shall direct thy paths."

Proverbs 3:5-6 KJV

CONTENTS

INTRODUCTION **11**

I THEORETICAL PART **12**

1 NATURAL RUBBER PROPERTIES AND NOMENCLATURE **13**

2 INGREDIENTS IN RUBBER COMPOSITION **15**

2.1 VULCANIZATION SYSTEMS 17

2.1.1 Sulfur 17
2.1.2 Accelerators 18
2.1.3 Activators 19

2.2 PROCESSING AIDS 19

2.3 FILLERS 21

2.3.1 Carbon black 21
2.3.2 Other fillers 22
2.3.3 Antidegradants 23

3 FEATURES OF VULCANIZATION OF NATURAL RUBBER **25**

4 COMPOUNDING AND PROCESSING **29**

4.1 COMPOUNDING TECHNIQUES 29

4.2 COMPOUNDING EQUIPMENT 31

4.2.1 Open mill 31
4.2.2 Internal mixers 32

4.3 PROCESSING TECHNIQUES 32

4.3.1 Compression molding 33

5 OZONE STABILITY OF NATURAL RUBBER **34**

5.1 OZONE MOLECULE 34

5.2 ATTACK OF OZONE 35

5.3 DEGRADATION CAUSED BY OZONE 36

5.4 OZONE STUDY 39

5.5 ANTIOZONANTS 40

6 MECHANICAL AND PHYSICAL TESTING OF RUBBER **42**

6.1 PREPARATION OF TEST SAMPLES 42

6.2 CURING CHARACTERISTICS 43

6.3 PHYSICAL TESTING OF RUBBER COMPOUNDS 45

6.3.1 Hardness 46
6.3.2 Tensile strength and elongation 46

II PRACTICAL PART **48**

7 MATERIALS AND PREPARATION OF COMPOSITIONS **49**

7.1 A BRIEF DESCRIPTION OF THE PERFORMED WORK 49
7.2 COMPOSITIONS 49
7.3 MATERIALS 51
7.3.1 Natural rubber 51
7.3.2 Soot 52
7.3.3 Processing oil 52
7.3.4 Main activator of vulcanization 52
7.3.5 Co-activator and dispersive agent 53
7.3.6 Vulcanizing agent 53
7.3.7 Accelerators 54
7.3.8 Antiozonant/antioxidant 54
7.4 PREPARATION OF THE MIXTURES 55
8 VULCANIZATION CHARACTERISTICS 59
9 PREPARATION OF TEST SAMPLES 65
9.1 PRESSING THE SAMPLE PLATES 65
9.2 PUNCHING THE SAMPLES FOR EXPERIMENTS 65
10 OZONE TESTING 68
11 PHYSICAL TESTING OF SAMPLES FROM THE SECOND ROUND OF THE EXPERIMENTS 77
11.1 HARDNESS TEST 77
11.2 TENSILE STRENGTH 79
CONCLUSION 88
BIBLIOGRAPHY 89
LIST OF FIGURES 94
LIST OF TABLES 96
LIST OF ABBREVIATIONS 97
APPENDICES 99

INTRODUCTION

In the last one hundred years, rubber has become an irreplaceable solution for many certain fields of applications. Due to its unique structure and properties, mainly elasticity at improved strength, rubber belongs to a specific class of polymers, called “elastomers”. Nowadays, they are widely used in the following areas: biomedical [1], marine [2], automotive and aerospace industry [3, 4], sports [5], electronics [6], construction [7], military [8], etc.

Together with a growing trend of sustainability, the demand in utilizing same material, rubber in particular, for a longer period of time is growing in order to reduce waste and promote the reuse of outwear rubbers in a circular economy [9]. In this regard, scientists actively explore how to improve properties and minimize the final cost of rubber products.

The most common rubber remains natural rubber (NR) [10], which is harshly affected by a number of environmental and weathering factors, such as temperature, UV light, water, humidity, oxygen, and ozone. The latter being often neglected or confused with the oxygen effect, although still harmful to rubber, and has to be taken into account as well [11]. Unfortunately, there are not many research papers studying the effect of ozone on NR, hence this field has not been completely studied yet. From another perspective, the papers that discuss the presence of different accelerators affecting rubber’s ozone resistance are almost non-existent, without even mentioning their different concentrations. Nevertheless, many commonly used accelerators have been utilized for decades.

Due to this concern, the topic of this Master’s Thesis reflects the aim of this work – to understand the influence of ozone on NR while changing the vulcanization systems and consequently their concentrations. It is believed that the conducted vulcanization process with different accelerators plays an important role in the final use at weathering conditions.

A theoretical part provides an overview of the most important aspects of NR properties, production of rubber compounds with further narrowing to vulcanization and ozonation. In the practical part, a visual evaluation and estimation of the developed surface area after ozonolysis are discussed together with the results from mechanical tests.

It is expected that this work will help scientists to understand more the nature of different amounts of accelerators’ concentrations on NR and how these rubber products may operate under ozone conditions.

I THEORETICAL PART

1 NATURAL RUBBER PROPERTIES AND NOMENCLATURE

Long before rubber came to Europe, native civilizations in America used latex from the tree *Hevea Brasiliensis* for creating water-proof things. In their lives, "ca-hu-chu" or the "crying tree" played a significant role in everyday life [12, 13].

Once the weeping tree has matured, it can be subjected to yield latex, cut by a technique called tapping. NR is obtained from this milky substance and on its chemical level consists predominantly of cis-1,4-polyisoprene with its hydrocarbon content reaching 95 % [13, 14], indicating its regular microstructure [15, 16]. It is a linear, high molecular weight, unsaturated polymer with long chains, composed of different-sized molecules [13] with empirical formula C_5H_8, while its structural formula is shown below in Figure 1.

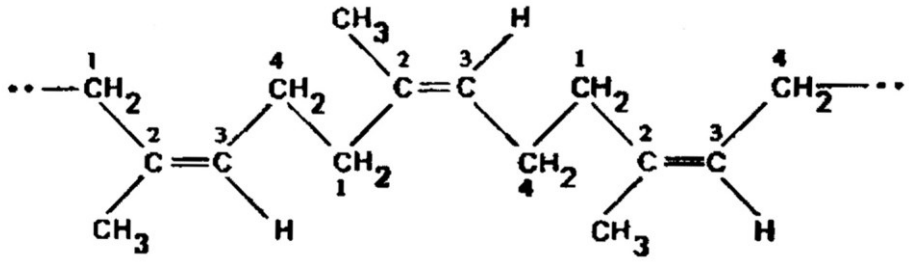


Figure 1 A structural formula of NR

(source: [16])

Despite majestic properties such as flexibility, waterproofing, and elasticity, there was a core challenge with NR, namely with a non-vulcanized one. In elevated temperatures, non-vulcanized rubber becomes sticky, and in cool temperatures, it shows brittleness, as well as it lacks strength overall. By good chance, Charles Goodyear in 1839 showed the world a vulcanization process [12, 17]. After the vulcanization, e.g. with sulfur, crosslinks are formed, representing bridges between macromolecular chains, indicating that the material cannot be reprocessed again or recycled due to the chemical bonding [12, 16].

Other important properties of NR include: low oxygen and ozone resistance [18], low swelling resistance towards hydrocarbon oil, moderate impermeability to both water and air, susceptibility to degradation by heat and light, low thermal conductivity [15, 17].

NR is a perfect representative of the term "elastomer", since it exhibits specific properties, such as: viscoelasticity, non-crystallinity, crosslinking, a low Young's modulus, and a large failure strain compared to other materials [15]. In essence, elastomers can undergo substantial deformation due to stretching, compressing, or bending and return to

their original shape once the stress is released. This behavior is due to their unique structure, which consist of long and flexible macromolecular chains, that are lightly crosslinked and can reconfigure themselves for even distribution of the applied stress. Due to covalent crosslinks, they prevent the slipping of macromolecule chains and return stressed chains to the initial position after stress release, preventing permanent deformation [12, 16].

Predominantly, raw NR is manufactured into blocks, which is referred to a technically specified rubber (TSR), as well as into sheets of conventional types, latter graded by International Standards of Quality and Packing. These types are referred to as ribbed smoked sheet (RSS), air-dried sheet (ADS), and crepe rubber. Depending on the final product, production methods vary [13, 19]. A simplified overview of production of NR grades is presented in Figure 2 below.

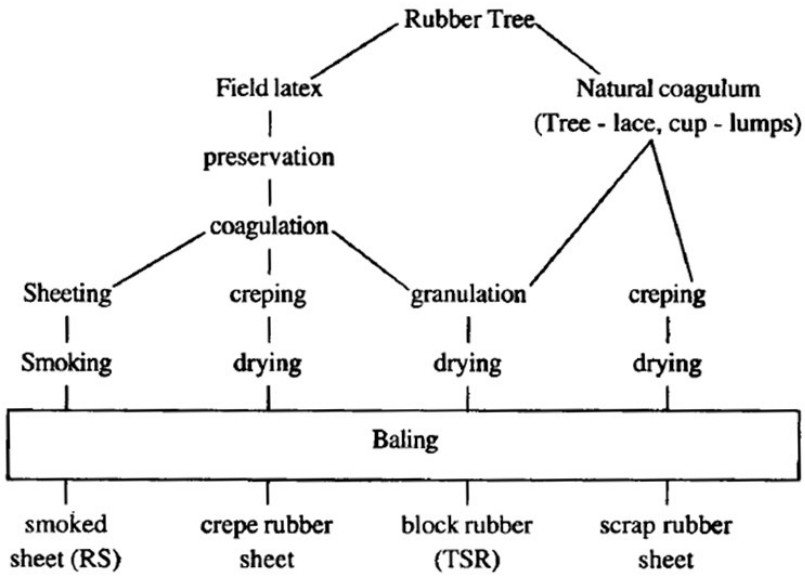


Figure 2 Flow line diagram for the production of different grades of NR

(source: [16])

Since 1920, Sri Lanka, Malaysia and Vietnam became the major producers of the raw rubber worldwide, covering 90 % of the world's rubber demand, together with later joined Thailand, India, Indonesia, and the Philippines [13, 16]. Due to its high demand, nowadays, rubber is produced in enormous amounts, in particular, 28.8 MMT (million metric tons) in 2023 [20]. According to the countries manufacturing block rubber, it withholds different characteristics, hence a nomenclature of TSR is distinguished by a place of origin in a following way: Malaysia (SMR), Indonesia (SIR), Thailand (STR), Vietnam (SVR), Sri Lanka (SLR), Singapore (SSR) [14, 21].

2 INGREDIENTS IN RUBBER COMPOSITION

In industry, raw NR is seldom used alone in the manufacture of rubber products. Compounding is a process of choosing the right ingredients with the right quantities and mixing them together with outcome material that meets the customer's requirements for a competitive price [16, 18]. Unfortunately, an ideal mathematical formulation to guide compounding does not exist. As a result, compounding is sometimes considered as half-art and half-science, since it is a combination of experience, knowledge, and intuition [12].

Without compounding and vulcanization, raw rubber has a number of following drawbacks [16]:

1. Weak strength
2. Softening at low temperatures
3. Easy molecular degradation in air
4. Hard to shape the final product

In this regard, raw NR is usually incorporated with so-called compounding ingredients. Formulation or recipe is a so-called heart in compounding [18]. These substances play different roles in rubber compounds and can be classified according to their functions presented in Table 1 [13, 16].

Table 1 Classification of main ingredients by their functions in a rubber compound

Ingredient	**Function**
Plasticizers	To enhance flexibility and elasticity in the final product as well as to improve the processability of rubber
Fillers and reinforcers	To modify the physical properties of rubber, for instance, resistance to deformation
Vulcanization systems	To increase the strength of the final product during its use
Processing oils	To disperse filler particles, which enhances the processability and flow of rubber
Antidegradants	To protect rubber products from environmental impact, for example, heat, light, ozone, oxygen, etc., which cause degradation

(source: [12, 22])

Beside mentioned main ingredients, there are additional ones, which are added to obtain some specific properties. These are presented in Table 2 below.

Table 2 Classification of additional ingredients by their functions in a rubber compound

Ingredient	**Function**
Pigments and dyes	To manufacture colored products
Deodorants	To achieve a pleasant smell in rubber products
Blowing agents	To create a cellular structure
Flame retardants	To inhibit the spread of flames when the rubber is on fire
Antistatic agents	To reduce or completely eliminate static electricity on the rubber surface
Miscellaneous	To provide additional properties during rubber mixing or in the final product

(source: [16])

A typical rubber formulation may contain 10 or more ingredients, sometimes several substances serving one function. An example sample of such recipe is presented in Table 3. Units for measuring each ingredient are accepted naturally to be in parts per hundred (phr). This unit shows a relationship of rubber, which has always 100 phr with other components. It simplifies calculation in formulation processes and ensures uniformity in the rubber mixture [12, 18].

Table 3 A formulation sample for a rubber compound

Ingredient	**phr**
Natural rubber	100
Filler	0–200
Plasticizer	0–40
Activator	0–40
Stabilizer	0–10
Vulcanizing agent	0.3–50
Accelerator	0.3–4

(source: [12])

The main task for a compounder is to find a balance between price, processing characteristics, and properties of the final product selecting the right ingredients. Optimal quality can be achieved only through careful monitoring of the product's field performance, selecting appropriate testing methods, and understanding rubber physics [13, 15].

2.1 Vulcanization systems

Vulcanization systems consist of three key ingredients, which are vulcanizing agents, accelerators, and activators [23]. The latter two combined create a synergistic effect during rubber curing [18].

"Vulcanizing agents" or sometimes called "curatives" are used in rubber compounding in order to create crosslinks among molecular chains generating a three-dimensional network [15]. There are two main groups of vulcanizers depending on the saturation of rubber. For simplicity, if the rubber is unsaturated, usually a widely spread sulfur vulcanizing agent is used, while if saturated, less common peroxides take place [13, 23].

At the same time, there are specific scenarios with other types of vulcanization, which include the following curatives: metal oxides, resins, sulfur donors, radiation, and urethane crosslinkers. These have found much smaller practical use in industry [12, 22].

2.1.1 Sulfur

The most widely used representative of a vulcanizing agent nowadays is an elemental sulfur. It is effective, in particular, with unsaturated elastomers, such as NR [23]. This curative exhibits an excellent balance between its price and performance [13, 22].

Sometimes, this curative is referred to as rhombic sulfur due to one of its allotropic structures consisting of eight sulfur atoms forming a puckered ring or a crown [13, 24]. Other forms, like monoclinic sulfur revert to the rhombic one upon cooling to the room temperature [25]. Rhombic sulfur is crystalline in nature and this structure is the most commonly encountered since it is considered to be the most stable at room temperature. Sulfur curative has a melting point of 115 °C and has a relatively low solubility in rubber compounds [22].

However, even 1 % w/w solubility in NR at room temperature and 7 % w/w at 100 °C is enough to migrate to the surface. This drawback is called "blooming", which affects the properties of a final product. It appears as a white powder on the rubber product by migrating from the matrix [13, 25]. If the amount of sulfur exceeds the amount required for crosslinking, it will come up to the surface [25].

Certainly, there exists an insoluble sulfur, which can help to prevent blooming. In its amorphous form, it remains relatively insoluble up to 100 °C during processing, exceeding which turns it into a rhombic soluble sulfur. At room temperature, it is insoluble in solvents and elastomers; hence it shows more stability by being trapped inside the product [22, 25].

2.1.2 Accelerators

The reaction between rubber and sulfur curative proceeds slowly even at elevated temperatures. The time required for NR to vulcanize containing only sulfur takes about 4 h at 140 °C, which is not very practical in industry [13]. The vulcanization rate is possible to be controlled by choosing the right accelerator [25]. Hence, the main purpose of developing accelerators is to save time during the vulcanization process and enhance the efficiency of crosslinking. It can be achieved by increasing the rate of curing by enabling sulfur to react with rubber more efficiently [15, 16]. Sometimes, several accelerators are used to speed up the vulcanization process, adding them in small amounts and forming a binary system [12]. Functionally, there are two types of accelerators – primary and secondary [18]. Primary accelerators provide significant scorch delay and offer moderate to fast curing, while secondary are usually scorchy and cause very fast curing. Meanwhile, scorch safety is the ability of rubber to resist pre-mature vulcanization during processing [22].

There are several key points, which have to be taken into account before selecting an accelerator [12]:

1. High solubility, which facilitates dispersion and avoids further blooming
2. Processing temperature
3. Scorch time, which refers to pre-mature vulcanization
4. Vulcanization method
5. Properties of the final product

The most common accelerators with their influence on vulcanization rate are listed in the Table 4.

Table 4 Comparison and classification of different accelerators

Chemical family	**Chemicals**	**Rate of vulcanization**	**Typical type**
Sulfenamides	CBS, TBBS, DCBS	Slow to moderate	Primary
Thiazoles	MBT, MBTS, ZMBT	Moderate	Both
Guanidines	DPG, TPG, DOTG	Slow	Secondary
Thiurams	TMTD, TETD, TMTM	Ultra-fast	Both
Dithiocarbamates	ZDBC, ZDEC, ZDMC	Ultra-fast	Secondary

(source: [13])

As can be seen, it is common to write abbreviations of chemicals in order to avoid calling their full names when preparing the recipe [18]. In addition to the presented classification, it is worth to describe their individual features. Sulfenamide accelerators gained the highest popularity in the tire industry due to their excellent scorch safety. Thiazoles are the most widely used by far providing good processing characteristics for many rubbers. Guanidines are considered to be safe due to their speed, but they can boost primary accelerators in a system. Thiurams ensure heat resistance with good aging. Dithocarbamates are commonly used exhibiting high crosslinking density, but low scorch safety [13, 21].

2.1.3 Activators

Activators in the vulcanizing system are used in order to mainly enhance the crosslinking efficiency during curing by facilitating the full potential of accelerators [13, 18]. Activators can be inorganic and organic chemicals, which have the ability to form complexes with accelerators, which in turn, aid to react more effectively with rubber [15, 16].

In most cases for sulfur-based vulcanization, two chemicals are used: inorganic metal oxides and organic fatty acids [18, 23]. The most popular among them are considered to be zinc oxide (ZnO) and stearic acid, respectively [12, 21]. Other representatives that are used less often include magnesium and lead oxide, as well as lauric acid [13, 22].

It was found out that without an accelerator, activators in the example of the synergy of ZnO and stearic acid are not very effective and vice versa [18, 23]. The synergy of ZnO and stearic acid comes from the latter's ability to convert ZnO into a rubber-solubilized form of zinc stearate being more reactive with accelerators [13, 22]. Moreover, fatty acids also enhance the dispersion of other chemicals acting as an additional plasticizer lowering the viscosity of the rubber compound, promoting processing characteristics [18, 23].

In addition to improved vulcanization, higher levels of ZnO in the recipe can help to prevent overvulcanization during curing, increase tensile strength and UV absorption acting as a pigmentation ingredient in a rubber compound [22, 24]. It is used in the manufacture of bulky thick products, where its good thermal conductivity and heat capacity contribute to more controlled, shorter, and even cure [22, 25].

2.2 Processing aids

In the literature, the terms plasticizer, softener, lubricant, dispersing agent, and processing oil/aid are used sometimes interchangeably in rubber processing [13, 21]. Although the

interpretations of these terms vary among different authors, all of these possible ingredients are used to enhance processability of rubber compound affecting the compound physically or chemically [12, 22]. In general, plasticizers must meet two main requirements to be used in processing: compatibility with rubber and not vaporizing at processing temperatures [16].

Some chemicals may also serve several functions improving the overall processing behavior of rubber compounds. These ingredients may affect rubber compound by [16, 18]:

1. lowering glass transition temperature
2. lowering viscosity
3. lowering molecular mass
4. improving filler dispersion by lubricating individual molecules
5. improving flowability
6. preventing rubber compound from adhering to hot machinery surfaces
7. enhancing final physical properties, such as flexibility, elasticity, etc.

In this regard, individual chemicals with their properties are discussed in this section. Examples of possible plasticizers are: petroleum, vegetable, and synthetic products. Petroleum-based products include: paraffin, aromatic, naphthenic oils, paraffin wax, and tar. Vegetable-based products include mostly fatty acids and salts. Synthetic products include mostly ester plasticizers. In more detail, mineral oils should be discussed, since they are the most frequently used for processing both natural and synthetic rubbers [13, 16].

All commercially used crude oils after refining contain high-boiling fractions, which is one of the requirements for utilizing them. They found popularity in both, saturated and unsaturated rubbers. These oils mainly consist of three different unit structures: unsaturated (aromatics), saturated (naphthenes), and structural units possessing saturated side chains (paraffins). Accordingly, these oils are classified into groups with preponderance in their structure [25].

Once choosing the most compatible oil, it depends on its polarity and whether it shares with rubber similar molecular units [22]. NR with double bonds is non-polar and works better with oil containing high aromatic content, giving the best processability, but poor odor and causes stains. Synthetic rubbers with different degrees of polarity and saturation, meet specifications with paraffinic oils having a less aging effect, less odor, and giving good color

to the compound. Naphthenic oil is often somewhere in the middle providing good properties for these both types of rubbers [13, 16]. If the oil is not compatible with rubber, it will "bleed" from the compound and will not promote the distribution of chemicals during mixing as well as worsen final physical properties [22, 25].

Another important factor for choosing the right oil type might be its stability to environmental factors. The best ability to resist oxygen has been found in paraffin oils. Oxidative instabilities are related to the presence of polar structures. In this regard, aromatic oils have the worst resistance to oxygen degradation, because of polar structure [22].

All these oils are presented with different viscosities on the market, which somewhat affect processing characteristics and final product properties. Viscosity Gravity Constant (VGC) is the main criteria representing the average aromaticity of an oil. Aromatic VGC < 0.95, naphthenic VGC = 0.85–0.90, paraffinic VGC < 0.85 [25].

2.3 Fillers

The last important ingredient in the rubber compound is called a filler. It consists of a group of chemicals, which modify the properties of rubber compounds during processing and final use [23]. Fillers usually fall into three main categories determining their role in a rubber compound: reinforcing, extending, and non-reinforcing (diluent). The most important reinforcing filler in the rubber industry remains carbon black (CB) enhancing the physical properties of vulcanized elastomer. Non-reinforcing fillers aim to reduce the cost of the final product by adding bulk to it, which does not interact with the compound [12, 15].

2.3.1 Carbon black

CB is a reinforcing black fine powder that improves the physical and mechanical properties of rubber compounds [13, 18]. Essentially, it is an elemental carbon with an amorphous molecular structure [12].

Over the years, many ways have been developed to obtain CB of different characteristics for specific needs, but fundamentally, manufacturing of soot is a simple incomplete combustion or thermal decomposition of organic substances, in particular, hydrocarbons [13, 22]. The most common methods for producing the soot include: furnace black, thermal black, and acetylene black processes [13, 16].

The main distinction among CBs lays in its characteristics, such as particle size, structure and surface area [16, 23].

Smaller CB particle sizes have shown a better reinforcing in rubber compounds. The sizes used commercially are in the range from 10 to 400 nm. At the same time, with the decrease in size, incorporation time, viscosity and heat generation of rubber mixture increase, resulting in poor soot dispersibility and potential scorch problems [16].

The structure of CB refers to the arrangement of its primary particles of 10–500 nm. These particles are hollow, semi-spherical structures made up of two to four turbostratic graphitic layers. X-ray diffraction studies reveal that CBs consist of tiny crystallites composed of parallel graphitic layers spaced about 0.35 nm apart [12, 13]. During CB manufacturing, these particles are fused together forming bigger aggregates of 100 nm to a few micrometers, which cannot be separated. The biggest structure is called an agglomerate with a size up to a few millimeters, formed from entangled clusters of aggregates by physical forces. Typically, a so-called low structure consists of 30 particles per aggregate, while a high structure may have over 200 [13, 18]. Generally, a higher structure of CB leads to a stiffer and less elastic unvulcanized compound, resulting in harder vulcanized materials [12, 16].

The surface of CB particles is physically active and capable of bonding with rubber radical chains. Chemically, the surface has been found to contain impurities such as phenolic, carboxylic, ketonic, and lactonic groups, along with traces of sulfur. These contaminants have a significant impact on the electrical conductance of rubber [12, 18].

To classify CB, the American Society of Testing Materials designed ASTM D1765 for grading. The first letter indicated the method used in the production of CB. N series “normal” used for the vast majority refers to curing furnace and thermal blacks, and S indicates “slow” curing methods. After the letter, a first number represents the particle size range in nm. The second and third numbers are of specific grade assigned by the manufacture corresponding to an ASTM list [16, 18].

2.3.2 Other fillers

Non-black fillers exist in a large variety for rubber compounding. The majority of this group represents clays, silicas, and calcium carbonates. Since it is impossible to discuss individual substances, fillers are classified into three groups proposed at the beginning of this section. Reinforcing fillers include: precipitated silica, calcium carbonate, and hard clays. All these fillers must have a fine size (less than 1 μm) adding strength to a rubber compound. Diluent fillers, which are mainly aimed to reduce the final cost include: soft clays, ground calcium

carbonate, and barytes [12, 22]. They also affect the processing parameters by reducing die swell, smooth calendaring behavior, and sharp-edge extrudates. Extending fillers add some special properties to the rubber compound: electrical conductivity, flame resistance, oil resistance, color, odor, aging resistance, etc. All of these can be also called miscellaneous fillers, traits of which depend as well on the particle size, structure, and surface chemistry. Typical representatives include: kaolin, talc, bentonite, mica, etc. [13, 16].

2.3.3 Antidegradants

The last in the group of fillers worth mentioning separately is antidegradant ingredients. Due to the unsaturated structure of rubber, it is more susceptible to the impact of oxygen and ozone on product properties in contrast to saturated rubber, which does not carry reactive double bonds [18, 21]. A consequence of such reactions is the loss of strength and elasticity of the final products [11]. Therefore, age resistors are being developed in order to prolong the service life of rubber [10]. However, all rubbers are degrading at the exposure to environmental conditions by the effect of light, temperature, weathering, and radiation due to a certain degree of unsaturation. All of these terms are referred to as aging [12, 13]. Although oxygen/ozone influence can be readily alleviated on rubber, it cannot be fully terminated even with the strongest ones, which in turn, may also cause staining of rubber compound [22, 25].

NR, polyisoprene, and butyl rubbers primarily degrade through chain scission, leading to weak, sticky, and softened material with surface tackiness. In contrast, styrene-butadiene rubber (SBR), ethylene propylene diene monomer rubber (EPDM), neoprene, polybutadiene, and acrylonitrile rubbers undergo degradation by crosslinking, resulting in brittle compounds with reduced elongation and flexibility [12, 18].

In general, antidegradants are distinguished into two classes – antioxidants and antiozonants, which sometimes present also additional properties beside to their primary function [13]. Antioxidants protect the rubber from oxygen degradation by slowing down its reaction with the material, while antiozonants prevent damage caused by ozone exposure [18]. The actual mechanisms of ozone degradation are discussed in a separate chapter.

There is a number of criteria, which are important when choosing an appropriate antidegradant, including: volatility, solubility, chemical stability, discoloration and staining, concentration cost [12, 18].

During compounding and final product use, if antidegradant is volatile, it worsens the service life of a product. Solubility is crucial as well since an antidegradant should be soluble in a rubber compound, but insoluble with substances the product may have a contact. Chemical stability, including resistance to heat, light, oxygen, and other additives, is essential for maximizing the product's service life. The optimum concentration level of antidegradant is hard to specify because its concentration will decrease over time reacting with oxygen [18, 23]. A wide variety of antidegradants are commercially available, and while it is not possible to cover them all, only the most important names are discussed [13].

A concentration of just 1–2 % oxygen is typically enough to cause significant deterioration of properties in any elastomer [12]. An effective antioxidant must be capable of capturing an oxygen-free radical and delocalizing the charge through resonance [24]. There are two major types of antioxidants – amines and phenolics. Although the former are more effective, they are also staining, hence it limits their application to black and dark rubbers, while phenols being less powerful, found a demand in white and bright rubber products. Both of them protect rubber against aging by scavenging harmful free radicals during the oxidative chain reaction [15, 16].

Even at low concentrations of around 5 ppm (parts per million) in air, ozone can trigger molecular degradation reactions at the double bonds in rubber. Once exposed to ozone (O_3), a white film on the rubber surface appears. It is fragile and cracks easily under strain. To prevent ozone damage, antiozonants are added to rubbers. These chemicals either strengthen the rubber's surface, slow down crack growth, or both [16, 22]. They function by migrating from the bulk of the compound to the surface, forming a protective film, where they are subjected to react with O_3, thereby preserving the component's integrity [13, 23]. Most used antiozonants act as antioxidants as well, offer antiflexing properties, but at the same time are expensive, discoloring, and staining [18, 22]. Using too little antiozonant can result in a more severe attack than if none were used at all [25].

The most popular representatives of phenolic antioxidants are: monophenols, bisphenols, thiobisphenols, polyphenols, and hydroquinone derivatives, 2,6-di-t-butyl-p-cresol, frequently (BHT). The most common among amines is polymerized 1,2-dihydro-2,2,4-trimethylquinoline (TMQ) [13, 24]. The most widely used antiozonants are para-phenylenediamines (PPDs) and waxes [12, 22].

3 FEATURES OF VULCANIZATION OF NATURAL RUBBER

In rubber processing, one of the most important processes, without a doubt is a vulcanization. In general, unvulcanized rubber is weak, lacks the ability to return to its original shape after mechanical deformation, and can be very sticky, as discussed before [26]. The vulcanization process turns raw rubber into a more stable, durable, and elastic material known as vulcanized rubber [17, 18]. It is a chemical process of crosslinking polymer molecules into larger molecules, which is carried out at relatively high temperatures (typically 140–220 °C) and pressure. Chemically crosslinked rubber is called a vulcanizate [15, 17].

One of the biggest effects of change is the swelling ability of vulcanized rubber. The introduction of crosslinks to raw rubber prevents its dissolution but provides a swelling ability. Chemically, crosslinks restrict the flow of chains past each other, but keep their movement due to kinetic energy resulting in high elasticity material [15, 17]. From another perspective, crosslinking reduces permanent deformation by enhancing the retractile force, which in turn increases elasticity and decreases plasticity, hence reducing the tendency to creep once a rubber sample is extended [24, 27]. The formation of a network with sulfur crosslinks is presented in Figure 3 below [26]:

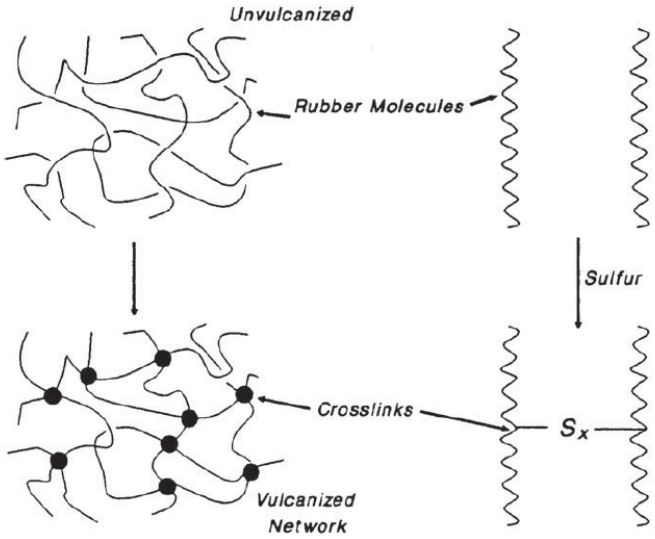


Figure 3 The presentation of rubber chains before and after the vulcanization process

(source: [26])

It is worth mentioning that various vulcanizing agents provide different effects on the final product influencing its properties, as well as concentrations of these agents [28]. A traditional method for curing NR remains the same with sulfur, which creates the most

complex 3D network, providing dimensional stability to the structure [27, 29]. It holds its popularity due to low price, wide availability, and a number of advantageous properties [15].

Due to the slow time of curing, blooming, and large heat generation, sulfur is usually used together with accelerators and activators creating a vulcanizing system for commercial purposes [29]. Overall, there are a number of advantages in utilizing a sulfur-based vulcanization system instead of sole sulfur, including: faster vulcanization process, easier process control, smaller required quantities of sulfur, smoother surface finish without blooming, as well as enhanced mechanical properties [12, 16].

A typical sulfur-based vulcanization formulation includes: ZnO (3–10 phr), stearic acid (1–4 phr), an accelerator (0.5–4 phr), and sulfur (0.5–3 phr), which together facilitate the curing process and optimize the rubber's final properties. A mechanism of curing involves both radical and ionic interactions and the whole picture of the process is complicated. A simplified scheme of the sulfur-based curing mechanism is presented below (equations 1–4) [12, 24]:

$$Ac + S_8 \rightarrow Ac - S_x - Ac \quad (1)$$

$$Ac - S_x - Ac + RH \rightarrow AcH + R - S_x - Ac \quad (2)$$

$$R - S_x - Ac + RH \rightarrow AcH + R - S_x - R \quad (3)$$

$$R - S_x - Ac \rightarrow cyclic\ sulphides + dienes + ZnS \quad (4)$$

$$R - S_x - Ac \rightarrow S_{x-1} + R - S - Ac$$

$$R - S_y - R \rightarrow S_{y-1} + R - S - R$$

$$R - S_{x+y} - R + Ac - S_2 - Ac \rightarrow Ac - S_{y+2} - Ac + R - S_x - R$$

In the beginning, the accelerator and activator (Ac) together react with sulfur (S_8) forming an active so-called "sulfurating agent" (1). The next step is the reaction between rubber chains (RH) and a sulfurating agent with the formation of polysulfidic pendant groups terminated by accelerator groups (2). In the third step, after abstracting another hydrogen from the rubber, a polysulfidic rubber-bound intermediate is formed containing polysulfidic crosslinks (3). Due to the side reactions presented in the (4) stage, a complex network can be formed. These side reactions include: degradation, desulfuration, creation of monosulfidic crosslinks, and sulfur exchange [12, 13].

The three biggest factors affecting the vulcanization process are: vulcanizing agents, temperature, and time of cure. A good vulcanizing system should provide rapid and effective crosslinking at the desired curing temperatures, as well as prevent pre-mature scorching at

lower temperatures [12]. Generally, there are three vulcanization systems in dependence of their efficiency. This classification presents the ratio of accelerator/sulfur (A/S) and is divided into: conventional (CV), semi-efficient (semi-EV), and efficient (EV) types. Different types of crosslinks can be formed depending on the A/S ratio. These are presented in the Table 5 below [15, 29]. Here, sulfur vulcanization offers flexibility, allowing to control the type of crosslinks providing properties suited for specific applications [15].

Table 5 Characterization of vulcanization systems

Vulcanization system	**CV**	**Semi-EV**	**EV**
Sulfur amount	2.0–3.5	1.0–1.7	0.3–0.8
Accelerator amount	1.0–0.4	2.5–1.0	6.0–2.5
Crosslink type	Polysulfidic	Poly-, di-, monosulfidic	Monosulfidic
Sulfur atoms per crosslink	10–15	5–10	4–5

(source: [12, 29])

Depending on the A/S ratio, different technological properties can be achieved. For instance, CV systems (C–S_x–C) with increased sulfur content, hence crosslinking, increase tensile and tear strengths, provide high compression set and good fatigue, but reduce heat resistance. However, higher temperatures may cause the breakage of polysulfidic links into mono- and disulfidic, decreasing the compound's strength and modulus [12, 22]. In contrast, EV systems (C–S–C) have great heat aging and thermal stability characteristics, but low compression set, abrasion resistance, as well as low tensile and tear strengths. A combination found in semi-EV systems (C–S–S–C) has a balance between both strength and heat aging properties [15, 27]. As can be seen, crosslinking agents substantially impact the physical and aging properties, but they have much less effect on thermal decomposition and burning [21, 28]. Another option to enhance aging resistance is the addition of antidegradants to rubber compounds [18, 21].

In addition to the described vulcanizing system containing sulfur, accelerator, and activator, one more ingredient often finds its use – a scorch retarder. It is a chemical, which increases the scorch time (induction time) and enhances processing safety, especially at low temperatures and with fast curing systems. To be more precise, they delay accelerator activity during processing and storage without decreasing the vulcanization rate. Once the compound reaches a vulcanization temperature, retarders lose their effectiveness and cease

without affecting the properties of the final product. Examples of retarders are organic acids, such as phthalic anhydride, benzoic acid, and salicylic acid [12, 18].

To illustrate the final properties, Figure 4 presents their dependence on crosslinking density. It shows a significant decrease in hysteresis, which is the ratio of viscous to elastic components in deformation resistance. It is a measure of energy loss that has been transferred to heat during deformation, which declines. Permanent set and friction coefficient decrease together with hysteresis because crosslinks prevent molecule slippage and tackiness. Tear strength, fatigue life, and toughness improve with a small degree of crosslinking, due to flexibility and energy dissipation, but eventually reach a peak and decline with excessive crosslink formation becoming rigid and brittle. Due to occurring brittleness, strength passes through a maximum further. Increasing crosslink density raises the modulus (stiffness) together with elastic recovery to the original shape [24, 26].

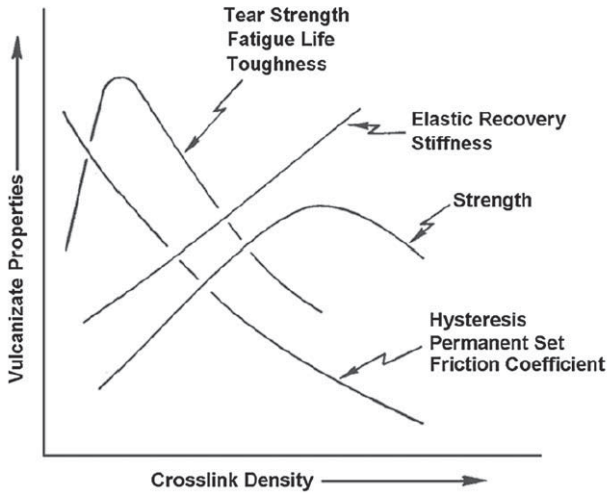


Figure 4 Effect of vulcanization on physical properties of the final product

(source: [26])

For a compounder, it is important to monitor the vulcanization process to achieve optimal performance. To conclude, vulcanization can be characterized by following parameters [16]:

1. Delay time (scorch time). It is the time from exposure of rubber to vulcanizing conditions, but before the actual vulcanization starts. It is significantly important for handling and molding the material
2. Vulcanization (cure) rate. It is the speed at which vulcanizate achieves the desired properties
3. Crosslinking. This level determines the final properties of a product

4 COMPOUNDING AND PROCESSING

Despite the good quality of raw ingredients, the type of mixer and quality control during compounding are extremely important as well in order to achieve final material with desired performance properties [12]. There are two key steps in compounding: mastication of raw rubber and mixing [16, 17]. The primary goal of compounding is to evenly disperse all ingredients in rubber with reduced viscosity, creating a rubber batch that can be effectively vulcanized creating a product with required properties [17, 22].

4.1 Compounding techniques

There are two main ways to start compounding – conventional and upside-down techniques. The choice depends on rubber formulation and the difference lies in the sequence of added ingredients [12, 13]. In conventional mixing, raw rubber is fed into the mixer for softening first. Naturally, raw NR is tough and needs to be pliable for processing [16]. Due to applied and generated heat, rubber undergoes the transition from elastic into a plastic state enhancing easier mixing. This step is called mastication or sometimes “plasticizing” of rubber. It is essential for NR to ensure its homogeneity and processability by decreasing its viscosity, making it receptive to the additives. The thermal breakdown of NR by changing its chain structure promotes viscoelasticity [23]. Regardless of the chosen method for compounding, a vulcanization system is added at the end [12, 23].

Once rubber shows immediate relaxation after deformations happening inside the mixer, it is ready to be fed with fillers. Incorporation of any additives except the vulcanizing system is called “masterbatching”. In order to prevent pre-mature vulcanization, the curing system is added separately, often on another mixer. Since rubber has already been softened and became pliable inside the mixer, chemical additives are blended together to reach a homogeneous dispersion of particles as well as proper viscosity [12, 23]. The main goal of dispersion is to reach the desired particle size by breaking agglomerates [13]. Generally, the higher the dispersion degree, the better the properties. Often to reach the desired dispersion and distribution, plasticizers and processing aids are added to the recipe. It is important to acknowledge dissipation during milling, hence masterbatching must be terminated before the degradation takes place. In some cases, compounder has to remill the masterbatch if it has not reached the desired dispersion and viscosity during the first milling [12, 23].

The last step, which is usually performed separately from the main mixing is an incorporation of a curing system. Time required for this step is shorter, since dispersion can

be reached faster. Temperature is lower as well, because the mass is a subject to vulcanization. This operation can be done on both, batch and continuous mixers, while Banbury series remain the most common [13, 23].

The upside-down technique is a variation of a traditional conventional one, although there are others as well. The upside-down method changes the sequence between rubber and fillers, making additives to combine in the mixer before the rubber is introduced. This method has found its use with synthetic rubbers, shortening the overall compounding process, but has some limitations with inability to disperse small filler particles effectively with high viscosity rubbers [12, 22].

In order to understand the optimum temperature for mixing a rubber compound, Figure 5 presents the dependence of plasticizing efficiency (molecular breakdown) on temperature. The first curve represents a mechanical breakdown of rubber, which happens during the increase in temperature, making rubber softer. It shows the decrease in viscosity due to the decrease in molecular weight. The second curve represents an increase of another breakdown – chain scission due to degradation by oxygen reactions above 80 °C. Curve number three is a combination of two previous curves, where their intersection at the temperatures 110–120 °C represents a minimum level of plasticizing efficiency. It is a place, where a rubber compound remains soft, but has not started to degrade yet, hence this temperature range is the best for compounding. However, to enhance mixing, the temperature rises up to 160 °C, which shortens the time [12, 16].

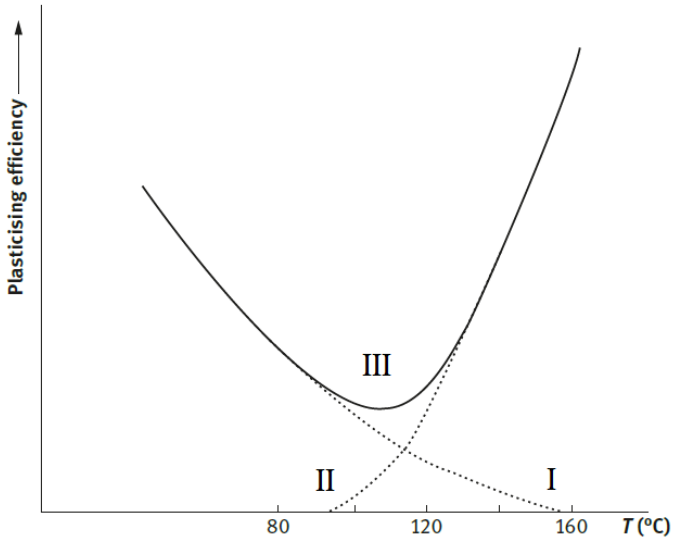


Figure 5 Effect of temperature on rubber breakdown in conventional mixing

(source: [12])

4.2 Compounding equipment

Machines used for compounding can be classified depending on the process continuity. Usually, a compound is mixed as a batch and for this operation, internal mixers are very common. Historically, an open mill or two-roll mixer was used, but this equipment has some significant drawbacks [16, 23]. There is a possibility to make this process continuous, where ingredients have to be fed at a specified time and set amount [16]. In any case, the aim of any equipment is to provide the best homogeneity for the rubber mixture as possible. Batch mixing consists of three operations: loading the ingredients, mixing, and discharging, while continuous mixing requires all these operations to be done continuously [12]. Examples of the latter mixers are: Multi-cut Transfermix, Double R mixer, Farrel continuous mixer (FCM), co-rotating twin-screw compounder, etc. [16].

4.2.1 Open mill

The earliest processing machine used for rubber compounding is called a two-roll mill or open mill [22]. It consists of two parallel counter-rotating metal rolls placed horizontally to each other and equipped with temperature control, shown in Figure 6A. Control of temperature takes place inside the rolls with channels, where the water, oil, or steam circulates heating up or cooling down the metal, the latter providing a good heat transfer. The rolls rotate towards each other by electric motor and gears. Between them exists an adjustable gap (nip) allowing rubber to pass through, mix and turn. The collected rubber mass in the nip is called a bank, the size of which is controlled by adjusting the gap. To increase the shear force, one roll has to rotate quicker. The difference in their speeds is called a friction ratio, which is usually in a range from 1:1.2 to 1:1.5. Due to this ratio, rubber usually forms a band around one roll. Mixing is done by an operator, who cuts the rubber and feeds it to the nip again. The higher their speed, the higher shear stress is generated. The main disadvantages of this method are its dust hazard, slow process speed, batch volume is heavily limited, and safety control is worse compared to internal mixers [13, 16]. On the other hand, it is efficient in breaking agglomerates, and good homogeneity over time can be achieved [18, 25]. Nowadays, it is mostly used for mastication, the last stage of adding vulcanizers, heating up and cooling down the rubber compound prepared by other means as well as sheeting it off to achieve a thin and uniform sheet of rubber. However, it can still be used for adding fillers in expensive compounds with limited amounts [13, 25].

4.2.2 Internal mixers

The most popular internal mixers remain Banbury, owing to H. Banbury who developed them intending to increase the productivity of the mixing process, presented Figure 6B. Internal mixers are general-purpose machines consisting of two parallel counter-rotating metal rolls or blades placed horizontally to each other inside an enclosed chamber; a ram or press, which is operated by pneumatic or hydraulic means allowing to feed the ingredients through a hopper in an upper position, while pressurizing and holding the compound in a lower position; a drop door, which opens upon cycle completion for discharging and fast removal of the mix. Blades can be placed tangentially or arranged for intermeshing with different variations [13, 18]. Rotors are powered by an electric or hydraulic motor with gears, controlled by a built-in tachometer. While tangential rotors may run at different speeds, intermeshing rotors must run at the same speed due to their geometry. Shearing occurs between the rotors and between rotor-chamber [12, 25]. However, intermeshing arrangement generates higher shear and dispersion than non-intermeshing, the latter being more suitable for tough rubber [13]. Shear stress and mixing time are determined by the size and shape of blades and their speed. It is usual to rotate them at high speed, which generates high stress and friction, increasing the temperature of the mix, which requires a powerful cooling system. Temperature is controlled by channels inside chamber walls, rotors, and sometimes the ram head for heat dissipation [18, 25]. The main advantage of internal mixers is the speed of the process, as well as better dispersion of ingredients [12, 18]. The main disadvantages are considered high cost and difficult maintenance of complex construction [16].

4.3 Processing Techniques

After the compounding process, a prepared rubber compound is ready to be formed (shaped) and vulcanized. Depending on the final product shape, processing techniques vary. Similarly, as in compounding, final processing can be divided into batch vulcanizing and continuous vulcanizing methods, although in the latter shaping and curing are performed separately [22]. Batch methods are the most common, where rubber compounds are heated in a pressurized mold. These methods include: compression molding, transfer molding, and injection molding. On the other hand, the most common continuous methods are: extrusion and calendaring [12, 17]. However, curing takes place in the following effective equipment: autoclave, hot air tunnel, fluidized bed, salt bath, microwave, etc. after shaping. Continuous way is mostly used for high-volume production [16].

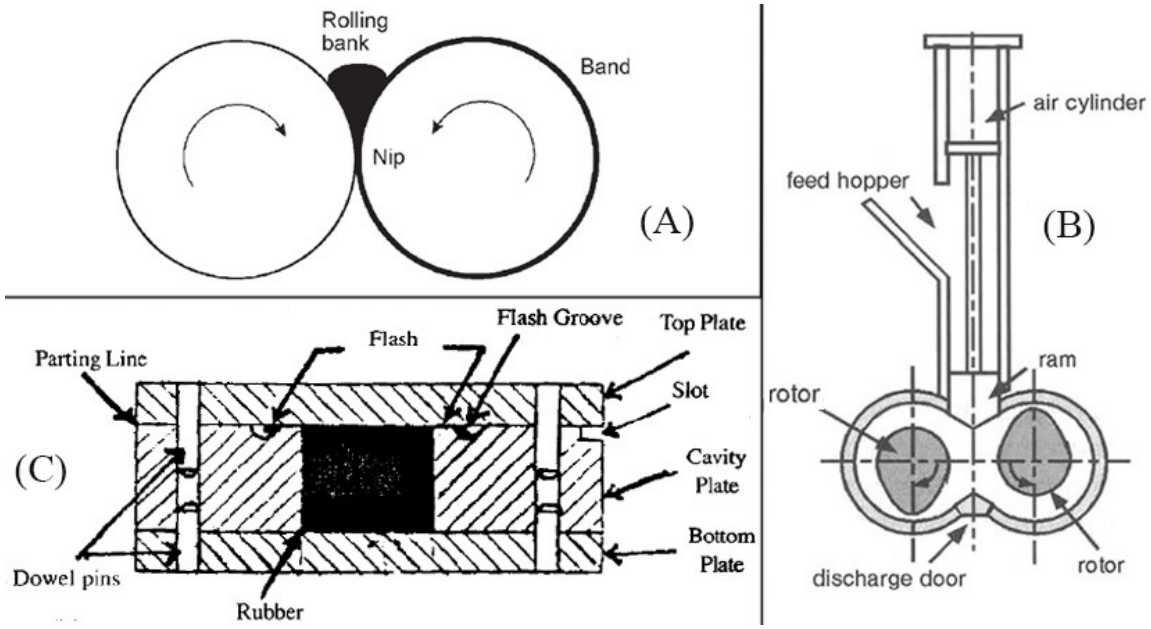


Figure 6 Schematic representation of open mill mixer (A), internal mixer (B), compression molding (C)

(source: A [13], B [22], C [16])

4.3.1 Compression molding

In this most popular method, rubber fills the empty volume in between two closed mold parts under high pressure, where it vulcanizes, as shown in Figure 6C. Usually, the loading of one cavity is done manually, which requires weighing the compound and cutting it to fit the size of a mold. The material, because of these operations is cold and the time for curing extends, which is a drawback [22]. It is important to calculate the proper weight, otherwise an overflow or underfill may happen. Typically, the mold is overfilled with 10–20 % more compound to ensure the fullness of molds, which is sometimes called “flash grove” [16]. Once the material has been placed on the lower part of the mold, the upper part closes it and compresses the material forcing it to deform into the free volume. Both mold parts are usually equipped with a heating system. Temperature, pressure, and curing time vary for individual compounds and it is important to control these parameters. After discharge, a prepared product must come out easily and sometimes has to undergo secondary operations, such as trimming edges. The advantages of compression molding include: simple and less expensive molds compared to those used in other methods, the possibility to produce large product sizes, reduced waste overflow, and quick mold change [12, 23]. This method is excellent for the small production, but also suitable for molds with multiple cavities [17].

5 OZONE STABILITY OF NATURAL RUBBER

During its service life, NR is sensitive to ozone degradation. Ozone is a harmful molecule that leads to NR surface cracks, hence degradation of physical properties [18, 30].

5.1 Ozone molecule

Ozone is a gas with pale blue color and has a characteristic smell of “freshness”. The name “ozone” comes historically from Greek language, where word “ozein” means “to smell”. In spite of imaginary friendliness for most of the people, it is in fact highly poisonous even at low concentrations [31].

Ozone, being an allotropic modification of oxygen, is synthesized naturally in the upper layers of the atmosphere, mostly in the stratosphere, troposphere, and ground level. The highest concentration can be found at 20 km altitude, where it plays a key role in blocking UV radiation. In the stratosphere it occurs due to sunlight forming an ozone layer, blocking completely UV-A, and filtering most of UV-B radiation from the sun [32]. The mechanism consists of molecular oxygen photolysis, where produced atomic oxygen reacts with another oxygen molecule forming O_3 [33]. In the troposphere, the major source of O_3 comes from nitrogen dioxide photodissociation, while at ground level, ozone appears by the reaction of NO_2 with volatile organic compounds (VOC), for example, appearing from combustion process emitted from industrial machines and cars [32, 34]. Ozone can be also generated from the passage of electric discharge through the air, causing high energy to break molecular oxygen, for instance, by lightning [31].

Ozone structure consists of three oxygen atoms, where every atom is connected by a single bond with another one, while the remaining negative charge is distributed across the O_3 molecule. Its steric hindrance does not allow it to form a triangular structure, where every oxygen atom could form a double bond. The main characteristics of ozone include a melting point of -195.5 °C and a boiling point of -111.9 °C, as well as a specific gravity of 2.144 [31]. A structural representation of ozone is shown in Figure 7 below.



Figure 7 Structural molecule of ozone

(source: [31])

Due to the industrial revolution, in particular, burning fossil fuels, ozone concentration in the atmosphere was generally lower before in 19th century. According to World Health Organization, a proposed threshold of 5 pphm (parts per hundred million) can have a negative impact on humans, vegetables, crops, animals, and other living organisms [31, 32]. In the outdoor atmosphere, the concentration of ozone at ground level is about 1 pphm [35]. However, ozone concentrations in highly polluted areas can reach up to 50 pphm easily nowadays. During the summer season, when the sun is more intense during longer days, ozone formation is increased. Consequently, levels of ozone are higher during the day and decrease overnight [34].

Being a better oxidizing agent due to higher reactivity compared to oxygen, ozone is used in sterilizing air, purifying water and finds use in other chemical applications. On the other hand, the toxicity of ozone can lead to serious health issues in the working environment, corrosion of some metals, plastics degradation etc. [31]. At the ground level, high concentrations of ozone readily react and deteriorate the properties of indoor surfaces, e.g., furniture, walls, and carpets with the production of VOC. These reactions result in the accelerated aging of materials, causing them to degrade quickly [32].

5.2 Attack of ozone

Among the most sensitive materials to ozone impact are rubbers. Only a few pphm of O_3 in the atmosphere can significantly damage rubber products, causing their cracking [18, 33]. This effect is much more noticeable once the rubber products are working under significant deformations of strain and compression. In highly polluted areas, it is common for standard tires to crack more significantly due to elevated ozone concentrations [32].

The ozone effect on rubber became apparent in the 1950s on US military vehicles, which have been mothballed since World War II. The tires on them were found to be useless [33]. Until then, no antidegradants against ozone were employed in rubber compounds, except paraffin wax to protect a product with a physical bloom barrier, hence for static conditions. Since that observation in the military, it became evident that a new type of chemicals has to be developed that can withstand ozone damage under cyclic deformations. At that time, the government initiated research that led to a discovery of N,N'-substituted p-phenylenediamines (PPDs), which turned out to be successful in protecting unsaturated rubber (e.g., polyisoprene, polybutadiene, chloroprene, etc.) from ozone attack [32]. The most common antiozonants in the rubber industry used nowadays are presented in Figure 8.

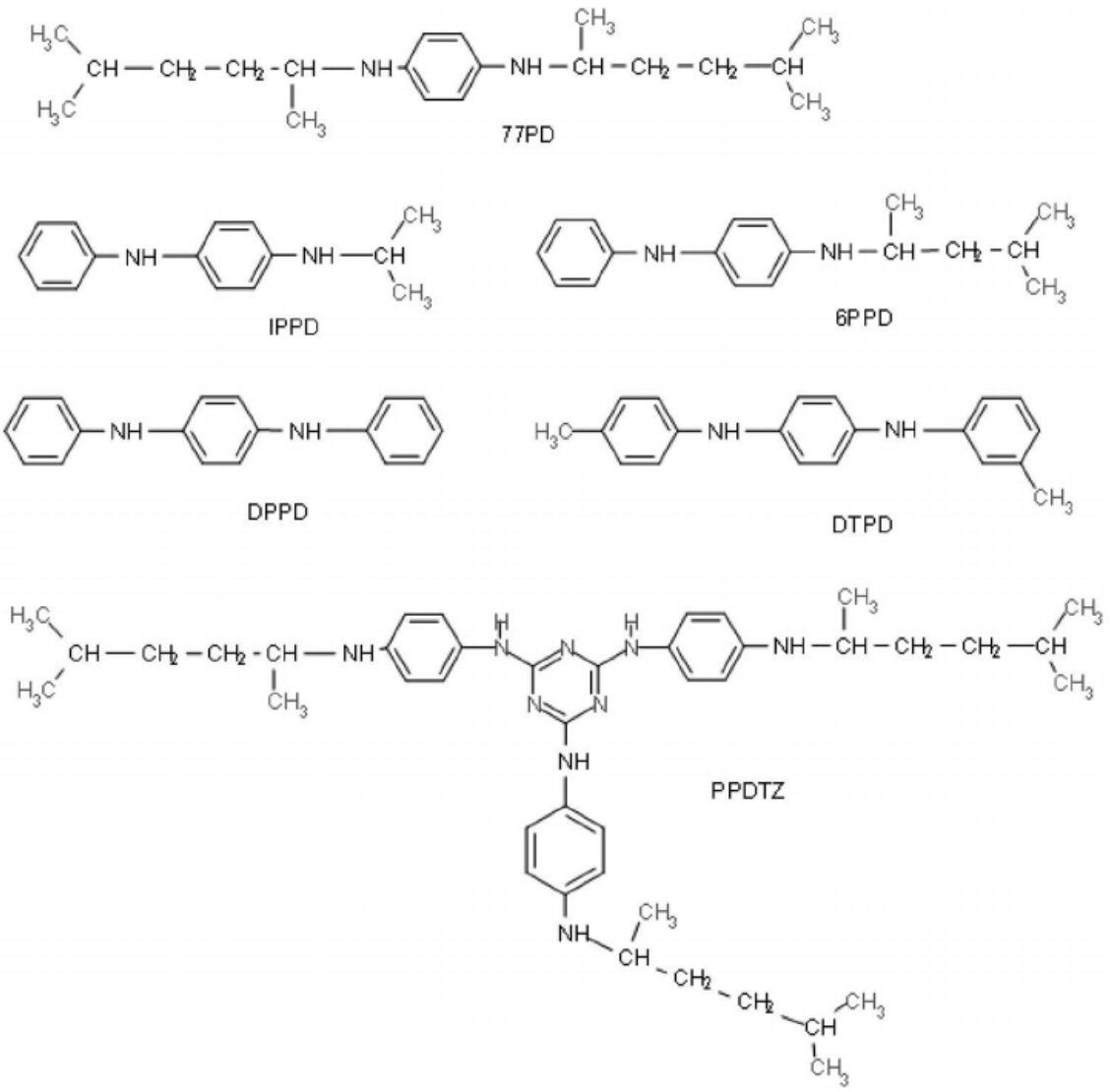


Figure 8 Chemical formulae of the most used antiozonants

(source: [32])

5.3 Degradation caused by ozone

As it was mentioned earlier, ozone cracking happens mostly to the products under tensile strength and compression. However, in the latter, the cracks will appear only in the regions where tensile stresses are induced. Ozone cannot penetrate far in this case, since it will soon encounter compressive rather than tensile stresses. Therefore, ozone cracking is not a significant issue for large elastomeric components, such as rubber bearings, which are used under compression [35]. If the rubber remains unstressed, a silver film on the product surface appears. This defect is called frosting, which is not as severe for physical properties as cracks [11, 21]. To summarize, degradation caused by ozone primarily attacks the surface and results in cracking and discoloration [18, 33].

When exposed to ozone, stretched unsaturated rubber forms surface cracks at right angles to the direction of the applied strain that progressively grow in depth and length, which eventually leads to the complete failure of the material [15, 36]. Even minor cracks, can drastically weaken the material and shorten its fatigue life. Over time, even minimal ozone levels are sufficient to cause material cracking. A large number of small, interconnected cracks is less damaging than a few isolated cracks, which can grow into deep, severe cuts over time [26, 37]. Once a minimum tearing energy is exceeded, typically with a tensile strain of 3–5 %, crack growth can readily occur. The tearing energy is the required energy to separate two surfaces in order for the crack to grow [34, 37]. The crack growth is also dependent on underlying chains' mobility, which can untangle and place double bonds for further ozone attack. Crosslinking can help to decrease mobility and reduce crack growth rate [33].

To conclude, there are four main factors affecting ozone degradation: ozone concentration, time of exposure, material strain, and chains' mobility. The higher these parameters are, the quicker cracks on the surface appear [11, 21]. The example of ozone exposure and its impact on NR is presented in Figure 9 with the following samples: (A) – unstretched, relaxed sample; (B) – sample under stretch; (C) – stretched sample degradation under ozone exposure [11].

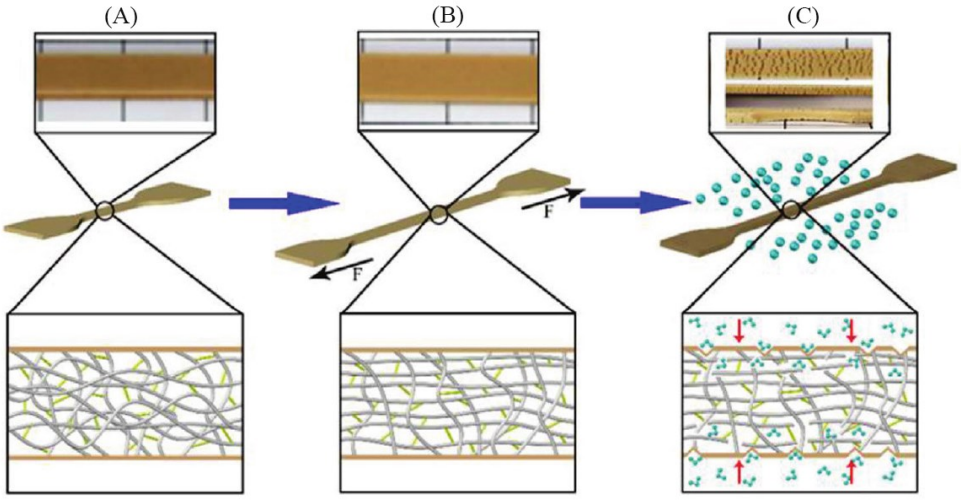


Figure 9 The changes in molecular structure of NR sample exposed under strain to ozone

(source: [11])

As mentioned before, ozone readily attacks rubber, which has unsaturation in the main chain [37]. Ozonolysis is a reaction between ozone and double bonds. In general, the ozonolysis process has been widely studied, but due to the complexity of NR, comprehensive

discussions on that topic are still missing. Therefore, most researchers concentrate on the alkenes example, the mechanism proposed by Criegee is widely accepted [31, 37]. The reaction of NR and ozone happens rapidly that happens with low activation energy [33, 38].

Figure 10 shows the Criegee mechanism, the electrophilic reaction of a basic monomer of NR and ozone. In step 1, highly reactive ozone attacks the double bonds in the polymer chain via a 1,3-dipolar cycloaddition, resulting in the formation of a primary ozonide, which rapidly rearranges through heterolytic cleavage of the oxygen-oxygen bond, resulting in the formation of a primary zwitterion. In step 2, this unstable primary zwitterion will break down into a carbonyl compound (aldehyde or ketone) and a secondary zwitterion [36, 38]. These intermediates then recombine in step 3 to form a secondary ozonide for stabilization [21, 31]. The last ozonide can undergo further reactions, such as thermolysis, photolysis, hydrolysis, and oxidation, depending on environmental conditions and producing final products like ketone derivatives. For NR, the ultimate result is chain scission, decreased molecular weight and hence its properties [15, 36]. With time, ozone may start to expose underlying unsaturation [34].

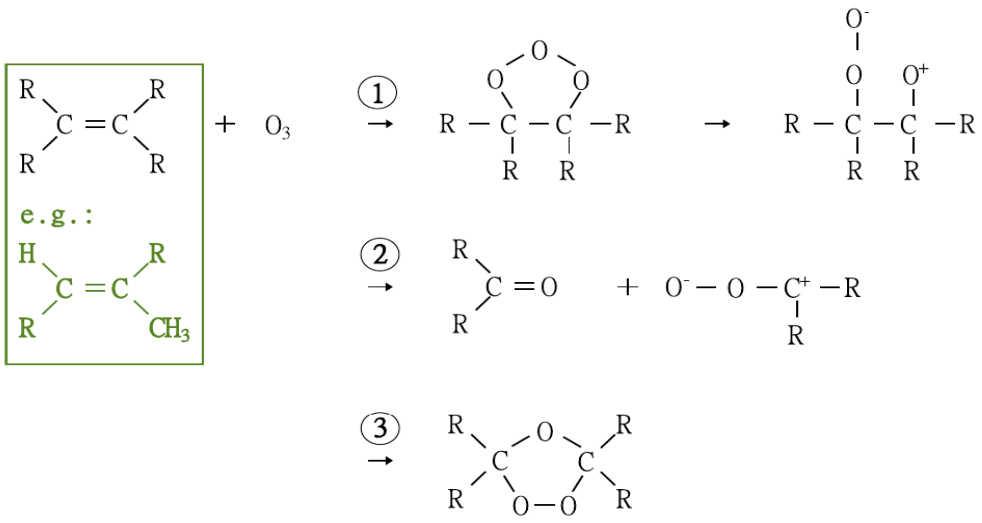


Figure 10 A Criegee's three-step mechanism of ozonolysis with basic NR monomer

(source: [36])

While the cracking of rubber is mainly described as ozone attacking rubber double bonds, it is important to note that ozone also interacts with sulfur crosslinks. However, these reactions with di- and polysulfides occur at least 50 times slower than the reactions with polyolefins. An example of such reaction with crosslinks is presented in equation (5) below [33]:

$$RSSSR + O_3 \rightarrow SO_2 + RSO_2 - O - SO_2R\ (+HOH) \rightarrow 2RSO_2H \qquad (5)$$

5.4 Ozone study

To determine whether a rubber compound is reliable for a product, an ozone test involving its high concentrations is necessary to perform [39]. Due to the surface degradation, testing methods are designed to expose rubber samples to controlled ozone concentrations for a specific period of time. After exposure, the samples are examined for cracking to determine ozone resistance. Common testing techniques include stretching flat specimens under tension, bending triangular specimens around a mandrel, or flexing flat specimens dynamically in an ozone environment [33, 38].

In laboratory conditions, ozone is typically generated from air or oxygen utilizing an ozonizer, which applies a voltage of variable output from a transformer. Commercially, ozone is produced from cold and dry oxygen that passes through silent electrical discharge. To measure ozone concentration, the gas has to pass through two wash bottles containing potassium iodide solution buffered to pH = 6.8. The coming solution is then acidified, and the liberated iodine can be determined by titrating with a 0.1 N sodium thiosulfate solution. This is a traditional method and its reactions are shown in equations (6-7) below. The total volume of gas can be measured using a calibrated flow meter [31, 37].

$$O_3 + 2KI + HOH \rightarrow O_2 + 2KOH + I_2 \quad (6)$$

$$I_2 + 2Na_2S_2O_3 \rightarrow Na_2S_4O_6 + 2NaI \quad (7)$$

Standard ozone tests are performed according to the Bayer method, which allows to assess the amount and length of the cracks [33]. They are typically conducted in a specialized ozone chamber, where the ozone concentration is controlled, usually ranging from 25 to 200 pphm circulating for e.g., 72 h. The other two parameters that have to be controlled are temperature and humidity. At high temperatures, ozone becomes unstable, while high humidity can decrease the reaction rate between ozone and rubber. In this regard, the standard temperature for testing is usually 40±1 °C and humidity has to be kept low. ASTM International published different standards for conducting ozone tests, for instance, ASTM D1149, ASTM D1171, ASTM D3395, as well as ISO with their standards like ISO 1431 [15, 18]. These accelerated tests are useful for comparing different rubber compounds, but they are not fully accurate for predicting the long-term performance of rubber in real-world conditions [33, 38]. Generally, if the cracks are not observed after these experiments, it means that the material has a good resistance to ozone cracking [35].

5.5 Antiozonants

Since ozonation mainly affects the surface, it is important to incorporate additives, which can provide surface protection. An ideal antiozonant would be a substance that can effectively disperse in a rubber compound, but after processing blooms to the surface providing an effective physical or chemical barrier against ozone [37, 38]. Other important requirements include: low toxicity and non-discoloring for non-black rubbers, as well as non-staining for light-colored rubbers along with persistent activity during service life [37].

Ozone resistance can be evaluated by both static and dynamic tests. Static conditions preserve protective wax barriers on the material, while dynamic flexing conditions, which cause these barriers to weaken and rupture, can better simulate real-world dynamic conditions. Consequently, dynamic tests are more effective for assessing the relative effectiveness of antiozonants like p-phenylenediamines (PPDs) [15, 18]. Both of these antiozonant types have low molecular weight and bloom to the surface [34, 38].

Under static conditions, rubber surface has to be covered, which can be accomplished with hydrocarbon waxes, such as paraffinic or microcrystalline. Paraffinic waxes consist mainly of hydrocarbons with straight chains and relatively low molecular weight [34, 37]. Due to their linear structure, these waxes are highly crystalline and can form large, well-defined crystals with a melting point of 38–74 °C. In contrast, microcrystalline waxes are derived from heavier petroleum residues and have a higher molecular weight. The structure of microcrystalline waxes is predominantly branched, resulting in smaller and more irregular crystals that melt at the temperature range of 57–100 °C. The thicker the crystallized film of bloomed wax appears at the surface, the better the protection against ozone. The film thickness depends on the solubility, temperature, as well as on diffusion rate of the static antiozonant. Bloom appears when the amount of wax in rubber exceeds its ability to dissolve within the rubber matrix. When the temperature is lower than 40 °C, it reduces the solubility, while small-sized wax molecules readily migrate to the surface, increasing the thickness of the bloom. In contrast, high temperature possesses a disadvantage, because the wax becomes too soluble and loses the ability to form enough thickness on the product surface. With regard to microcrystalline waxes, higher temperature promotes their migration to the surface, hence they can perform better at these conditions. Commonly, blends of both waxes are used [15, 33]. Their main advantages are: non-discoloring, no effect on vulcanization, and low cost. The main disadvantages are: inability to protect rubber products from dynamic strain, high temperature dependence, and surface appearance, which can be easily ruptured [31, 37].

The scavenging mechanism under dynamic conditions explains that migrated antiozonants to the surface react more quickly with outside ozone, rather than ozone attacking double bonds of rubber, hence protecting the material from degradation. As a result, the reaction rate decreases over time coming to a complete cease. Spectroscopic analysis of the surface confirmed the presence of unreacted antiozonant and its ozonized derivatives, but no evidence of ozonized rubber [33]. This reaction creates a protective layer with amine ozonide products, which acts as a barrier to prevent O_3 from penetrating deeper inside [38, 39]. Over time, as the surface antiozonant is consumed, more antiozonant diffuses from the rubber bulk to the surface, ensuring continuous protection against ozone [34]. Again, the migration efficiency is influenced by temperature, the degree of crosslinking, solubility, and diffusion rate [36]. The simplified mechanism of the example of antiozonant 6PPD with ozone is presented in Figure 11. In this reaction, the aryl alkyl-substituted NH group is more reactive than the bisaryl-substituted NH group due to the former higher charge density, because of the alkyl electron-donating group, while aryl groups are less electron-donating, hence reducing the charge density on the nitrogen atom [33].

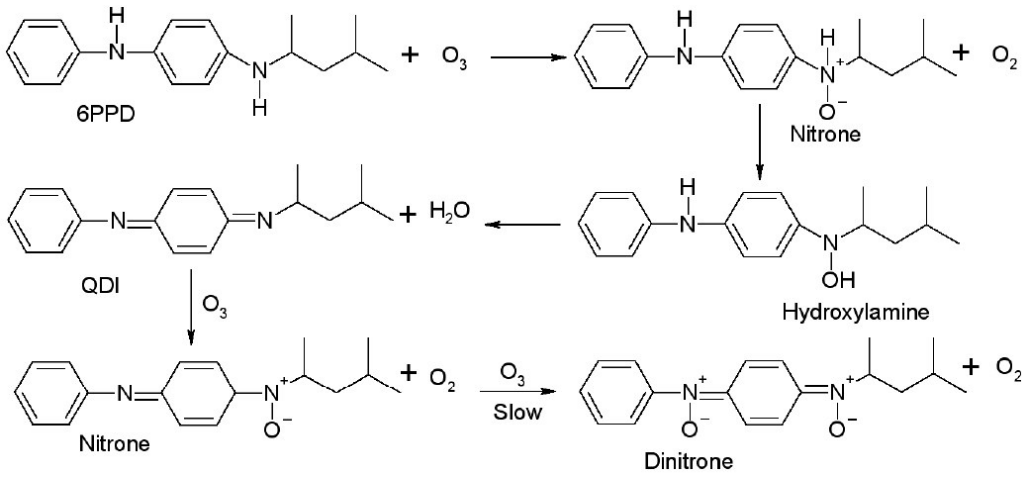


Figure 11 Ozonation mechanism with 6PPD antiozonant

(source: [33])

Conventional antiozonants like 6PPD offer effective protection against oxygen and ozone, but this protection is relatively short, up to 5 years. Other disadvantages of 6PPD include: volatilization, staining, discoloring, and high toxicity. In response to the service life of conventional antiozonants and their other disadvantages, toxicity in particular, there is a clear, high demand to develop new classes of long-lasting non-toxic antiozonants [34, 37]. In spite of development of new antiozonants, former still hold a lead with the balance of properties, demand, and cost [33].

6 MECHANICAL AND PHYSICAL TESTING OF RUBBER

For a rubber product to exhibit desired properties, its rubber compound has to be tested to comply with quality control, which further determines its suitability for a specific application [16]. Most of these tests are performed to evaluate processability and assess the physical properties of rubber after vulcanization [23]. Processing mainly depends on the viscosity and elasticity of compounds, which is reflected in measuring curing characteristics and Mooney viscosity [12, 18]. The following curing parameters are tested: scorch time, cure time, torques, and reversion, which are usually measured for any rubber compound to understand its vulcanization behavior, while the Mooney viscometer measures the relative viscosity. In order to measure physical properties, the following main tests are performed: hardness, tensile strength, and elongation at break. When a product has specific applications, other tests can be performed, such as heat resistance, compression set, impact strength, abrasion resistance, tear strength, resilience, flex resistance, weather tests, oil resistance, etc. [21, 23]. All these methods have been standardized at both national and international levels, while there is a trend to use standards from International Standards Organization (ISO). The main aim of creating standards is to eliminate the possibility of variations between separate researchers [13].

6.1 Preparation of test samples

Before any testing, it is important to prepare a sample for an experiment. In the vast majority of measurements, the geometry of the test sample plays a crucial role. Therefore, the shapes and sizes of samples have to be well-defined according to standards. In order to obtain the required geometry, a test piece usually has to be cut out and/or buffed [13]. Other important sample parameters, which must be controlled include: the production method of a sample, storage, and testing conditions [16].

ISO-23529-2016 states, quote: “For all tests, the minimum time between forming the material and testing shall be 16 h.” and quote “For product tests, whenever possible, the time between vulcanization and testing should not exceed 3 months.”. It indicates that physical testing shall not be performed immediately after product manufacture due to the subject of temperature, humidity, and other conditions, which have not reached equilibrium with the test sample yet, as for the same reason not exceed longer than 3 months, while these conditions may affect the rubber compound. The storage temperature and humidity are not critical since conditioning occurs later, but a reasonable range is from 10 to 30 °C with

humidity under 80 %. Additionally, different compounds should be kept separate in order to prevent the migration of ingredients [13]. These measures are important for reproducibility of these tests by others for comparison and legitimacy [16].

6.2 Curing characteristics

As it was discussed before, processability plays a crucial role in the production of the final products, since the exact measured parameters allow to make this process as efficient as possible with good estimation of the final properties [25]. Rheometry is among the basic techniques used to investigate the rheological characteristics of a rubber compound in its industry. It helps to monitor and achieve the desired curing parameters, such as: scorch time or safety time, minimum and maximum torques, cure time, as well as viscoelastic properties. Nowadays, two types of rheometers are widely used: oscillating disk rheometer (ODR) and moving die rheometer (MDR). The last one is basically an improved version of ODR, which was developed in 1963 by Alpha Technologies [12, 18].

The difference in the equipment structure is a biconical disk in ODR instead of a rotor disk in Mooney Viscometer. Biconical disk according to standards has a diameter of 35.5 mm. The sample must have a cylindrical shape, which is usually punched out with a diameter of 30 mm and a thickness of 12.5 mm. This test piece has to be placed inside a cavity consisting of two parts, the lower being fixed and the upper movable, both with heating platens. During the experiment, the cavity closes, seals under pressure, and is heated to the test temperature. A biconical disk embeds in the specimen and starts sinusoidal oscillations with a constant frequency of 1.7 Hz and typical rotary amplitude of 1°, 3°, or 5°. Typical testing temperature varies from 100 °C to 250 °C, depending on the expected curing temperature. From an applied shear stress, it is possible to get a torque measurement (resistance) and understand the curing behavior of a specific rubber compound [16, 25].

As it was mentioned, ODR performs the measurements at actual curing temperatures. It measures changes in torque (shear modulus) during occurring crosslinks by heating. The torque or force required to move the disk depends on the stiffness of the rubber compound and is measured by a torque arm transducer. With the vulcanization progress, the viscosity of a compound rises and it requires greater torque to oscillate. The instrument continuously records and plots a graph dependence of torque on time, commonly known as an ODR trace or simply a cure curve [12, 23]. An example of such a curve is presented below in Figure 12 generated by both, ODR and MDR [23].

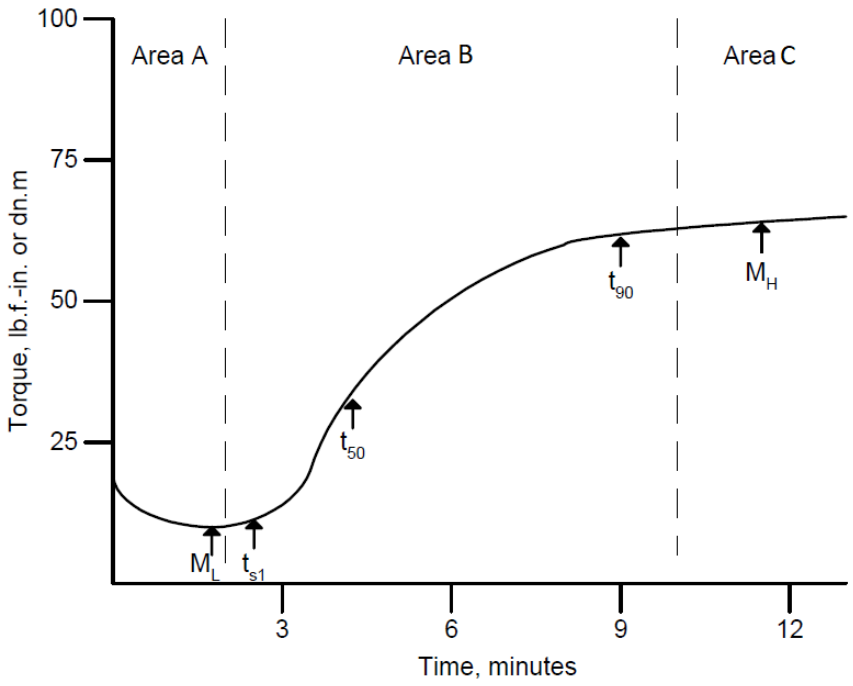


Figure 12 An example of a vulcanization curve

(source: [23])

The graph shows the most important parameters to consider before curing the compound. There are three sections of the graph, which represent:

1. Area A – viscosity of a compound
2. Area B – rate of cure
3. Area C – state of cure

In the A area, M_L represents a minimal torque, which is a value for compound viscosity before vulcanization. In area B, t_{s1} – is a time for torque to increase 1 unit above M_L, which is important to understand the safety time before a compound starts to vulcanize (scorch time). t_{50} and t_{90} are the times when vulcanization of a compound reaches 50 %, and 90 % respectively of maximum torque development M_H, which is a measure of the cure state and presented in area C. t_{90} is also known as "optimum cure time", which is accepted as the practical endpoint to terminate further vulcanization. With this regard, the end of the curve may have three possibilities to develop. The first option is to maintain a horizontal level, creating a plateau, indicating the end of the vulcanization process. The second option is to rise slowly, which leads to overcure, making rubber stiffer. The last option is to slowly decline, which is also called reversion – it leads to a breakdown of a vulcanized network, weakening the rubber compound [12, 23].

There are several issues with ODR, which lead to the development of a more modern version MDR [12, 18]:

1. The rotating disk, which is not heated, does not allow a specimen to reach a test temperature quickly enough, which means that its scorch values are not accurate
2. Mechanical influence of biconical disk shears the rubber compound, affecting the outcome of isothermal and dynamic properties
3. Finally, the test specimen has to be pried off the rotor, due to the construction difficulties of using a barrier film. It makes an ODR difficult to operate

Due to these limitations, a moving die rheometer was developed in order to overcome these problems. It consists of two dies, which form a biconical cavity. A sample should be placed in between these dies, both of which are sealed, pressurized, and constantly heated, and one of which makes the sinusoidal oscillations at the same frequency and amplitude as ODR [13, 25]. As the specimen gets stiffer, a torque increases, monitored by a reaction torque transducer, which is directly connected to a torque transducer; such structure increases test sensitivity which is called signal-to-noise. The advantages of MDR allow test samples to run tests much quicker and more accurately under the same conditions than ODR. Another advantage of rotorless curemeters is a separate measurement of elastic and viscous responses. In this case, a second viscous curve appears on the graph allowing to better analyze the flowability and processing of the rubber compound [12, 18].

An even more advanced rotorless rheometer is called Rubber Process Analyzer (RPA), where both dies have the ability to oscillate and measure the curing characteristics, as well as analyze the viscoelastic properties of both cured and uncured rubber, perform strain and frequency sweeps, and evaluate filler dispersion and the Payne effect [12, 18]. It is a very sophisticated equipment, where the oscillation rate, temperature, and strain level can all be precisely adjusted [25].

6.3 Physical testing of rubber compounds

Mechanical testing as a part of physical testing involves different methods to evaluate the final properties whether they meet desirable requirements of the products. The most general and common tests for rubber materials include: hardness testing, tensile strength and elongation at break [21].

6.3.1 Hardness

Hardness is the most popular, inexpensive, and quick physical testing of rubber, which allows to obtain a modulus by evaluating the resistance of cured rubber to a deformation done by a rigid indenter, to which a force is applied [21]. The higher the hardness, the less elastic is the compound. The softer the specimen, the less it pushes back the indenter [12].

However, hardness test results may greatly vary on the same sample piece [23]. There are two ways of handling the testing. The first one is called – an International Hardness, which normally uses a hemispherical or ball indenter, to which a dead load (constant force) is applied and the result is measured in International Rubber Hardness Degrees (IRHD) units described in ISO 48-2. The measurements of IRHD are held on a so-called dead-load hardness tester. The other method involves a force applied to an indenter by a spring, which presses into a rubber. It is called a Durometer Hardness Method, described in ISO 48-4. The first type is considered to be more accurate, but the last is simpler and quicker [13, 18].

Durometers can be hand-held or mounted on a stand [23]. The hardness method has two main variations – Shore A and Shore D. Type A is used for soft materials; the applied force is lower and the indenter has a rounded blunt cone. Type D is used for hard materials; the applied force is higher and the indenter has the shape of a sharp tip [16].

The standard thickness of the IRHD test piece is from 8 to 10 mm but can vary since this method is also used for thinner samples. Shore A and D typical thickness is at least 6 mm [16]. Due to the viscoelasticity of rubber, a Shore tester shows the maximum value once an indenter reaches the maximum penetration and then this value decreases [12]. Despite its accuracy and poor repeatability, hardness testing will most probably continue to remain a standard test in the rubber industry [23].

6.3.2 Tensile strength and elongation

Stress-strain tests are considered much more informative and useful in the rubber industry [23]. ISO 37 describes the procedure to measure the following properties: ultimate tensile strength, ultimate elongation at break, and elongation modulus [18]. The essence of this method is to determine how much stress can one specimen withstand before it reaches a breaking point at a certain elongation [22]. These properties are measured on tensile strength machines, which require specimens of different possible shapes, such as dumbbells, rings, or straight strips. Once centrally fixated in clams, the specimen is stretched at a traverse rate, the most popular being a constant 500 mm/min and the relationship between applied force

and registered deformation is calculated [16, 18]. One test round should consist of at least two to three samples [16, 23].

When the specimen breaks at the maximum stress during elongation, it is called an ultimate tensile strength, measured in "Pa". Ultimate elongation measures the applied strain at which a specimen breaks, defined in "%". A modulus is basically an applied stress per cross-sectional area at a given elongation, usually measured at 100 % and 300 % [18, 23]. Figure 13 shows an example of a typical stress-strain curve for a rubber specimen with detailed characteristics [13]. Although it is possible to measure Young's modulus due to the linear portion on a curve as well, it is too small to get an accurate result [12].

Outcome results mainly depend on material properties, specimen dimensions, and test conditions [13, 21]. Tensile strength is calculated as the dependence of breaking force (N) on the initial cross-sectional area of a specimen (m^2). Elongation at break is calculated as the dependence of a difference between final length and gauge length on gauge length, expressed in percentages. Gauge length is the initial length of a sample between the so-called gauge marks, which represent the reference clams' marks. Modulus is the dependence of the force at a certain elongation on the cross-sectional area of a specimen (m^2) [12, 16].

The main advantage of the tensile strength method is the possibility to understand the consistency of a rubber batch, in particular, its mixing and dispersion, presence of contamination, and curing [12, 18].

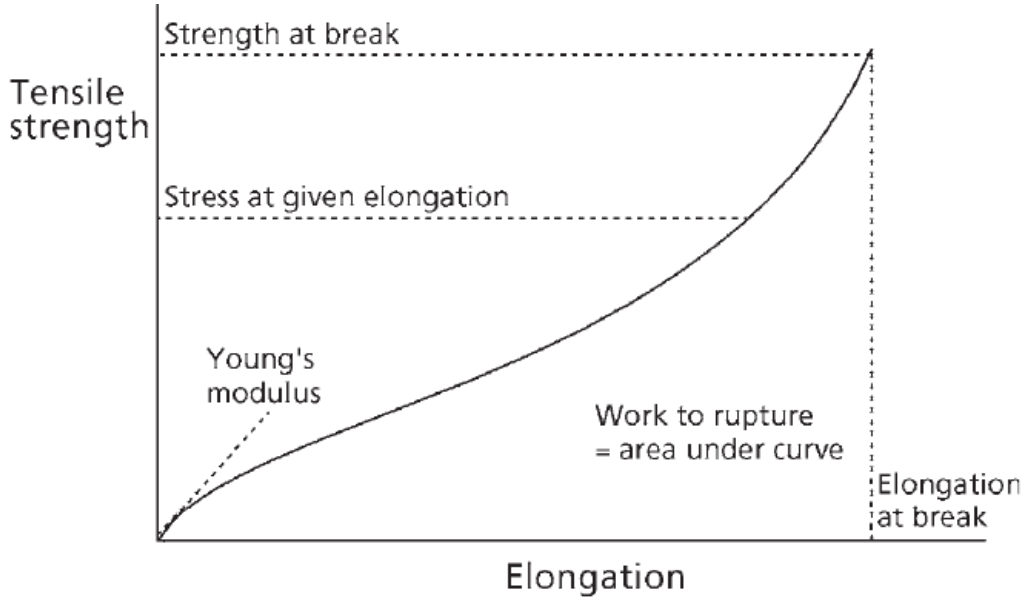


Figure 13 A representative stress-strain curve

(source: [13])

II PRACTICAL PART

7 MATERIALS AND PREPARATION OF COMPOSITIONS

The main goals of the practical part are to investigate the influence of different vulcanization systems on the ozone stability of rubber compounds by evaluating the new surface area as well as to perform mechanical tests to observe the possible correlations between the results.

7.1 A brief description of the performed work

In the practical section, seven different compositions were prepared, each with a unique accelerator. In total, two rounds of experiments took place. The first round contained four compositions, and nine samples were formulated for each, while in the second round, the other three compositions contained six samples each. All these samples from both rounds had different concentrations of an accelerator. Vulcanized samples were then exposed to ozone circulation and observed at specific intervals using an optical microscope. Ozone tests help to determine at which concentration of an accelerator and at what time point of the ozone exposure a sample develops cracks, indicating the ozone effect. Additionally, all compounds from the second round underwent tensile strength as well as hardness testing to identify possible correlations between mechanical properties and ozone degradation. Mechanical tests (hardness test and tensile test) reveal how the obtained data correspond to the sample's actual mechanical properties, providing insights into their durability and potential applications under environmental impact.

7.2 Compositions

For the experiments, a base compound consisted of NR, CB, processing oil, activator, and co-activator/dispersive agent. The vulcanizing agent was added along with the accelerator, the latter at varying concentrations. Antiozonant 6PPD was added only to the second composition to observe any changes with the first composition consisting solely of the TBBS accelerator.

As it was said, two rounds of experiments took place at varying concentrations. It was interesting to observe how an antiozonant performs comparing to the sole composition with the same accelerator, as well as to the composition with another accelerator. The first round contained 9 concentrations, while the second was adjusted only to 6 after understanding the behavior of the concentration effect. In addition, the observation times during ozonation after the first round were also changed with a focus on the beginning, since the cracks' development is generally more engaging at the start. At the same time, a third accelerator

was introduced into the second round to observe the complex changes between accelerators based on their rate of vulcanization. It was also a subject of reproducibility of measurements.

The types of accelerators were added as follows. For the first round: the first composition used TBBS (referred to as TBBS-1), the second used TBBS and 6PPD antioxidant (referred to as TBPD-1), the third used TBBS (referred to as TBBS-2), the fourth used MBTS (referred to as MBTS-1). For the second round, the fifth composition used TBBS (referred to as TBBS-3), the sixth used MBTS (referred to as MBTS-2), and the seventh used TMTD (referred to as TMTD-1). Tables for the first round with concentrations are presented in Appendix 1. A Table 6 shows the composition for the second round.

Based on the described vulcanization systems, A/S concentration ratio indicates it in the tables – conventional (CV) for the range ~0.1–0.5, semi-efficient (SEM) for the range ~0.5–2.5, and efficient (EV) for the range ~2.5–20. The number of samples increases by 1 with the increase of the accelerator's concentration. In the following naming, a specific sample is written according to its referring concentration with "_" straight after the composition's name. For example: MBTS-2_2 means that a sample was vulcanized with MBTS accelerator, "-2" means that it is a second composition with such accelerator, and "_2" means the actual accelerator's concentration of the sample, which is 0.5 phr. This composition possesses a conventional vulcanization system and the A/S ratio is 0.2.

Table 6 Compositions from the second round of experiments

	Loading in phr					
A/S ratio	**0.1 CV**	**0.2 CV**	**0.7 SEV**	**1 SEV**	**2.5 EV**	**3 EV**
Ingredients / ***Samples***	**1**	**2**	**3**	**4**	**5**	**6**
NR SVR-CV60	100.00	100.00	100.00	100.00	100.00	100.00
N220	58.00	58.00	58.00	58.00	58.00	58.00
Tudalen oil 11	6.00	6.00	6.00	6.00	6.00	6.00
ZnO	5.00	5.00	5.00	5.00	5.00	5.00
Stearic acid	3.00	3.00	3.00	3.00	3.00	3.00
Accelerator	**0.25**	**0.50**	**1.75**	**2.50**	**6.25**	**7.50**
Sulfur OT33	2.50	2.50	2.50	2.50	2.50	2.50
Sum	**174.75**	**175.00**	**176.25**	**177.00**	**180.75**	**182.00**

The input raw materials were weighed on laboratory scales with an accuracy of 0.01 g, in the correct amounts according to the calculated weights. For easy and dust-free handling during mixing masterbatches in the kneader, the input chemicals except rubber were weighed in ethylene-vinyl acetate (EVA) bags as follows: the first bag contained the activator along with the dispersing agent, the second bag contained 2/3 of the soot, and the third bag contained the remaining 1/3 of the soot and the processing oil. The composition containing the antioxidant/antiozonant 6PPD received it from the first bag. After obtaining the base mixture, the last portions containing the accelerator and vulcanizing agent were weighed separately, each with different concentrations, which were added to the compositions during the last stage.

7.3 Materials

7.3.1 Natural rubber

The basis for creating rubber compounds was NR (cis-1,4-polyisoprene) NR SVR-CV60. This abbreviation can be broken down as follows: SVR stands for a Standard Vietnamese Rubber and CV60 refers to the Constant Viscosity grade, which indicates the Mooney Viscosity of 60 ML (large rotor). Characteristics are presented in Table 7.

Its color is yellow, suppliers indicate that this grade exhibits high elasticity and tear resistance together with an outstanding tensile strength [40]. Possible applications include: the tire industry, seals, vibration dampers, engine mounts, conveyor belts, etc. [30, 41].

Table 7 Characteristics of NR SVR-CV60

Characteristic	**Value**	**Test method**
Dirt content, wt.% max	0.02	TCVN 6089:2004
Ash content, wt.% max	0.40	TCVN 6087:2004
Nitrogen content, wt.% max	0.60	TCVN 6091:2004
Volatile content, wt.% max	0.80	TCVN 6088:2004
Plasticity retention index, min	60	TCVN 6092:2004
Mooney viscosity, ML	60 (±5)	TCVN 6090:2004

(source: [40])

7.3.2 Soot

CB with a trade name VULCAN® 6 type N220 from Cabot Corporation (USA) was used, meeting the ASTM N220 standard. The manufacturer states that this grade is greatly suitable for tire threads, which require better wear, as well as tear and cut/chip resistance. N220 offers outstanding extrusion characteristics and is easy to be dispersed [42]. Characteristics are shown below in Table 8.

Table 8 Characteristics of CB VULCAN® 6 type N220

Characteristic	**Value**	**Test method**
Iodine adsorption number, mg/kg	121	ASTM D1510
Oil absorption number (OAN), ml/100 g	114	ASTM D2414
OAN after crushing (COAN), ml/100 g	98	ASTM D3493
Tinting strength, %	115	ASTM D3265
STSA surface area, m^2/g	104	ASTM D6556

(source: [42])

7.3.3 Processing oil

Tudalen oil type 11 is a solvent-refined, paraffinic oil used as a processing oil from Hansen & Rosenthal Company (Germany) with characteristics presented below in Table 9. It is a paraffinic oil with good viscosity characteristics, mostly used in tire threads [43].

Table 9 Characteristics of Tudalen oil type 11

Characteristic	**Value**
Viscosity gravity constant	0.815
Density at 15 °C, kg/m^3	869.8
Pour point, °C	-15
Kinematic viscosity at 40 °C, mm^2/sec	31.6
Aniline point, °C	103.7

(source: [43])

7.3.4 Main activator of vulcanization

ZnO type S6 was purchased from SlovZink, a.s. (Slovakia), and used as an activator in the vulcanization process. This product is in the form of soft, white, amorphous powder,

obtained by the oxidation of zinc vapors. The product's purity is 99.0 min. %. Loss on ignition test (LOI) shows 0.5 %. A specific surface by BET method is 4.0–7.5 m^2/g [44].

7.3.5 Co-activator and dispersive agent

Stearic acid with a tradename Stearin TEFACID® RG from AAK Czech Republic s.r.o. (Czech Republic) was used to work in tandem with ZnO as activators, as well as to play the role of a dispersive agent in order to ensure an even cure. In essence, it consists not only of stearic acid, but it is a mixture with palmitic and other fatty acids [45]. Characteristics are below in Table 10.

Table 10 Characteristics of TEFACID® RG stearic acid

Characteristic	**Value**
Melting point, °C	53–61
Acid number, mg KOH/g	194–210
Saponification number, mg KOH/g	195–211
Iodine number, g/100 g	<8

(source: [45])

7.3.6 Vulcanizing agent

Insoluble sulfur with a trade name CRYSTEX™ OT 33 from Eastman Chemical Company (USA) was used as a vulcanizing agent. CRYSTEX is a trademark, OT stands for oil-treated and 33 is its value in "%". It is a non-blooming polymeric sulfur, which is insoluble in elastomers, and has found most of its applications in tires. This sulfur type is both non-staining and non-discoloring [46]. Characteristics are presented in Table 11 below.

Table 11 Characteristics of sulfur CRYSTEX™ OT 33

Characteristic	**Value**
Oil treated powder, %	33
Specific gravity at 20 °C	1.43
Bulk density packed, kg/m^3	600–800
Bulk density unpacked, kg/m^3	400–600
Mean particle size, µm	<30

(source: [46])

7.3.7 Accelerators

In this work, three different accelerators were used: N-tertiarybutyl-2-benzothiazole sulfenamide (TBBS), Dibenzothiazole disulfide (MBTS), Tetramethylthiuram disulfide (TMTD), where the first is the slowest providing good scorch safety, the second is moderate and the latter is the fastest one. All of them were received from Shandong Dongchang Fine Chemical Technology Co., Ltd. (China), and can be used in a variety of rubber goods. Characteristics are provided below in Table 12.

Table 12 Characteristics of TBBS, MBTS and TMTD

Characteristic / Accelerator	TBBS	MBTS	TMTD
Ash content, %	<0.3	<0.5	<0.3
Melting point, °C	>104	>166	>142
Purity, %	>96	>96	>96

(source: [47–49])

7.3.8 Antiozonant/antioxidant

A thermal antiozonant and antioxidant DUSANTOX® 6PPD (N-(1,3-dimethylbutyl)-N'-phenyl-p-phenylenediamine) from the company Duslo, a.s. (Slovakia) was used in one composition. Producer affirms that 6PPD has great solubility in rubbers and is considered to be the most effective antidegradant available commercially providing excellent protection against ozone in both static and dynamic conditions [50]. The basic parameters are presented in Table 13 below.

Table 13 Characteristics of DUSANTOX® 6PPD

Characteristic	Value
Purity, wt.% min	97
Melting point, °C	44–50
Cinematic viscosity at 60 °C, mm^2/sec	>50
Ash content, wt.%	>0.1
Specific gravity, kg/m^3	1.056

(source: [50])

7.4 Preparation of the mixtures

The first round of rubber compounds took place by mixing ingredients in the Banbury mixer by Pomini Farrel, model Midget (USA), shown in Figure 14. In the first stage, a masterbatch was prepared, which is a premix composed of rubber, soot, processing oil, activator, and co-activator/dispersive agent.

The rotor speed of the kneader was set to 50 rpm. The temperature on the temperature control unit was set to 90 °C, but due to the high friction of the mixture against the walls of the kneader and the kneading blades, the actual temperature rose to approximately 135 °C, depending on the individual mixture. The entire mixing cycle lasted approximately 5 min. In the beginning, the rubber was fed into the kneader and mixed for 30 sec in order to break and heat it up, facilitating its processability. After that, the first bag of ZnO and stearic acid was introduced and mixed for another 30 sec. Later, the second bag containing 2/3 of CB was added to a kneader and mixed for 120 sec. Lastly, the third bag with the remaining 1/3 of soot and processing oil was thrown inside and the whole mixture was mixed for another 120 sec. In total, the entire rubber mixture was mixed for approximately 300 sec from the beginning of kneading, excluding the time of adding the ingredients.



Figure 14 A Banbury mixer by Pomini Farrel, model Midget

(source: own elaboration)

Before feeding new raw materials to the kneader, the ram was lifted, and after dosing the chemicals, the ram was always lowered to compress all input materials. The beginning of the kneading started once the ram compressed the input rubber, and the end of the process represents opening the bottom door to discharge the masterbatch.

The second round of rubber compounds was performed by the same technique and conditions, but on a bigger kneader from Everplast Machinery Co., Ltd., model SYD–2L (Taiwan), shown in Figure 15.



Figure 15 A kneader from Everplast Machinery Co., Ltd., model SYD–2L

(source: own elaboration)

Later, the mixture was discharged from the kneader and cooled on an open mill Farrel G-2603 (Spain), with 150 mm rolls' diameter and 330 mm of working length sized, presented in Figure 16. The two-roll mill was temperature-controlled at 60 °C, with the front roll set to 18 rpm and the rear roll set to 20 rpm. The mixture was thoroughly cut and folded, and the gap width was gradually adjusted to ensure proper mixing of the mixture for at least 5 min. The rubber masterbatch was finally put to rest for 1–2 h.



Figure 16 A mixing mill Farrel G-2603, 150×330 mm

(source: own elaboration)

In the second stage, a small-volume Brabender kneader, model F-10572 (Western Germany) was used to mix a masterbatch with different ratios of A/S. The machine is shown in Figure 17 below. After the rubber mixture had rested, it was cut into strips with scissors and prepared for another mixing cycle. The rotor speed of the kneader was set to 35 rpm. The temperature in the device was set to 85 ℃ and, due to friction, the actual temperature increased to approximately 100 ℃. At the beginning, approximately 3/5 of the masterbatch of the required amount for one sample was introduced into the kneader to mix for 20 sec in order to reach the desired temperature to facilitate its processability, followed by the vulcanization system consisting of sulfur and accelerator. It was mixed for another 10 sec and lastly, the remaining part of the masterbatch was added at 30 sec from the start. After the whole mix became pliable, the rotor speed was increased to 40 rpm. The entire mixing cycle lasted 150 sec or 2.5 min until the equipment was stopped and dismantled to discharge the prepared mixture and prepare the inside of the chamber by cleaning for the next one. The discharged rubber mixture was again cooled down on the same open mill and rolled as in the first stage, as mentioned above.

An overall summary of the rubber compounding is presented below in Table 16. To prepare individual samples for various tests, the rubber mixtures were rolled on the two-roll mill into thin sheets from which samples for testing were prepared.

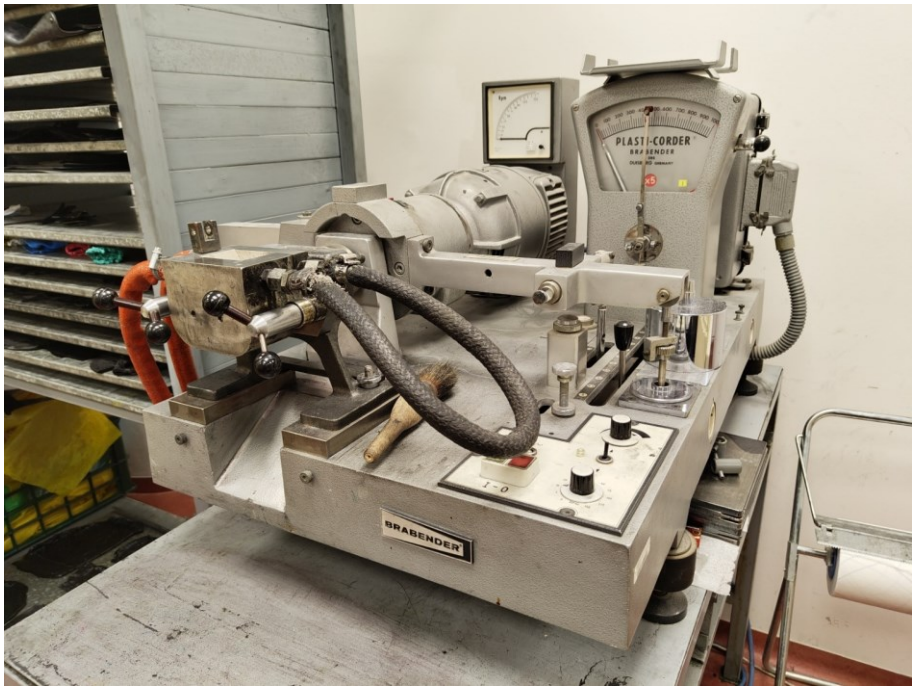


Figure 17 A Brabender kneader, model F-10572

(source: own elaboration)

Table 14 A procedure of rubber compounding

Machine	Ingredient	Addition time, sec
Banbury mixer	NR SVR-CV60	0
	First bag: ZnO and stearic acid (+6PPD)	30
	Second bag: 2/3 of soot	60
	Third bag: 1/3 of soot and processing oil	180
Discharge at 300 sec		
Cooling down on the Open mill for 300 sec with a following rest		
Brabender kneader	3/5 of masterbatch	0
	Vulcanization system	20
	2/5 of masterbatch	30
Discharge at 150 sec		
Cooling down on the Open mill with following rest		

8 VULCANIZATION CHARACTERISTICS

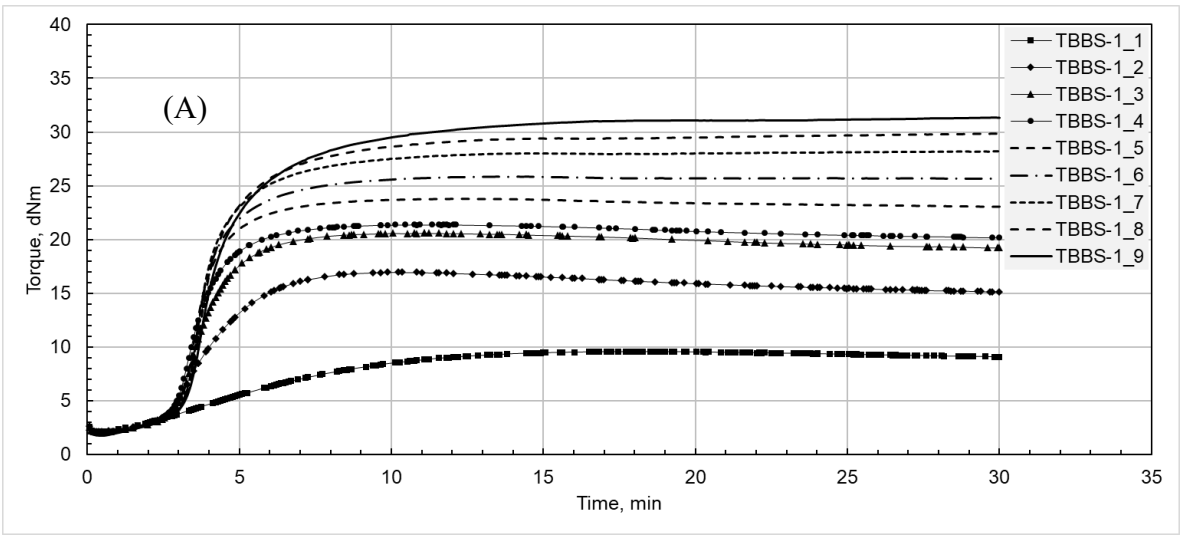
Measurements of basic vulcanization characteristics were conducted on Polymer Process Analyzer PPA-1 from Alpha Technologies (USA) for the first round, and on Premier MDR 3D rheometer also from Alpha Technologies (USA) for the second round. Both rheometers are presented in Figure 18. The samples were cut out from rubber sheets using supplied punchers together with these machines. Test characteristics for measurements were as follows: temperature of 160 °C with a usual measurement time of 30 min. The measurements were performed at least 24 h after mixing the compounds.

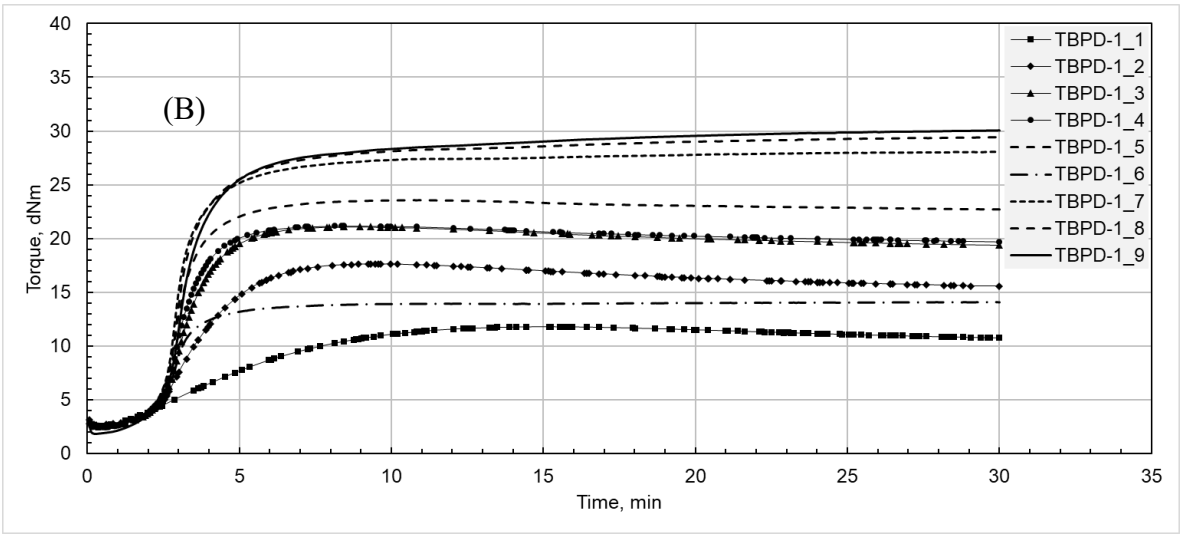


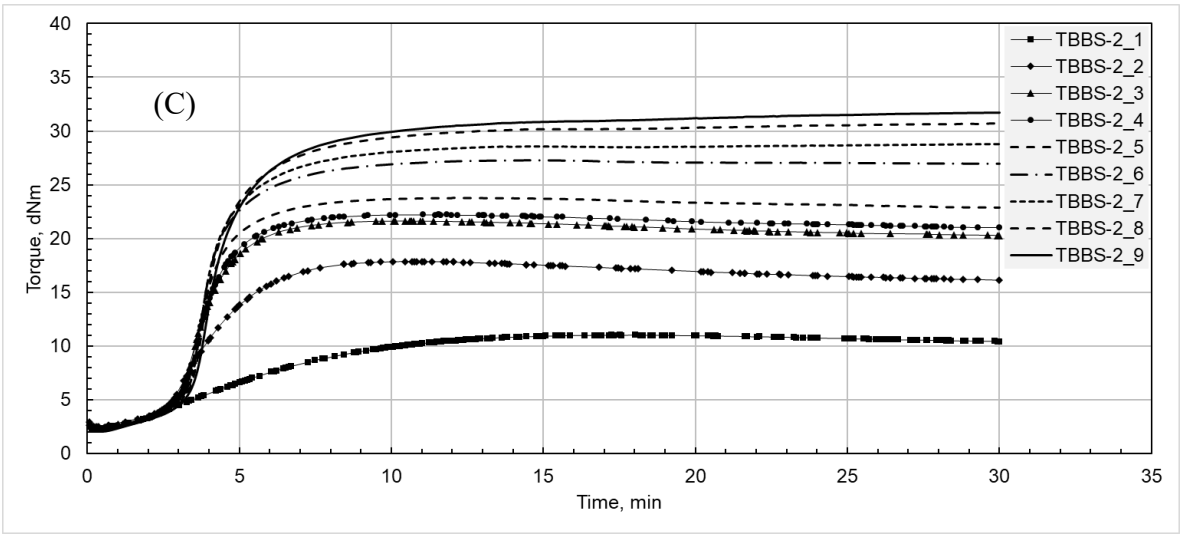
Figure 18 Polymer Process Analyzer PPA-1 (left) and Premier MDR 3D (right) from Alpha Technologies

(source: PPA-1 [own elaboration], Premier MDR 3D [51])

The results are presented below, showing the vulcanization curves of the individual compounds and illustrating the dependence of torque (dNm) on time (min). Curves for the first round of experiments are shown in Figure 19, whereas the ones from the second round are shown in Figure 20. Corresponding sets of vulcanization result data are presented in Table 15 for the first round and in Table 16 for the second round.


(A)
Torque, dNm
Time, min
TBBS-1_1
TBBS-1_2
TBBS-1_3
TBBS-1_4
TBBS-1_5
TBBS-1_6
TBBS-1_7
TBBS-1_8
TBBS-1_9


(B)
Torque, dNm
Time, min
TBPD-1_1
TBPD-1_2
TBPD-1_3
TBPD-1_4
TBPD-1_5
TBPD-1_6
TBPD-1_7
TBPD-1_8
TBPD-1_9


(C)
Torque, dNm
Time, min
TBBS-2_1
TBBS-2_2
TBBS-2_3
TBBS-2_4
TBBS-2_5
TBBS-2_6
TBBS-2_7
TBBS-2_8
TBBS-2_9

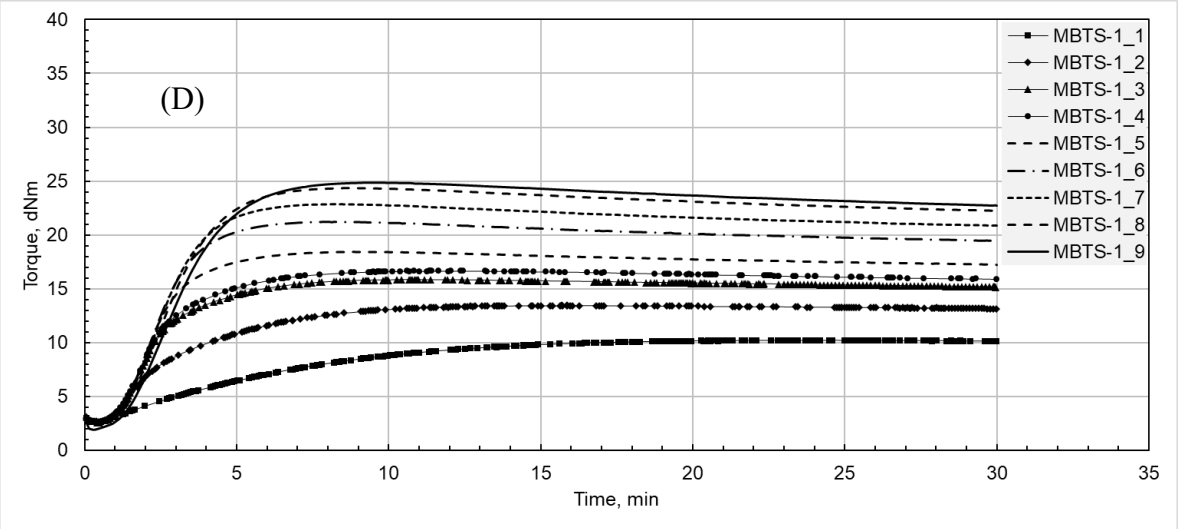


Figure 19 Vulcanization curves from the first round of experiments: (A) – TBBS-1, (B) – TBPD-1, (C) – TBBS-2, (D) – MBTS-1

Table 15 Vulcanization characteristics from the first round of experiments

Composition	M_L, dNm	M_H, dNm	t_{90}, min	t_{s1}, min	**Composition**	M_L, dNm	M_H, dNm	t_{90}, min	t_{s1}, min
TBBS-1_1	2.12	9.58	11.12	2.24	**TBBS-2_1**	2.22	11.04	10.65	1.82
TBBS-1_2	2.12	16.97	6.33	2.24	**TBBS-2_2**	2.51	17.87	6.48	2.03
TBBS-1_3	2.05	20.61	5.61	2.28	**TBBS-2_3**	2.47	21.64	5.58	2.09
TBBS-1_4	2.05	21.39	5.31	2.21	**TBBS-2_4**	2.39	22.25	5.55	2.06
TBBS-1_5	2.02	23.79	5.36	2.19	**TBBS-2_5**	1.93	23.82	5.60	1.74
TBBS-1_6	1.95	25.85	5.84	2.25	**TBBS-2_6**	2.34	27.28	6.11	1.99
TBBS-1_7	1.86	28.18	6.36	2.17	**TBBS-2_7**	2.17	28.70	6.41	1.99
TBBS-1_8	1.81	29.89	7.07	2.13	**TBBS-2_8**	2.12	30.74	7.15	1.92
TBBS-1_9	1.77	31.38	8.13	2.08	**TBBS-2_9**	2.05	31.68	7.73	1.87
TBPD-1_1	2.53	11.80	9.42	1.73	**MBTS-1_1**	2.62	10.22	12.69	1.50
TBPD-1_2	2.64	17.62	5.89	1.94	**MBTS-1_2**	2.64	13.45	7.47	1.15
TBPD-1_3	2.59	21.11	4.85	1.91	**MBTS-1_3**	2.58	15.84	5.14	1.08
TBPD-1_4	2.47	21.17	4.51	1.78	**MBTS-1_4**	2.61	16.69	5.22	1.06
TBPD-1_5	2.42	23.61	4.57	1.80	**MBTS-1_5**	2.59	18.43	4.28	1.05
TBPD-1_6	2.52	14.11	4.57	1.84	**MBTS-1_6**	2.48	21.22	4.21	1.04
TBPD-1_7	2.25	28.11	5.27	1.68	**MBTS-1_7**	2.40	22.85	4.41	1.07
TBPD-1_8	2.22	29.43	6.08	1.70	**MBTS-1_8**	2.33	24.36	4.86	1.07
TBPD-1_9	1.83	30.07	6.53	1.60	**MBTS-1_9**	1.92	24.85	5.29	1.12

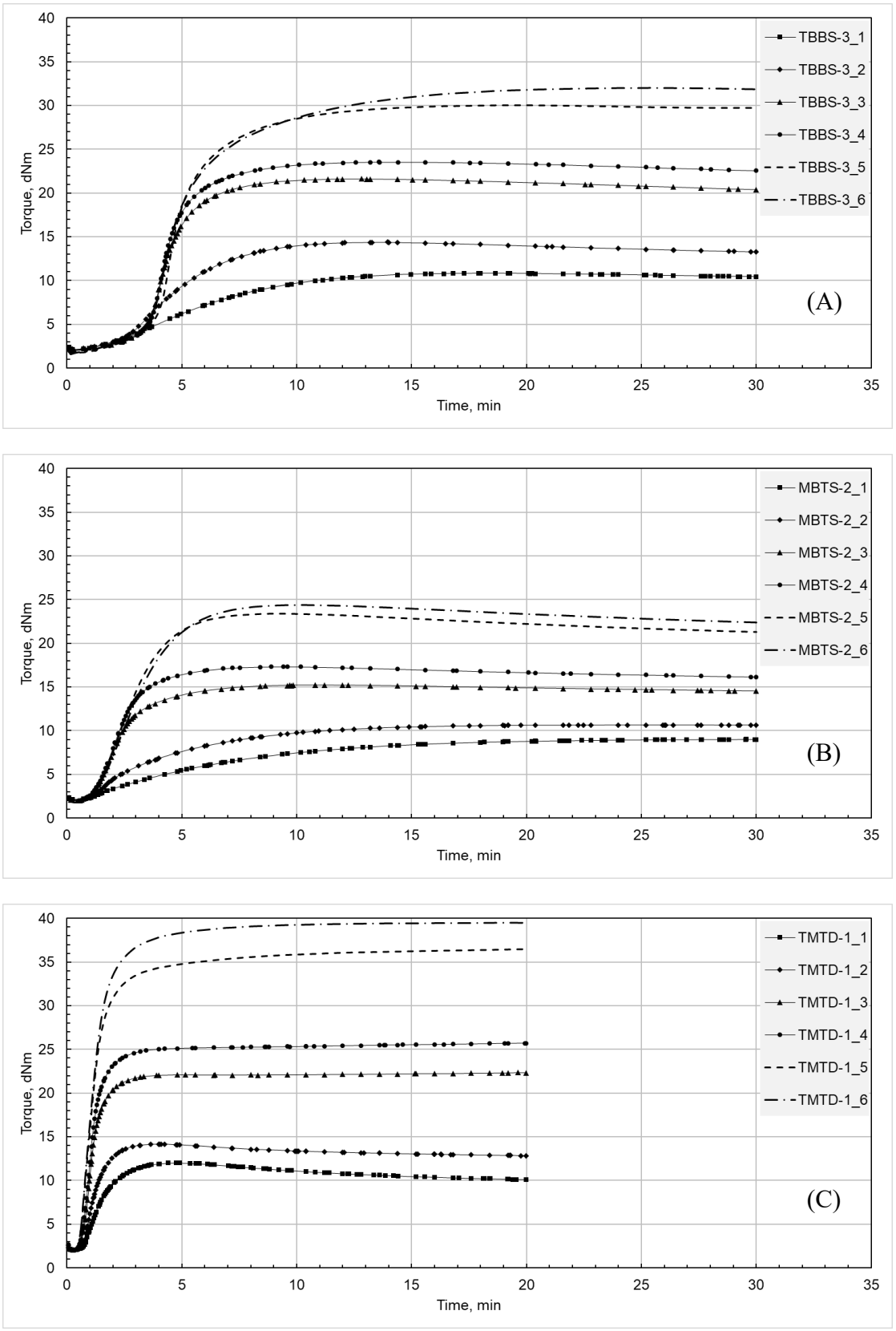


Figure 20 Vulcanization curves from the second round of experiments: (A) – TBBS-3, (B) – MBTS-2, (C) – TMTD-1

Table 16 Vulcanization characteristics from the second round of experiments

Composition	M_L, dNm	M_H, dNm	t_{90}, min	t_{s1}, min
TBBS-3_1	2.12	10.83	10.79	2.23
TBBS-3_2	2.13	14.38	8.14	2.12
TBBS-3_3	2.03	21.62	6.41	2.39
TBBS-3_4	1.95	23.50	6.62	2.41
TBBS-3_5	1.70	30.03	8.23	2.12
TBBS-3_6	1.57	32.04	10.51	1.76
MBTS-2_1	2.11	9.01	14.45	1.74
MBTS-2_2	2.10	10.66	10.28	1.42
MBTS-2_3	1.99	15.21	4.75	1.14
MBTS-2_4	1.94	17.32	4.19	1.13
MBTS-2_5	1.83	23.43	4.90	1.12
MBTS-2_6	1.76	24.39	5.46	1.13
TMTD-1_1	2.09	12.01	2.74	0.83
TMTD-1_2	2.06	14.16	2.12	0.79
TMTD-1_3	2.10	22.34	1.98	0.63
TMTD-1_4	2.03	25.72	2.07	0.59
TMTD-1_5	2.01	36.45	2.70	0.53
TMTD-1_6	1.92	39.51	2.58	0.52

At first, it is important to note that the graphs of compositions containing TBBS as well as MBTS accelerators look alike at the same concentrations among themselves respectively through two rounds of measurements, which indicates a good reproducibility of the experiment. It is highly probable that with an increase of the accelerator's concentration, the torque rises with M_H values accordingly, since the number of crosslinks increases, hence the rubber compound becomes stiffer. An exception is visible with the sample TBPD-1_6, which is definitely off the normal range in the concentration increase and could be caused by an unknown error since the plateau was reached quite quickly. In some cases during the first round of experiments, certain curves, particularly those of the highest concentration samples, show slight over-vulcanization behavior toward the end. It is visible, in particular, in TBBS-1_9, TBPD-1_9, and TBBS-2_9. However, at the second-round measurements, the highest

concentration curves rise less, with a small exception in TMTD-1_5; most probably due to the different homogeneity, since the mixing was done on different equipment. Some of the curves also show a slight reversion, for example, TBBS-1_2, TBPD-1_2, TBBS-2_2, MBTS-1_8, MBTS-1_9, MBTS-2_5, and MBTS-2_6. Due to the faster vulcanization, measurements of TMTD samples' characteristics were shortened to 20 min.

From the presented tables, a trend of minimum torque M_L in all compositions either straightly decreases or passes through a maximum together with the increase in accelerator's concentrations. This could happen due to a possible decrease in the viscosity of the mixtures caused by the mobility of chains. In comparison, the maximum torque M_H increases in all compositions, due to the higher crosslinking degree, except the mentioned TBPD-1_6. The passage through a minimum is also observed in all compositions in the t_{90} value – time of 90% of cure. It is an indicator that with the increase of concentration in the compositions, the vulcanization time shortens and the cure undergoes quicker first, although this time increases again, which could be the reason of reduced chain mobility and steric hindrance with an excess of accelerator. There is no particular trend observed in the scorch time values among concentrations, although they are still equally important for a compounder to understand where a processing safety window is, before scorching takes place.

An easier overview shows Table 17, which groups the vulcanization characteristics by average values. In the second round, it is clear now that scorch time decreases with the faster accelerator. Composition TBPD-1 with an antiozonant 6PPD from the first round plays the same role with t_{s1} compared with TBBS-1 and TBBS-2, tending to decrease t_{90} as well. In general, t_{90} falls with the faster accelerator, while M_L rises slightly. M_H values are clearly the lowest for MBTS samples in both rounds. The times correspond with the literature [23].

Table 17 The average values of vulcanization characteristics among compositions

Composition	$\boldsymbol{M_L}$, dNm	$\boldsymbol{M_H}$, dNm	$\boldsymbol{t_{90}}$, min	$\boldsymbol{t_{s1}}$, min
TBBS-1	1.97	23.07	6.79	2.20
TBPD-1	2.39	21.89	5.74	1.78
TBBS-2	2.24	23.89	6.81	1.95
MBTS-1	2.46	18.66	5.95	1.13
TBBS-3	1.92	22.07	8.45	2.17
MBTS-2	1.96	16.67	7.34	1.28
TMTD-1	2.04	25.03	2.37	0.65

9 PREPARATION OF TEST SAMPLES

Test plates were prepared from the compounds using a compression molding method, from which test samples were cut out utilizing a puncher. These samples were then tested in an ozone chamber. Additionally, other sets of samples were cut from the pressed plates and used for both tensile strength and hardness testing. All compounds were pre-heated on an open mill Farrel G-2603, 150×330 mm (Spain) before compressing, with the rolls heated to 60 °C. The rubber compound sheets were rolled to a thickness of approximately 3 mm, with the front roll rotating at 12 rpm and the rear roll at 15 rpm.

9.1 Pressing the sample plates

Pressing was carried out on a press model P–11E from Blanické strojírny (Czech Republic) at a temperature of 160 °C, corresponding to the temperature of measured vulcanization characteristics. The applied pressure after sample degassing was around 250 bar. Vulcanization times correspond to those measured on a rheometer without any change, since the thickness of the plates did not require it.

Rubber plates with dimensions of 150×150×2 mm were molded from the prepared rubber compounds. The mold consisted of three parts – two metal plates as an outer surface and a square-shaped cavity, where the rubber compound was put. After closing the mold, it was slid inside the compressing unit and pressed. It was desirable to obtain an effect called "overflow", where a small extent of rubber was coming out of the square-shaped part. In this regard, it was ensured that sample plates maintain the same thickness, eliminating further error factors. The weight for all plates was calculated by taking into account the approximate density of the compounds (1.2 g/cm^3), multiplied by the volume of the plate (45 cm^3). Hence, the amount of approximately 48 g was cut from a compound in the form of stripes and weighed. Figure 21 shows a compressing machine with an open mold at the front.

9.2 Punching the samples for experiments

From the already prepared plates, samples for the ozone experiment were punched at a manual hydraulic press from Polymertest (Czech Republic), presented in Figure 22. It was done using a punching knife with dimensions 125×13 mm, as shown in Figure 23. These ozonated samples were consequently used for comparison with non-ozonated ones later. For hardness and tensile strength testing, a hydraulic punching machine ZPS 06102 P1 (Czech Republic) with the same cutting knife was used, as shown in Figure 24.



Figure 21 A compressing machine P–11E from Blanické strojírny

(source: own elaboration)



Figure 22 A manual hydraulic press from Polymertest

(source: own elaboration)

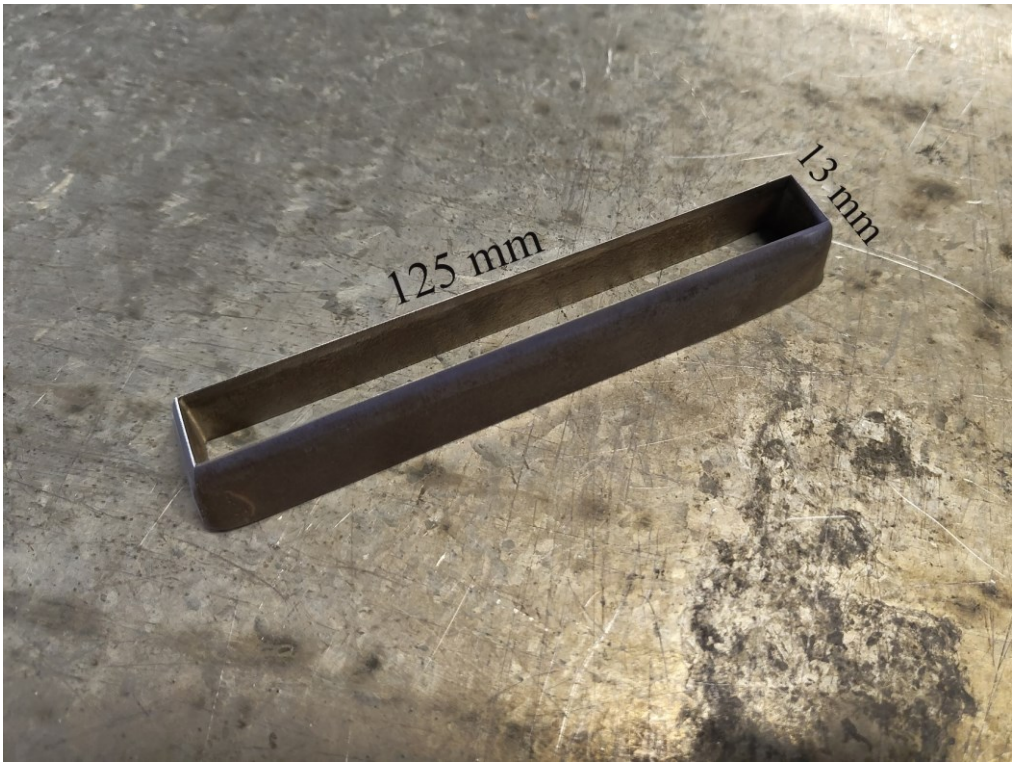


Figure 23 A punching knife

(source: own elaboration)



Figure 24 A hydraulic punching machine ZPS 06102 P1

(source: own elaboration)

10 OZONE TESTING

The prepared samples were fixed in special holders and stretched by 20 %, with the length from 100 mm to 120 mm in order to expose and increase the surface under static strain, otherwise, the effect of ozone would be less powerful. These holders, shown in Figure 25 (left) as an example with a fixated rubber sample, were placed inside the ozone chamber vertically, ensuring the samples did not touch each other, allowing free access for ozone exposure. The name of the ozone cabinet is Ozone Check - UV by Gibitre Instruments S.r.l. (Italy), shown in Figure 25 (right). Once the test had begun, ozone started to flow into the sealed chamber, and the holders began to rotate to ensure an even ozone circulation from the bottom of the unit. The ozone chamber used UV light to produce ozone.

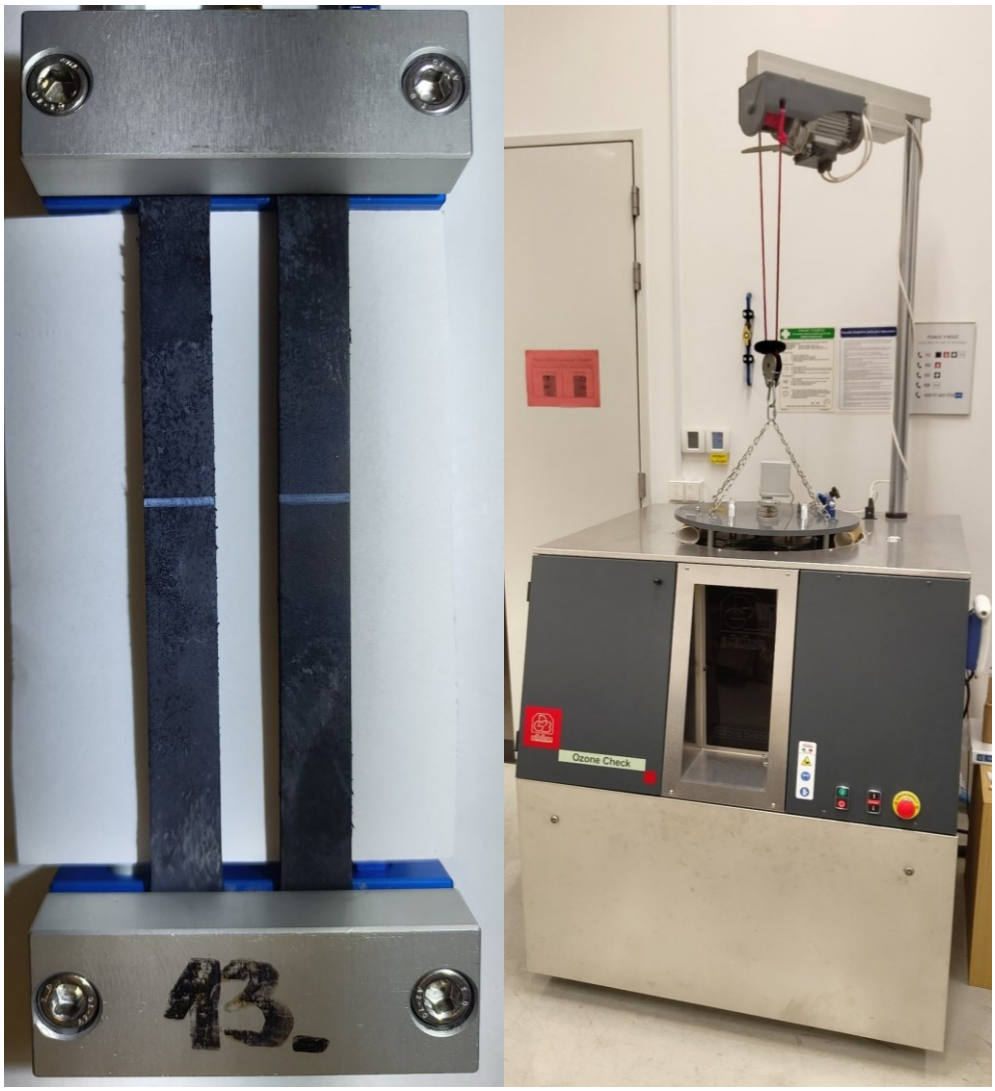


Figure 25 A rubber holder with a fixated rubber sample (left) and an ozone cabinet Ozone Check - UV by Gibitre Instruments S.r.l. (right)

(source: own elaboration)

Figure 26 shows a representative graph of the tests with the conditions that were kept the same through all experiments. The temperature was consistently set to 40 °C, with 50 % humidity and an ozone concentration of 50 pphm in both experimental rounds. In the first round, the test was paused at 3, 6, 12, 24, 48, 72, and terminated completely at 96 h. In the second round, the times were adjusted to 2, 4, 6, 8, 12, 24, 48, 72, and terminated at 96 h to observe changes with greater precision at the beginning. At each of these time points, the ozone circulation was paused, the holders with samples were removed from the chamber, and photos were taken using a digital microscope model DVM2500 from Leica Microsystems GmbH (Germany), shown in Figure 27, to document any changes on the surface of the samples. After the photos were taken, the samples were returned to the chamber, and the experiment continued until the next time point. It is important to mention that samples were not released from the holders until the experiment was complete at the end. The samples from the second round were used for further tensile strength testing.

The second round of experiments was performed additionally with the aim to make photo shooting with better precision through time points, registering the one representative area on the sample, which had been chosen randomly before the experiment (0 h) started, marked with a white color, hence the developing of the crack area would be accurate to follow. Due to a large size area, it was impossible to capture the whole sample in one photo.

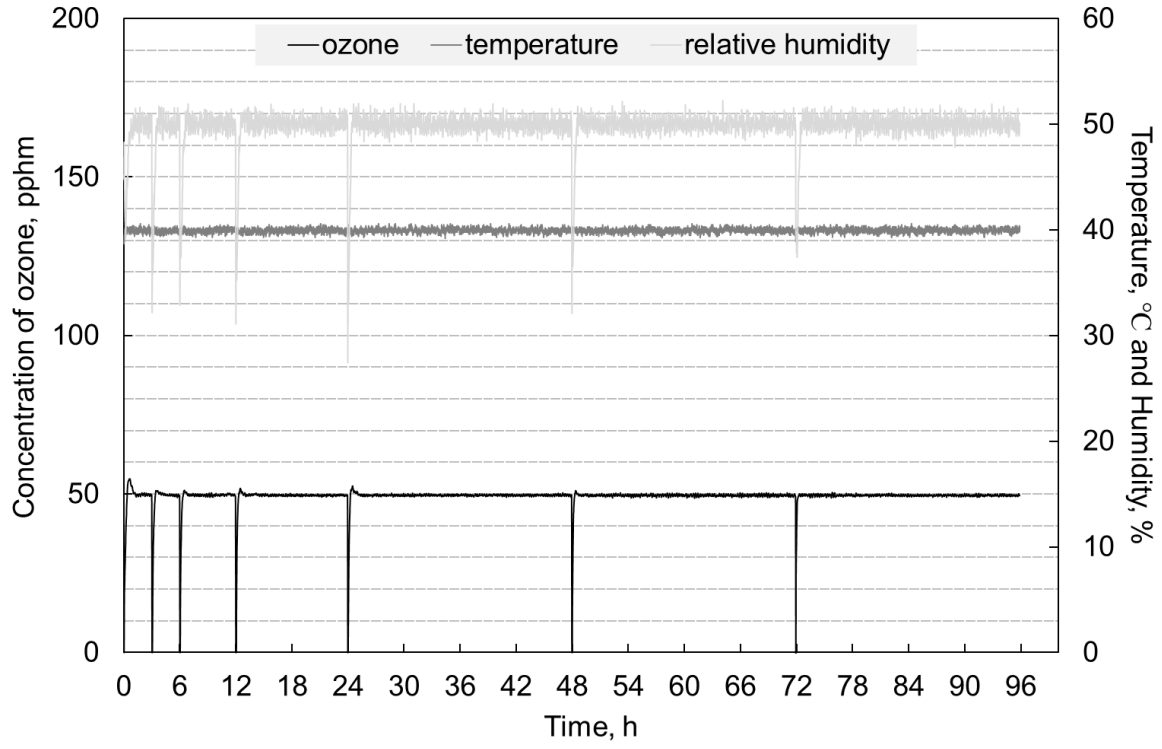


Figure 26 A representative graph of the tests on the example of TBBS-2

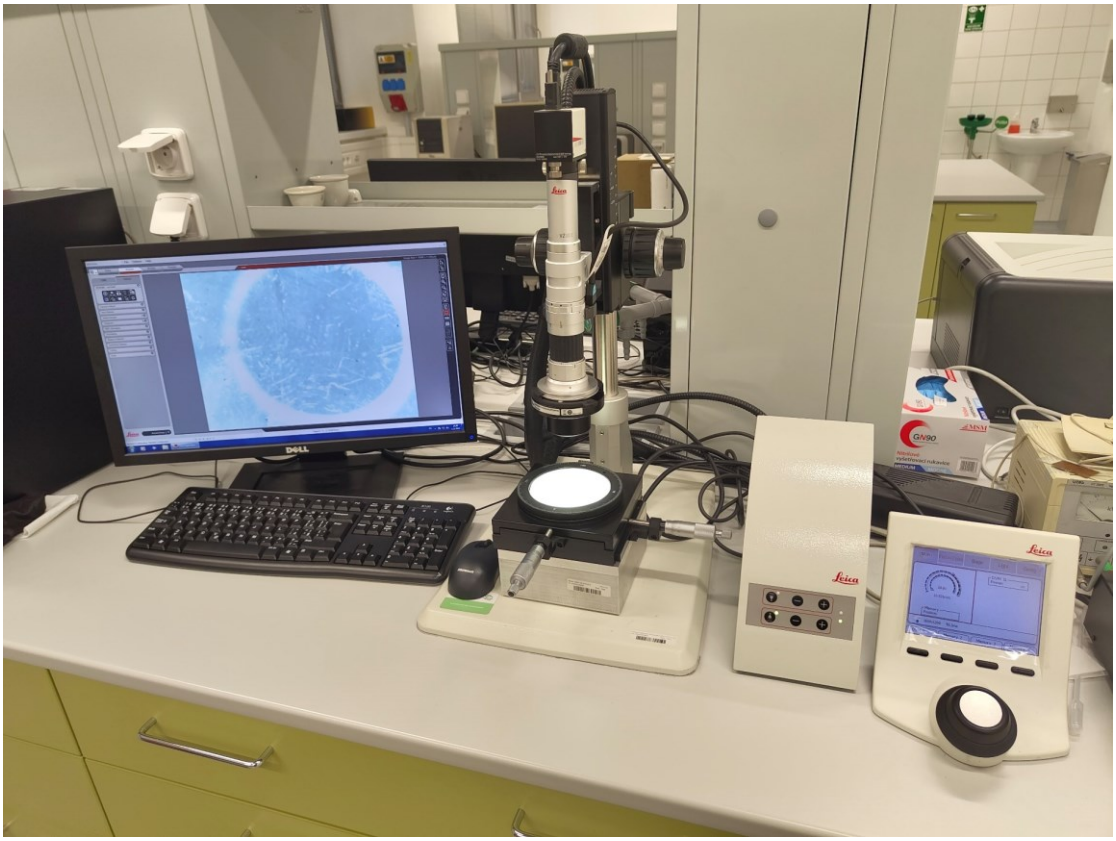


Figure 27 A digital microscope model DVM2500 from Leica Microsystems GmbH

(source: own elaboration)

Each holder carried two samples at the time of one experiment. Besides, a few samples have undergone the experiment twice in order to catch an area, which contains the most trustworthy development, with a reference to the repetition of samples containing TBBS accelerator. Sometimes, the majority of cracks could appear just in one place, which could happen due to localized stress, surface imperfection, impurities, ununiform dispersion, or migration of ingredients. However, only one sample of each concentration of a composition is shown in this work, due to the bulkiness of the space. Outcome photos of the first round are presented in Appendix 2, and the second round in Appendix 3.

To evaluate the development of cracks' formation, a Matlab program was used with an own-designed application. The task of it was to evaluate the total surface area of cracks, which appears and grows or closes over time on every sample. It worked on the basis of a grayscale representation of the sample, ranging from 0 (black) to 255 (white). The threshold was a subject of change, introducing a human error of the executer. In addition, it was sometimes complicated to highlight just the new surface and not the impurities of the sample due to the similarities in grey tones, hence a threshold had to be adjusted.

An example of a fair good highlighting is presented in Figure 28 below. Every photo was cropped identically as follows: 1.3 mm on the left side, 1.3 mm on the right side, 0.1 mm from the top, and 0.1 mm from the bottom. It was done due to the program peculiarity that highlighted the borders as cracks. After that a threshold was applied and the program calculated the highlighting area. The created graphs with a visible representation of the crack growth are presented in Figure 29 for TBBS-3, in Figure 30 for MBTS-2 and in Figure 31 for TMTD-1.They are based on the obtained results from Matlab software and are presented in Table 18 for TBBS-3, in Table 19 for MBTS-2 and in Table 20 for TMTD-1.

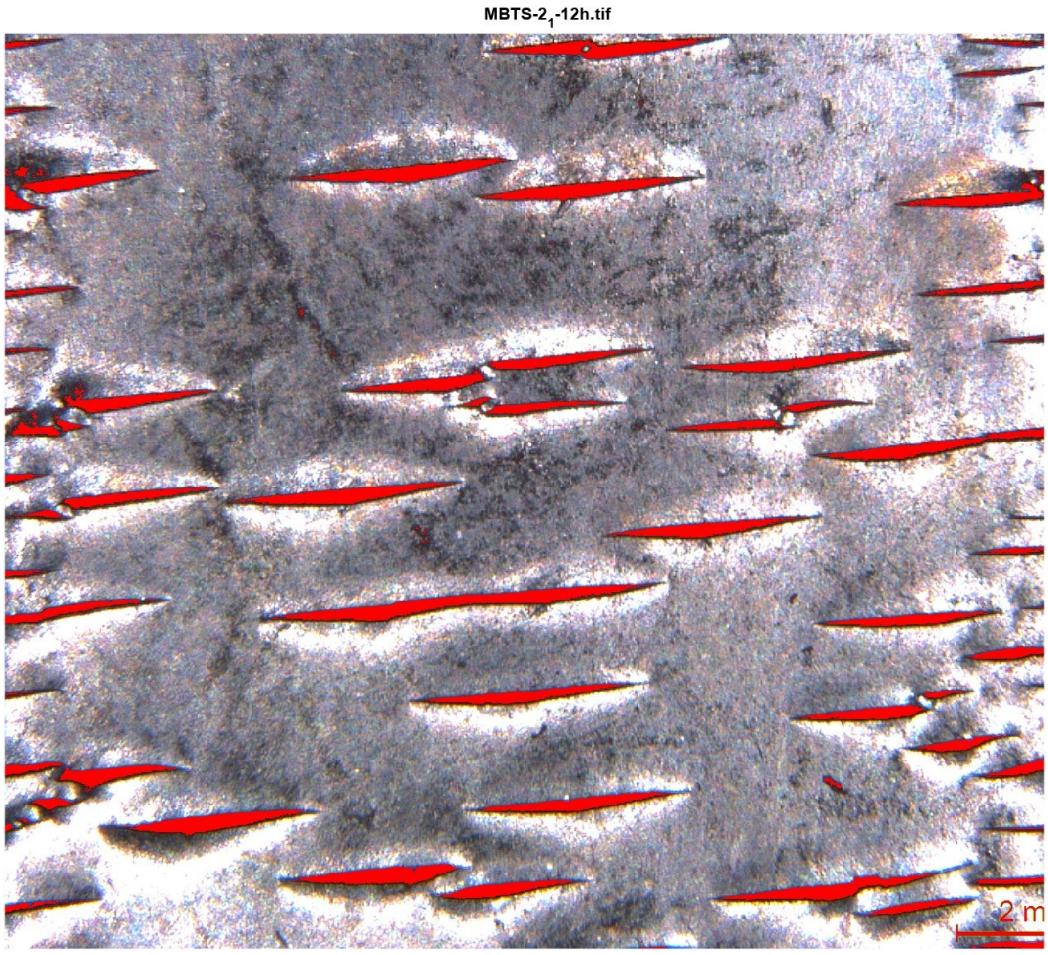


Figure 28 An example of highlighting the cracks in Matlab software

The first round of experiments was left without evaluation due to the inability to see an accurate trend of cracks development; the photos were taken not of the same area, affecting the final results. Therefore, ozonated samples from the first round are presented as a reference. Nevertheless, the visual evaluation of the photos from the first round is presented below, since they still contain valuable information about crack growth.

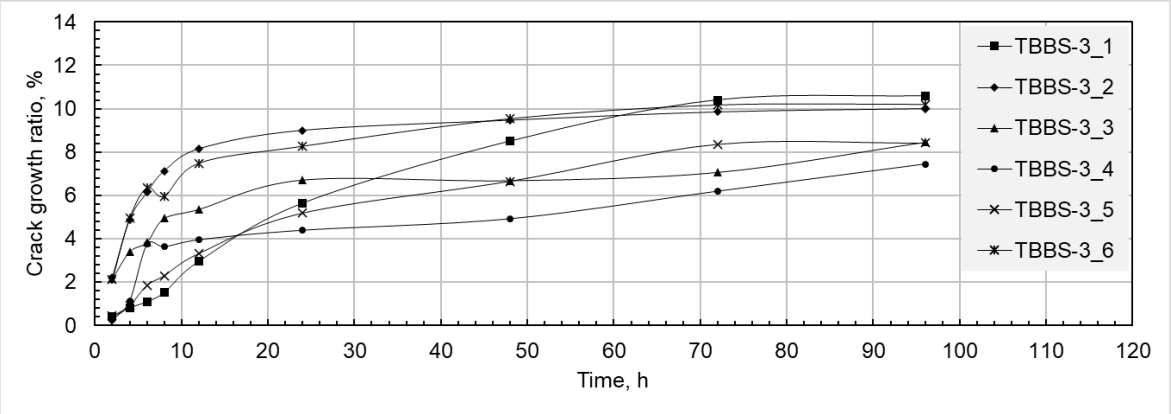


Figure 29 A visual representation of crack growth in TBBS-3

Table 18 Evaluation of surface area of TBBS-3 composition in "%"

Time	TBBS-3_1	TBBS-3_2	TBBS-3_3	TBBS-3_4	TBBS-3_5	TBBS-3_6
2 h	0.39	2.22	2.15	0.23	0.43	2.12
4 h	0.81	4.89	3.40	1.14	0.92	4.95
6 h	1.10	6.14	3.85	3.74	1.85	6.37
8 h	1.52	7.13	4.95	3.63	2.30	5.97
12 h	2.96	8.15	5.36	3.95	3.32	7.49
24 h	5.64	9.00	6.72	4.39	5.18	8.27
48 h	8.50	9.47	6.69	4.92	6.65	9.54
72 h	10.40	9.85	7.07	6.19	8.35	10.17
96 h	10.59	10.00	8.46	7.44	8.41	10.20

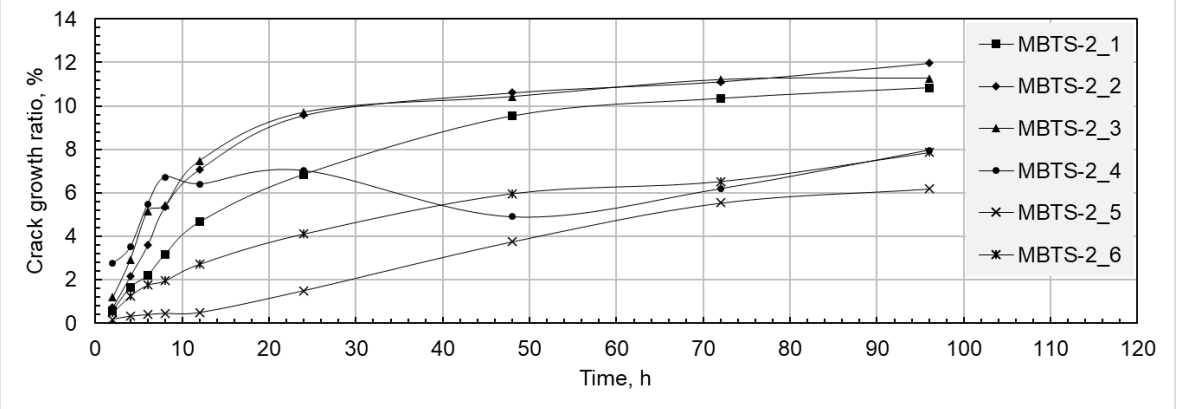


Figure 30 A visual representation of crack growth in MBTS-2

Table 19 Evaluation of surface area of MBTS-2 composition in "%"

Time	MBTS-2_1	MBTS-2_2	MBTS-2_3	MBTS-2_4	MBTS-2_5	MBTS-2_6
2 h	0.58	0.72	1.20	2.76	0.18	0.47
4 h	1.65	2.15	2.93	3.53	0.32	1.25
6 h	2.20	3.58	5.16	5.48	0.39	1.75
8 h	3.17	5.35	5.44	6.73	0.45	1.95
12 h	4.66	7.08	7.49	6.41	0.49	2.72
24 h	6.85	9.57	9.71	7.02	1.50	4.11
48 h	9.54	10.61	10.43	4.90	3.75	5.97
72 h	10.35	11.12	11.21	6.19	5.54	6.53
96 h	10.84	11.97	11.28	7.95	6.19	7.86

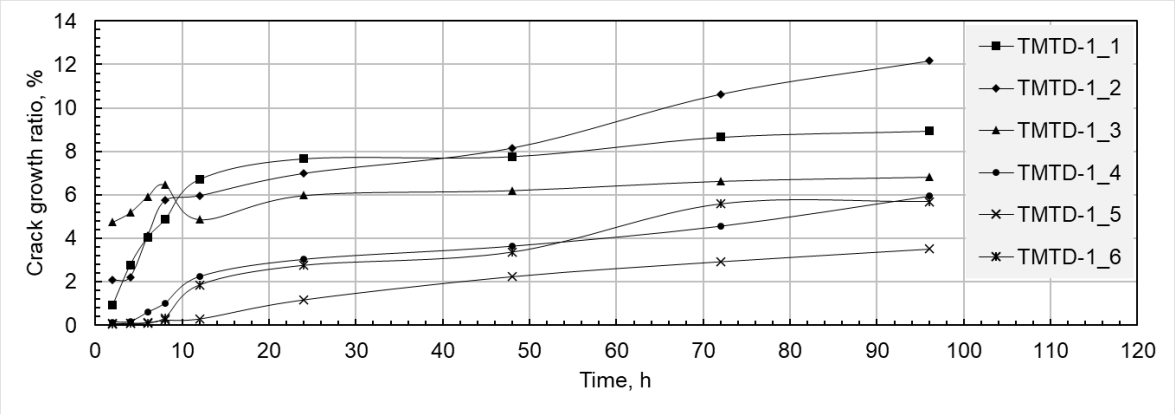


Figure 31 A visual representation of crack growth in TMTD-1

Starting with a visual representation, the results from both rounds shall be divided at first for evaluation, since the conditions of taking the photos differ as well as time points and concentrations, making it difficult to compare. It has to be kept in mind that the photos from the first round were taken horizontally, while the second round was taken vertically, explaining the directions of crack growth. Another critical point is the scale of the taken photos. Photos from the first round were taken at 1 mm, while the second round with 2 mm in order to show a larger area for photo shooting, capturing more information. The color of the different samples should not be taken into account. The one true identical feature that happens throughout both rounds is the development of cracks under the influence of ozone.

Table 20 Evaluation of surface area of TMTD-1 composition in "%"

Time	TMTD-1_1	TMTD-1_2	TMTD-1_3	TMTD-1_4	TMTD-1_5	TMTD-1_6
2 h	0.94	2.07	4.75	0.14	0.07	0.06
4 h	2.78	2.22	5.19	0.17	0.08	0.07
6 h	4.05	4.11	5.93	0.59	0.11	0.10
8 h	4.86	5.75	6.46	1.01	0.23	0.34
12 h	6.72	5.97	4.87	2.24	0.29	1.85
24 h	7.66	6.99	5.98	3.03	1.17	2.75
48 h	7.76	8.16	6.21	3.64	2.24	3.36
72 h	8.65	10.64	6.64	4.56	2.93	5.58
96 h	8.93	12.17	6.83	5.94	3.51	5.69

To begin with, TBBS-1 and TBBS-2 compositions look almost identical, indicating good reproducibility with similar results. The first sample with a 0.1 CV ratio shows the development of big cracks with blisters over time starting from 3 h. With an increase of accelerator content TBBS, the rubber is able to withstand ozone influence longer every time, starting from 0.3 CV concentration. However, tiny cracks appear from this concentration starting at 3 h, which can grow to some small degree over time. This effect is also called "crazing" [39]. In fact, the trendline passes through a minimum, and at 1.5 SEV the crazing is almost invisible. The big cracks start to appear again at the concentration 2.0 SEV and higher. It seems the amount of TBBS affects the small crack size appearance only in this range, while effective systems 2.5 EV and 3.0 EV turn to develop middle-sized cracks.

MBTS-1 composition shows a different behavior. At the lowest concentration of 0.1 CV, it degrades with blisters, starting approximately at the same time as TBBS-1 and TBBS-2 compositions – 24 h, although no cracks are visible. From the 0.3 CV concentration, MBTS starts to develop visible medium-range cracks at 3 h that somewhat grow over time. The next 0.6 CV concentration shows a crazing effect, turning the cracks into smaller and well-distributed all over the sample area, visible at 3 h, which grow again over time. This behavior continues until 1.5 SEV concentration, where bigger cracks start to appear again at the last hours of the experiment and this trend lasts until the highest and the last 3.0 EV system.

In contrast, TBPD-1 shares similarities with pure TBBS compositions. The difference can be seen in 1.5 SEV concentration, where big cracks appear over time starting with small

ones at 3 h, while TBBS compositions remain almost untouched, having a faint crazing on the surface. At this time point, TBPD-1 mostly reflects MBTS-1. With a higher concentration at 2.0 SEV, even bigger cracks appear, but with the following efficient systems 2.5 EV and 3.0 EV, TBPD-1 behaves similarly to TBBS compositions.

To summarize, it was found that there are no certain trends that could help to predict the behavior of cracks' development at a certain time at a particular concentration of an accelerator. At the same time, TBBS-1 and TBBS-2 show similar results, indicating a good reproducibility of the experiment. Between TBBS compositions, it has been found that the clearest samples dispose with the concentration from 0.3 CV to 1.5 SEV, while the biggest cracks with blisters appear at the very beginning at 0.1 CV. TBPD-1 shows similar behavior and the evidence of antiozonant does not play almost any role until 1.5 SEV, where the cracking becomes worse compared to TBBS compositions. At this point, it was agreed to exclude a composition containing 6PPD from the second round. MBTS-1 composition does not show cracks at the very beginning, but blisters. However, the best results are presented from 0.6 CV until 1.0 SEV, the last being the clearest one.

In the second round, adjusting the time with a focus to the beginning uncovers an obvious fact that the cracks, most probably, start to appear almost immediately after the beginning of ozone aging. Throughout all concentrations, the blisters do not appear anymore, which could be evidence of better compounding and processability of the second round. All three compositions develop cracks over time but to a different extent.

At the starting concentration of 0.1 CV, the fastest accelerator TMTD develops the highest number of cracks, MBTS moderate, and TBBS the lowest, while the size of the cracks has an opposite trend. With the increase just by doubling the accelerator amount, in 0.2 CV system, TBBS-3 develops small cracks that grow over time, while TMTD-1 has a crazing effect and MBTS-2 remains almost the same as in the previous concentration. At 0.7 SEV concentration, TBBS-3 turns into crazing the same as TMTD-1, showing similar behavior, while MBTS-2 starts to develop a higher number of a bit smaller cracks. The following 1 SEV concentration MBTS-2 turns into crazing, while TBBS-3 remains almost the same, and TMTD-1 actually remains almost clear for up to 24 h. 2.5 SEV concentration shows similar results for TMTD-1, while on TBBS-3 and MBTS-2 start to appear small cracks that grow over time, the last preserving clearness until 6 h. The last 3 EV concentration affects TBBS-3 in a similar way, but with a higher number of tiny cracks that turn into crazing afterwards, while MBTS-2 develops medium cracking over time, and

TMTD-1 shows crazing at 12 h. Unfortunately, no evidence of a certain trend is observed in this round either. The clearest samples can be observed at 1 SEV – TMTD-1_4 up to 24 h and at 2.5 EV – MBTS-2_5 up to 6 h and TMTD-1_5 up to 12 h.

After the comparison TBBS and MBTS compositions through the first and second rounds, the following can be concluded. Conventional and semi-effective systems show mostly similar results among TBBS and MBTS samples respectively, with large cracks appearing at the lowest concentration and following crazing until 1 SEV. Efficient system 2.5 EV differs somewhat between MBTS-1 and MBTS-2, where MBTS-1 starts to appear small cracks at 3 h that grow over time, while MBTS-2 remains almost clear until 6 h with growing big cracks afterwards. The last 3.0 EV differs as well, TBBS-3 shows tiny cracks that turn into crazing afterwards, while TBBS-1 and TBBS-2 develop just big cracks. MBTS-1 and MBTS-2 show similar behavior at this concentration. To summarize, most of the samples show similar behavior among their compositions with particular accelerators respectively, although it is not possible to definitely predict the behavior at specific concentrations. However, it can be also summarized that most of the samples develop in a matter they show at the beginning of the experiment, whether these are small to moderate/big cracks, number of them, or crazing effect, growing with the longer ozone exposure.

The visual evaluation second round, can be compared with presented graphs and tables. A so-called “crack growth ratio” measured in “%” shows the calculated highlighted area depending on the total area of the photo. Keeping in mind that these values are not so accurate, measured with an executor error, hence they mostly show a trend of crack growth. In this regard, the crack growth ratio (CGR) plays only an informative role to build a trend.

All in all, it is complicated to predict the behavior of a particular concentration at a particular time point. The highest CGR at the end among TBBS-3 shows TBBS-3_1 with 0.1 CV and the lowest has TBBS-3_4 with 1 SEV. The highest CGR at the end among MBTS-2 shows MBTS-2_2 with 0.2 CV and the lowest has MBTS-2_5 with 2.5 EV. The highest CGR among all shows TMTD-1_2 of 0.2 CV and the lowest CGR shows TMTD-1_5 of 2.5 EV. The evaluated CGR by Matlab software mostly correspond to the visual data, which are further compared with the results from mechanical experiments.

In conclusion, the lowest CGR values, in most cases, are observed at the middle SEV systems. In general, the best performance for the samples containing TBBS accelerator are SEV systems, MBTS are mostly better in the middle-high SEV, while TMTD compositions show good results in both SEV and the best in EV systems.

11 PHYSICAL TESTING OF SAMPLES FROM THE SECOND ROUND OF THE EXPERIMENTS

This last section provides the last experiments that have been performed only for the second round of experiments – hardness testing and tensile strength tests, the latter evaluating tensile strength and elongation at break. The hardness test utilizes only non-ozonated samples since the ones that have underwent ozonation are too soft and could not show accurate values. Tensile strength, on the other hand, shows both ozonated and non-ozonated samples to compare the differences.

11.1 Hardness test

The hardness test of rubber compounds was performed based on the Shore A method and measured on Bareiss model BS 61 II (Canada) durometer, shown in Figure 32. The test condition was a standard laboratory temperature of 23 °C according to the Durometer Hardness Method, described in ISO 48-4. Every vulcanized non-ozonized sample was subjected to five measurements taken at different locations on one of the sample's surfaces. After 3 sec from the beginning of pressing the sample by indenter, the readings were registered and the median value was established, presented in Table 21. Figure 33 shows a comparable representation of the results.



Figure 32 A Bareiss model BS 61 II durometer

(source: own elaboration)

Table 21 Median results of the hardness test

A/S ratio	0.1 CV	0.2 CV	0.7 SEV	1 SEV	2.5 EV	3 EV
Composition \ Samples	1	2	3	4	5	6
TBBS-3	59.5	62.8	70.1	70.2	75.7	79.4
MBTS-2	58.6	61.4	64.7	67.4	74.1	75.2
TMTD-1	63.7	68.4	76.0	76.7	82.7	82.7

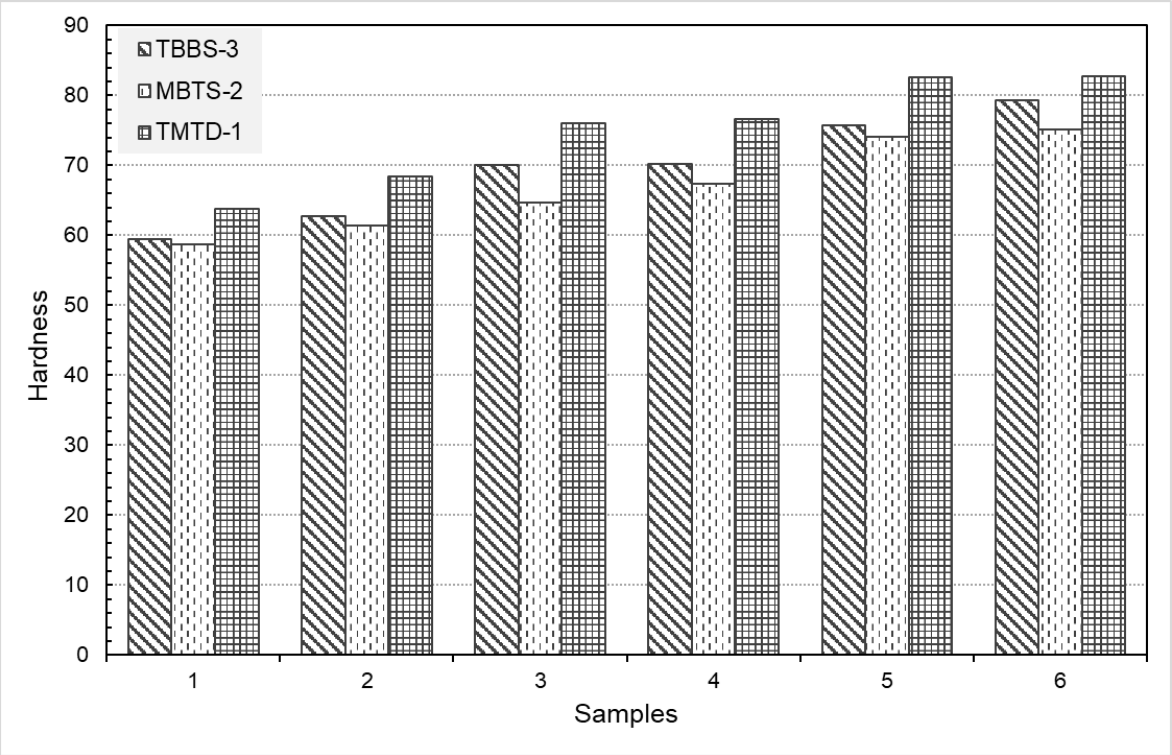


Figure 33 A representation of a hardness Shore A test for non-ozonized samples

As can be seen from the graph, a trend is visible for non-ozonated samples. The values of the indenter depth grow together with the increase of concentration in all compositions. It seems that TMTD-1 composition is the most resistant to indentation, while TBBS-3 is moderate and MBTS-2 is the least resistant. Other authors utilizing CBS, MBT, and TMTD accelerators, although with different composition formulations and only EV systems, came across the same trend, where the values for hardness test increase in the order: MBT, CBS, TMTD [52]. With the increase of accelerator's concentration, the stiffness and subsequent hardness rise as well, since the crosslinking density values become higher with the torque increase that has been confirmed in Vulcanization characteristics chapter [53].

11.2 Tensile strength

Tensile strength experiments were conducted for both ozonized and non-ozonized rubber samples in order to compare the differences and estimate the effect of ozone. The testing was done according to ISO 37 on a Tensometer T10D by Alpha Technologies (USA), shown in Figure 34. The gauge length or the distance between grips was set to 65 mm, and the strain rate was 500 mm/min. Tests were performed at a standard laboratory temperature of 23 °C. The number of strained non-ozonized samples of one accelerator and concentration was three, whereas the number of ozonized ones of the same accelerator and same concentration ranged from 2 to 4, due to the limitation of ozonized samples. Those that have been severely cracked or completely burst were unable to be fixated and strained on the extensometer. The results are presented in Table 22, which contains the following abbreviations: breaking stress (BS) measured in "MPa", elongation at break (EB), measured in "%", and standard deviation (SD) of the value. A number of the sample represents the column "#". To distinguish the samples of the same concentration whether it was ozonated, an "o" letter is inserted after the name of the accelerator. In addition, tables of modules, which measure the stress required to stretch a sample to a specific elongation are presented in Appendix 4.

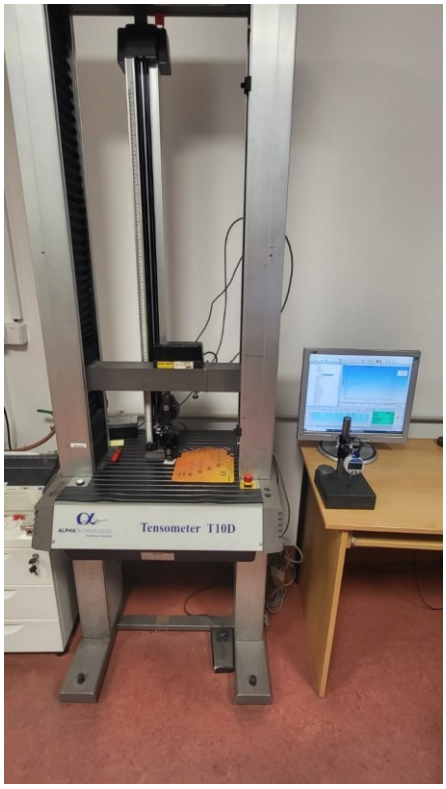


Figure 34 A tensometer T10D by Alpha Technologies

(source: own elaboration)

Table 22 Results obtained from the tensile strength test

#	BS TBBS-3	SD	BS TBBSo-3	SD	EB TBBS-3	SD	EB TBBSo-3	SD
1	5.90	1.50	0.83	0.50	315.95	45.58	121.48	59.06
2	9.22	0.24	2.46	0.56	410.91	5.50	232.69	45.94
3	13.58	1.38	6.24	0.94	416.26	34.03	282.98	24.84
4	14.36	2.99	8.49	0.34	427.75	78.17	323.80	6.06
5	9.39	3.04	4.07	0.21	213.70	62.45	112.10	0.74
6	9.66	0.24	4.79	0.04	191.15	8.56	114.15	1.23

#	BS MBTS-2	SD	BS MBTSo-2	SD	EB MBTS-2	SD	EB MBTSo-2	SD
1	5.56	0.98	0.45	0.24	339.11	54.51	120.31	12.55
2	7.27	0.09	0.72	0.05	394.24	2.59	138.44	4.03
3	12.94	0.50	4.79	0.94	524.89	12.51	356.42	44.14
4	13.84	0.53	5.62	0.14	521.18	18.00	369.60	7.34
5	17.56	0.57	4.56	0.16	502.75	20.11	222.02	9.09
6	16.48	0.20	2.70	0.16	460.00	4.50	144.02	10.91

#	BS TMTD-1	SD	BS TMTDo-1	SD	EB TMTD-1	SD	EB TMTDo-1	SD
1	13.00	0.38	2.75	0.23	484.93	11.49	234.42	15.44
2	13.79	0.22	5.21	0.67	476.32	7.76	325.83	28.84
3	13.26	1.29	8.26	0.30	323.68	30.25	271.18	14.79
4	12.53	0.27	7.26	0.40	268.88	5.03	194.26	19.00
5	6.78	0.13	4.52	0.10	103.59	4.37	70.15	21.82
6	7.30	0.63	4.59	0.29	94.02	10.69	61.28	3.26

The following Figure 35 and Figure 36 show the visual representation of the data between the ozonated and non-ozonated compositions containing one specific accelerator respectively. The following Figure 37 and Figure 38 show the visual representation of the data separately between ozonated and non-ozonated samples of different accelerators respectively.

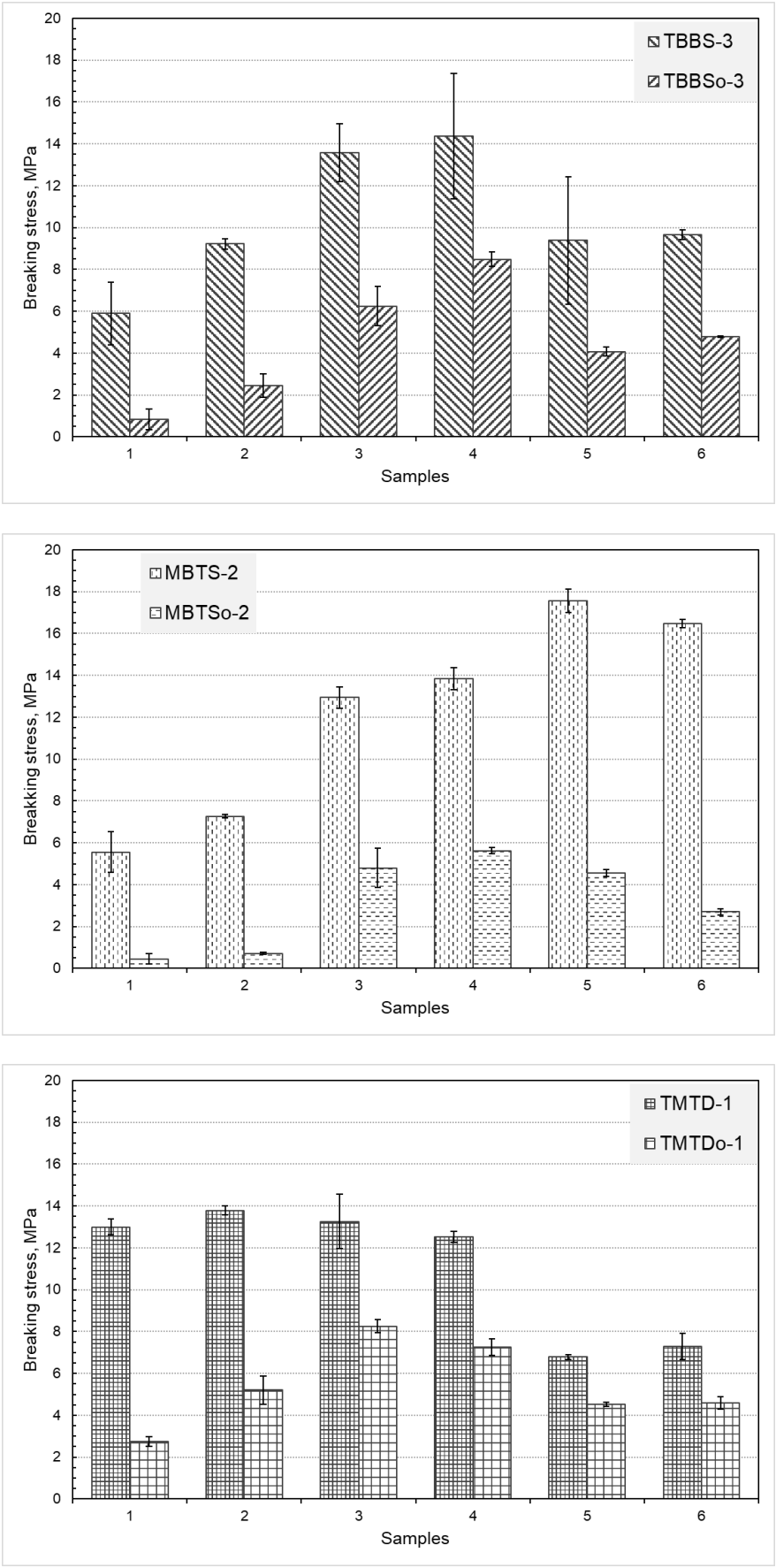


Figure 35 Breaking stress results between non-ozonated and ozonated samples

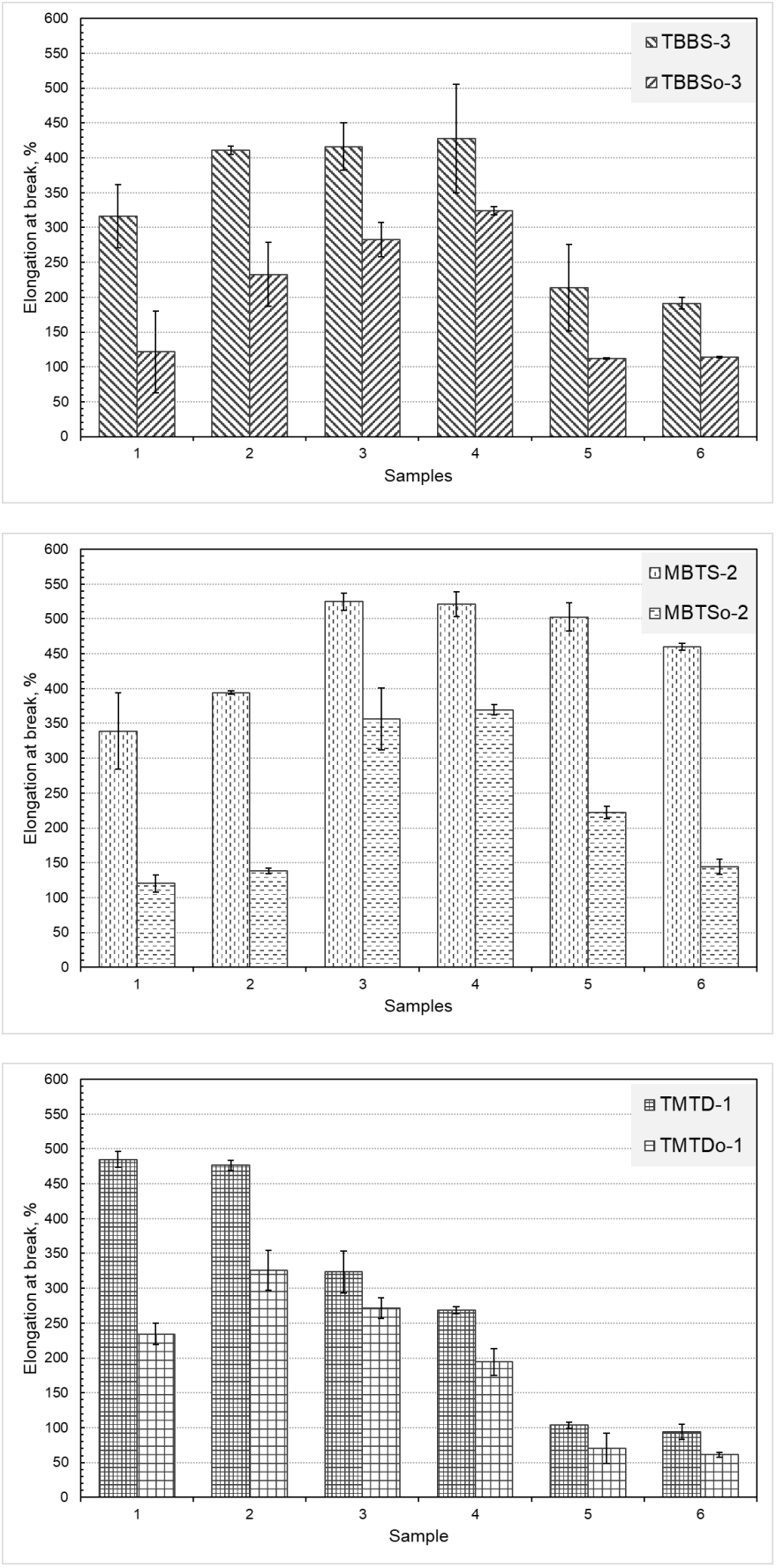


Figure 36 Elongation at break results between non-ozonated and ozonated samples

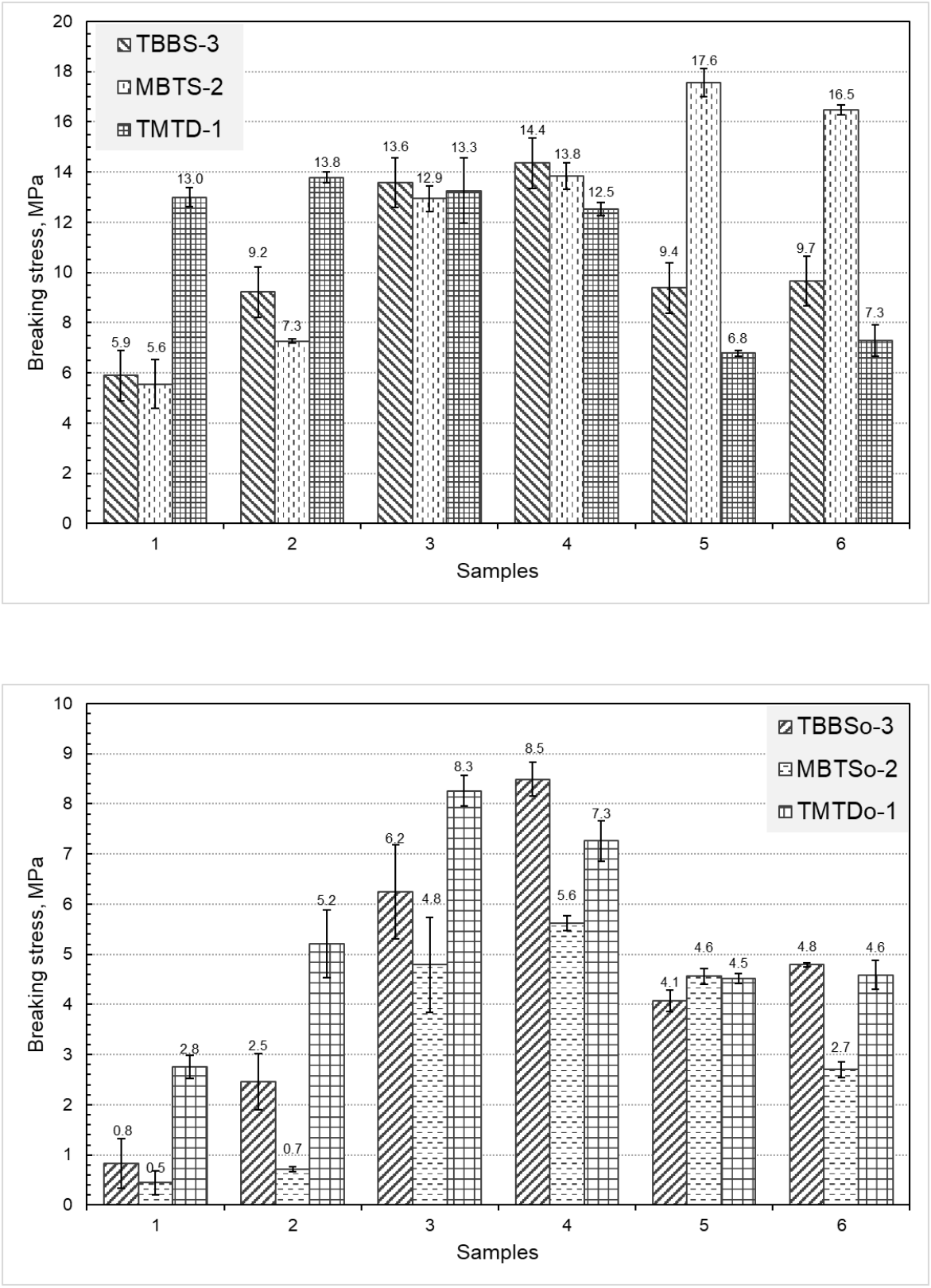
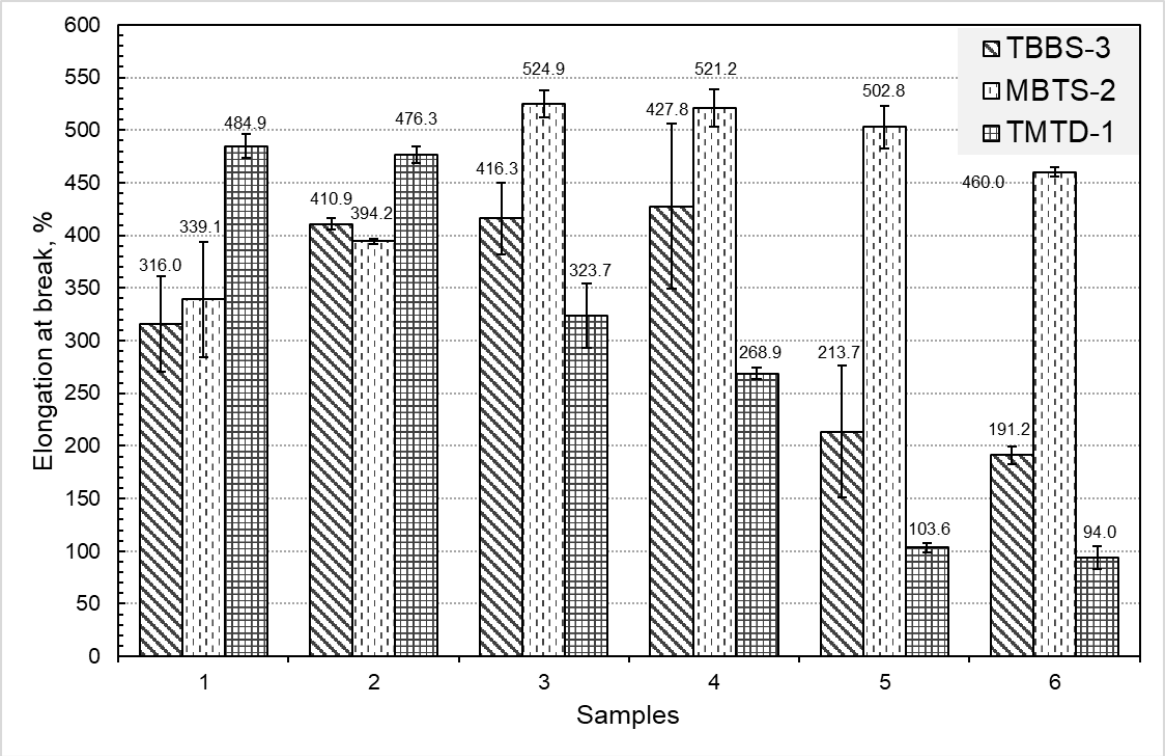


Figure 37 Breaking stress comparison between ozonated and non-ozonated samples respectively

The graphs of breaking stress at varying elongation modules between the compositions containing one accelerator are presented in Appendix 5.



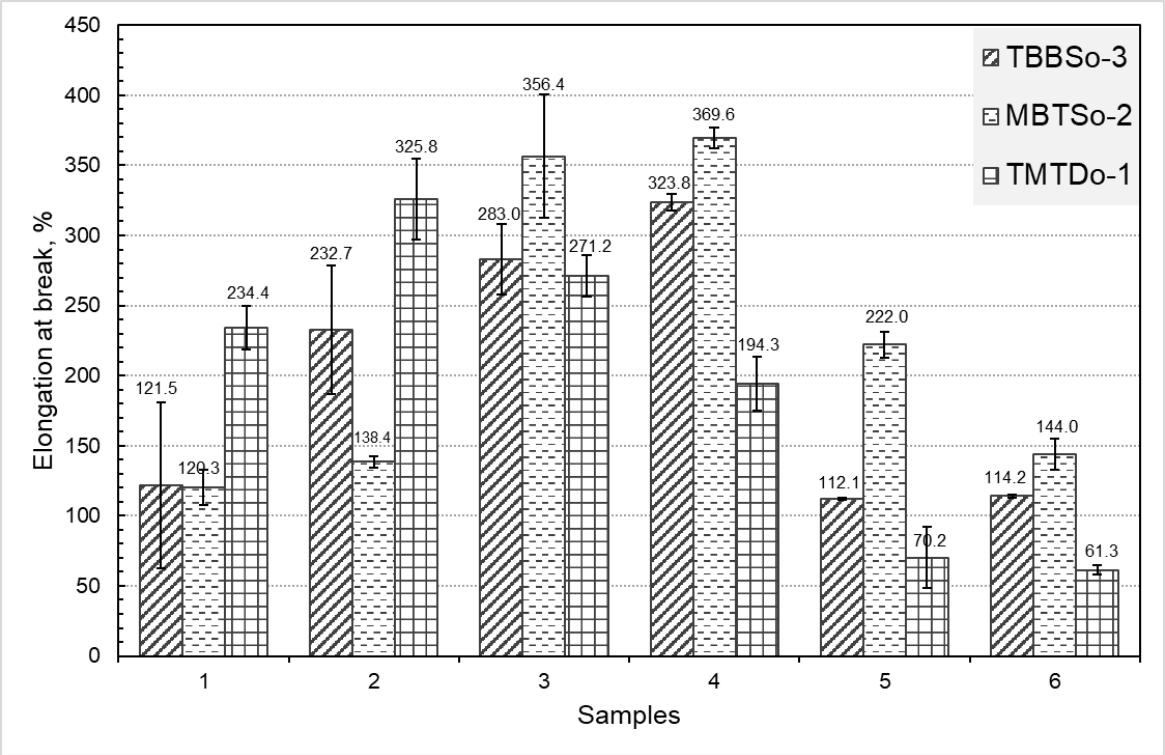


Figure 38 Elongation at break comparison between ozonated and non-ozonated samples respectively

The graphs of breaking stress at a certain elongation module between the compositions containing different accelerators are presented in Appendix 6.

Figure 35 and Figure 36 show obvious results that ozonated samples performed worse in both breaking stress and elongation at break comparing to their non-ozonated samples. TBBS-3 and TBBS-3o show an expected behavior, when the BS and EB rise until the fourth samples at 1 SEV, while the fifth at 2.5 EV and sixth at 3 EV ones drop, the latter rising slightly at the end, except the sixth non-ozonated sample at 3 EV for EB. In the case of MBTS-2 and MBTS-2o, the behavior is somewhat similar. The maximum point for non-ozonated samples is reached in the fourth sample at 1 SEV, while for ozonated it differs with the fifth sample at 2.5 EV for BS and the third sample at 0.7 SEV for EB. The last comparison between TMTD-1 and TMTD-1o shows a different behavior. The maximum for non-ozonated samples is reached with the second sample at 0.2 CV, and the minimum is at the fifth sample at 2.5 SEV for BS, while the first sample at 0.1 CV is the largest at EB, after which the values drop through further concentrations. Ozonated samples pass through a maximum at the third sample at 0.7 SEV with a slight rise at the last concentration at 3 EV for BS, while the second sample at 0.2 CV reaches the maximum for EB with the minimum point at the last concentration.

After filtering the values, Figure 37 shows a comprehensible view in BS in two graphs for ozonated and non-ozonated samples respectively, while Figure 38 shows it for EB. Firstly, BS is discussed. At the beginning, the values rise for CV concentrations respectively, showing a picture of TMTD-1 and TMTD-1o performing the best, TBBS-3 and TBBS-3o moderate, and MBTS-2 and MBTS-2o the worst. The behavior changes, looking at MBTS-2, which reaches a maximum at the fifth sample at 2.5 EV, overshooting at this and last concentrations all others, while MBTS-2o passes through a maximum at the fourth sample at 1 SEV, but being the biggest only in fifth at 2.5 EV and falling again the last at the sixth at 3 EV. TBBS-3 and TBBS-3o hold the lead until the fourth sample at 1 SEV, but TBBS-3 becomes the second for fifth at 2.5 EV and sixth 3 EV concentrations, while TBBS-3o falls the last at fifth 2.5 EV, but rises to the first place again for the sixth 3 EV sample. TMTD-1 loses its lead at the third sample at 0.7 SEV and becomes last till the end from the fourth 1 SEV. TMTD-1o, on the other hand, after reaching the highest point among others at the third sample at 0.7 SEV, becomes the second afterward till the end.

Figure 38 representing EB does not really correspond to BS and has to be discussed separately. TMTD-1 and TMTD-1o show the leadership for CV concentrations, but fall to the last place since then. MBTS-1 and MBTS-1o show the opposite – being the second and third for the CV concentrations respectively and climbs to the first place from the third 0.7

SEV concentration. TBBS-3 has the last place for the first sample at 0.1 CV but rises to the second place starting from the second sample at 0.2 CV. TBBS-3o remains the second place through all concentrations.

From the tables in Appendix 4 and graphs in Appendix 5 and Appendix 6 representing modules, it can be concluded that TBBS-3 reaches the elongation of 300 % for CV and SEV concentrations, the values of breaking stress increase together with concentrations, while TBBS-3o reaches M300 only for SEV concentrations. MBTS-2 compositions perform the best, all reaching 300 %, but MBTS-2o shows these values only for SEV concentrations. TMTD-1 performs the worst, reaching 300 % only for the first three concentrations, while TMTD-1o reaches 100 % except for EV concentrations, and 300 % is reached only by the 0.2 CV concentration. Without a doubt, all non-ozonated samples performed better than corresponding ozonated ones.

The breaking stress reached in modules for TBBS-3 and TBBS-3o varies, but there is a distinguishing mark in the third sample at 0.7 SEV, where the difference between the following modules becomes less far from each other, compared to the two previous CV concentrations, reaching 0.6 MPa maximum difference. The same rise in values for ozonated samples can be said for MBTS-2o, while TMTD-1o shows this behavior from the beginning. The last remark from the graphs comparing samples at certain elongations, MBTS compositions always perform the worst, TBBS moderate, and TMTD the best among all concentrations.

From the obtained results, it can be certainly confirmed that different accelerators affect the performance of the rubber composition differently, which cannot be accurately predicted, but a general trend is, nevertheless, visible. A team of authors in their similar research state that BS values pass through a maximum for CBS (same group of Sulfenamides with TBBS) and MBTS compositions, while only TBzTD (same family of Thiurams with TMTD) decreased its values with the increase of its concentrations, meaning that the amount of polysulfidic linkages are not proportional to A/S ratios for all accelerators [54]. The possible connection with the increase of BS and EB values from the beginning, occurs due to the polysulfidic linkages, which do not appear in the high proportion with the low accelerator's amount, and a crosslink distribution is poor. A team of authors [55] found out that the amount of polysulfidic linkages in a rubber composition with TBBS decreases with an increase of sulfur content, which correlates with the obtained results, hence the higher A/S ratio means less polysulfidic linkages and following decrease in mechanical properties.

A similar behavior of the curves has been shown in [56], investigating CBS accelerator at varying concentrations, where at the SEV system the curve passed through a maximum in BS. Authors discuss that the drop after a certain concentration can be explained by excessive crosslinking, which restricts the movement of chains. Authors state that with the addition of more accelerator, a large crosslinking network is formed with short free chains in between, which, in turn, are capable of limiting the orientation and extension of the molecular chains around crosslinks during deformation forces, leading to the appearance of cracks and lowering the physical properties. A slight increase in BS in TBBS-3 and TMTD-1 can be explained by the creation of crystallites in short-chain regions, trying to reinforce the whole structure. This phenomenon cannot be seen in MBTS-2 due to the later decrease of BS at 2.5 EV systems, but it is quite possible to appear at higher EV systems. Authors emphasize that mechanical properties depend on crosslinking density, the size and distribution of crosslinks, and their ability to crystallize during applied stretching [56].

Moreover, the obtained results mostly correspond to the obtained ozonated samples as well, from the summary of which can be concluded that **the best lowest results of CGR, which are mostly reached with SEV ratios for TBBS-3 and MBTS-2 correspond to the highest BS and EB values**, as well as to the visual evaluation, where the crazing effect at SEV mostly occurs. **The highest BS values for TMTD are reached for same concentration range as TBBS-3 and MBTS-2, while the highest EB values are shown for CV concentrations.** These, however, do not correspond to the visual representation, indicating the lowest CGR at SEV and EV concentrations. All in all, the best way is to study each accelerator separately, which could lead to different behaviors even among the same family group.

CONCLUSION

This Master's Thesis is focused on the investigation of the induced ozone impact in time on NR compositions consisting of different accelerators and their concentrations.

The practical part presents seven compositions, divided into two rounds, both containing different concentrations. The first round contained two compositions with TBBS, one with MBTS accelerators and one with TBBS and 6PPD antiozonant. The second round contained three compositions with TBBS, MBTS, and TMTD accelerators respectively. Samples from both rounds were subjected to induced ozone test in an ozone chamber, and all photos obtained under the microscope were visually evaluated, while the area of cracks from the second round was additionally evaluated with Matlab software and these samples underwent mechanical testing afterwards, comparing them with non-ozonated siblings.

The visual evaluation of ozonated photos shows that TBBS and MBTS compositions had good reproducibility respectively, having the best results between high CV and moderate SEV concentrations with the lowest number of large cracks. TBPD shows a similar behavior as TBBS compositions in this range. In contrast, compositions with TMTD accelerator show the lowest number of cracks in low EV concentrations. It was also observed that the samples are more likely to get damaged in the same way as they started at the beginning, which happens almost immediately after the start of ozone aging. These results were confirmed with CGR values obtained from own-designed application in Matlab software.

Hardness test for non-ozonated samples show an increasing trend with their growing concentrations in all compositions, the highest TMTD, moderate TBBS, and last MBTS. It was confirmed that a crazing effect has a less tremendous effect in comparison with occurred big cracks by a tensile strength. The highest values for BS and EB mostly correspond to the discussed photo results for TBBS and MBTS compositions, where SEV system shows the lowest CGR values, while TMTD composition shows the highest BS in between CV and SEV systems, but EB in CV systems. Non-ozonated siblings of TBBS and MBTS mostly show the same behavior, certainly with the higher values, while TMTD compositions show similarly for BS, but its EB is the highest in low concentrations of CV system. The best way is to study each accelerator separately and observe the outcome.

Lastly, by selecting an appropriate accelerator and its concentration, it is possible not only to influence the mechanical properties of the rubber product, but also to mitigate the effect of the ozone exposure, extending its service life.

BIBLIOGRAPHY

[1] GUERRA, Nayrim Brizuela, Giovana SANT'ANA PEGORIN, Miguel Henrique BORATTO, Natan Roberto DE BARROS, Carlos Frederico DE OLIVEIRA GRAEFF a Rondinelli Donizetti HERCULANO. *Biomedical applications of natural rubber latex from the rubber tree Hevea brasiliensis* [online]. B.m.: Elsevier Ltd. 1. červenec 2021. ISSN 18730191. Dostupné z: doi:10.1016/j.msec.2021.112126

[2] AMAECHI, Chiemela Victor, Facheng WANG, Idris Ahmed JA'E, Aaron ABOSHIO, Agbomerie Charles ODIJIE a Jianqiao YE. *A literature review on the technologies of bonded hoses for marine applications* [online]. B.m.: Taylor and Francis Ltd. 2022. ISSN 17445302. Dostupné z: doi:10.1080/17445302.2022.2027682

[3] MELICHERČÍK, Ján, Tomáš KUVIK, Jozef KRILEK a Iveta ČABALOVÁ. Design of the Crusher for Plastic and Rubber Waste Produced in Automotive Industry. *FME Transactions* [online]. 2021, 49(3), 734–739. ISSN 2406128X. Dostupné z: doi:10.5937/fme2103734M

[4] ALKARRANI, Hessa, Ghada ALMISNED a H. O. TEKIN. A benchmarking analysis on different rubber materials: towards customisation of lightweight and effective radiation protection solutions for aerospace and electronic applications. *Journal of Rubber Research* [online]. 2024. ISSN 15111768. Dostupné z: doi:10.1007/s42464-024-00272-4

[5] GOMES, Filipa O., M. Rosário ROCHA, Arminda ALVES a Nuno RATOLA. *A review of potentially harmful chemicals in crumb rubber used in synthetic football pitches* [online]. B.m.: Elsevier B.V. 5. květen 2021. ISSN 18733336. Dostupné z: doi:10.1016/j.jhazmat.2020.124998

[6] DISSANAYAKE, D. G.K., D. U. WEERASINGHE, L. M. THEBUWANAGE a U. A.A.N. BANDARA. An environmentally friendly sound insulation material from post-industrial textile waste and natural rubber. *Journal of Building Engineering* [online]. 2021, 33. ISSN 23527102. Dostupné z: doi:10.1016/j.jobe.2020.101606

[7] AL-ATTAR, Alyaa A., Hussein M. HAMADA, Bassam A. TAYEH a Paul O. AWOYERA. Exploring engineering properties of waste tire rubber for construction applications- A review of recent advances. In: *Materials Today: Proceedings* [online]. B.m.: Elsevier Ltd, 2021, s. 1–17. ISSN 22147853. Dostupné z: doi:10.1016/j.matpr.2022.03.228

[8] NICOLIN, Bogdan Adrian a Ilie NICOLIN. Tire Selection for a Military Training Aircraft. *Macromolecular Symposia* [online]. 2023, 411(1). ISSN 15213900. Dostupné z: doi:10.1002/masy.202200184

[9] HSIEH, Hsi Huang, Kai Chao YAO, Ching Hsin WANG, Chih Han CHEN a Shu Hua HUANG. Using a Circular Economy and Supply Chain as a Framework for Remanufactured Products in the Rubber Recycling Industry. *Sustainability (Switzerland)* [online]. 2024, 16(7). ISSN 20711050. Dostupné z: doi:10.3390/su16072824

[10] STATISTA. Natural rubber global production worldwide from 2000 to H1 2023. *https://www.statista.com/statistics/275387/global-natural-rubber-production/* [online]. [vid. 2025-03-20]. Dostupné z: https://www.statista.com/statistics/275387/global-natural-rubber-production/

[11] ZHENG, Tingting, Xiaoqian ZHENG, Shengqi ZHAN, Jing ZHOU a Shuangquan LIAO. Study on the ozone aging mechanism of Natural Rubber. *Polymer Degradation and Stability* [online]. 2021, 186. ISSN 01413910. Dostupné z: doi:10.1016/j.polymdegradstab.2021.109514

[12] PRINCI, Elisabetta. *Rubber: Science and technology* [online]. B.m.: De Gruyter, 2019 [vid. 2025-03-18]. ISBN 9783110640328. Dostupné z: doi:10.1515/9783110640328/EPUB
[13] WHITE, J.R. a S.K. DE. *Rubber Technologist's Handbook* [online]. Shawbury: Rapra Technology Limited, 2001. ISBN 1859572626. Dostupné z: http://www.rapra.net
[14] SABU, Thomas, RAJISHA K. R., Maria HANNA J., Chin Chan HAN a Laly POTHEN A. *Natural rubber materials. Volume 1, Blends and IPNs*. B.m.: RSC Publishing, 2014. ISBN 9781680158083.
[15] SAMSURI, Azemi. Degradation of Natural Rubber and Synthetic Elastomers. *Shreir's Corrosion* [online]. 2010, 2407–2438 [vid. 2025-03-18]. Dostupné z: doi:10.1016/B978-044452787-5.00117-7
[16] SUBRAMANIAM, Kanthappu. *Fundamentals of rubber technology*. Colombo: K.Subramaniam, 2002. ISBN 9559795708.
[17] RAGHAVAN VIJAYARAM, Thoguluva. A technical review on rubber. *International Journal on Design and Manufacturing Technologies* [online]. 2009, 3(1), 25–37 [vid. 2025-03-18]. ISSN 09739106. Dostupné z: doi:10.18000/IJODAM.70043
[18] DICK, John S. *Rubber Technology* [online]. B.m.: Carl Hanser Verlag GmbH & Co. KG, 2020 [vid. 2025-03-18]. ISBN 9781569906156. Dostupné z: doi:https://doi.org/10.1016/C2017-0-01398-8
[19] BHOWMICK, Anil K. a Howard STEPHENS. *Handbook of Elastomers* [online]. B.m.: CRC Press, 2000 [vid. 2025-03-18]. ISBN 9780429177231. Dostupné z: doi:10.1201/9781482270365/HANDBOOK-ELASTOMERS-ANIL-BHOWMICK-HOWARD-STEPHENS
[20] STATISTA. Production of rubber worldwide from 2000 to 2023. *https://www.statista.com/statistics/618804/total-global-natural-and-synthetic-rubber-production/* [online]. [vid. 2025-03-20]. Dostupné z: https://www.statista.com/statistics/618804/total-global-natural-and-synthetic-rubber-production/
[21] SETHURAJ, M R a N M MATHEW. *Natural rubber: Biology, cultivation and technology* [online]. B.m.: Elsevier Science, 2012 [vid. 2025-03-18]. ISBN 9780444597809. Dostupné z: https://books.google.com/books?id=-rHXxqRjWuIC&pgis=1
[22] P. M., Visakh, Thomas SABU, Chandra ARUP K. a Mathew AJI. P. *Advances in Elastomers I* [online]. Berlin, Heidelberg: Springer Berlin Heidelberg, 2013 [vid. 2025-03-18]. Advanced Structured Materials. ISBN 978-3-642-20925-3. Dostupné z: doi:10.1007/978-3-642-20925-3
[23] CIULLO, Peter A. a Norman HEWITT. *The Rubber Formulary* [online]. New York: Noyes Publications/William Andrew Publishing, LLC, 1999 [vid. 2025-03-19]. ISBN 0815514344. Dostupné z: https://www.scribd.com/document/157647977/14344-fm-pdf
[24] HILL, David M. *Latex dipping: Science and technology* [online]. B.m.: De Gruyter, 2019 [vid. 2025-03-19]. ISBN 9783110638097. Dostupné z: doi:10.1515/9783110638097/EPUB
[25] SIMPSON, R. B.. *Rubber Basics*. Shawbury: Rapra Technology Limited, 2002. ISBN 9781859573075.
[26] MARK, James E., Burak ERMAN a C. Michael ROLAND. *The Science and Technology of Rubber, Fourth Edition* [online]. B.m.: Elsevier, 2013 [vid. 2025-03-19]. ISBN 9780123945846. Dostupné z: doi:10.1016/C2011-0-05820-9

[27] CHITTELLA, Harika, Li Wan YOON, Suganti RAMARAD a Zee Wei LAI. Rubber waste management: A review on methods, mechanism, and prospects. *Polymer Degradation and Stability* [online]. 2021, 194 [vid. 2025-03-18]. ISSN 0141-3910. Dostupné z: doi:10.1016/J.POLYMDEGRADSTAB.2021.109761

[28] NOR HASMANIZA HUSNA SHUHAIMI, Ishak NUR SYULEHA, Othman NADRAS, Ismail HANAFI a Sasidharan SREENIVASAN. Effect of different types of vulcanization systems on the mechanical properties of natural rubber vulcanizates in the presence of oil palm leaves-based antioxidant. *Journal of Elastomers and Plastics* [online]. 2014, 46(8), 747–764 [vid. 2025-03-18]. ISSN 15308006. Dostupné z: doi:10.1177/0095244313489910/ASSET/AAF64497-110F-4A33-9F26-60982D4FC80D/ASSETS/IMAGES/LARGE/10.1177_0095244313489910-FIG17.JPG

[29] HERNÁNDEZ, Marianella, Juan L. VALENTÍN, Miguel A. LÓPEZ-MANCHADO a Tiberio A. EZQUERRA. Influence of the vulcanization system on the dynamics and structure of natural rubber: Comparative study by means of broadband dielectric spectroscopy and solid-state NMR spectroscopy. *European Polymer Journal* [online]. 2015, 68, 90–103 [vid. 2025-03-18]. ISSN 00143057. Dostupné z: doi:10.1016/J.EURPOLYMJ.2015.04.021

[30] GENT, Alan Neville. *Pneumatic Tire* [online]. 2006 [vid. 2025-03-18]. Dostupné z: doi:DOTHS810561

[31] SOLANKY, S. S. a R. P. SINGH. Ozonolysis of natural rubber: A critical review. *Progress in Rubber and Plastics Technology* [online]. 2001, 17(1), 13–58 [vid. 2025-03-18]. ISSN 02667320. Dostupné z: doi:10.1177/147776060101700102/ASSET/32ADE22B-6427-4B57-95E8-D714A6EEC742/ASSETS/147776060101700102.FP.PNG

[32] CATALDO, Franco. Protection Mechanism of Rubbers from Ozone Attack. *Ozone: Science & Engineering* [online]. 2019, 41(4), 358–368 [vid. 2025-03-18]. ISSN 15476545. Dostupné z: doi:10.1080/01919512.2018.1542518

[33] HUNTINK, N. M., R. N. DATTA a J. W.M. NOORDERMEER. Addressing Durability of Rubber Compounds. *Rubber Chemistry and Technology* [online]. 2004, 77(3), 476–511 [vid. 2025-03-18]. ISSN 0035-9475. Dostupné z: doi:10.5254/1.3547833

[34] DATTA, R. N., N. M. HUNTINK, S. DATTA a A. G. TALMA. Rubber Vulcanizates Degradation and Stabilization. *Rubber Chemistry and Technology* [online]. 2007, 80(3), 436–480 [vid. 2025-03-18]. ISSN 0035-9475. Dostupné z: doi:10.5254/1.3548174

[35] SABU, Thomas, Maria HANNA J., Joy JITHIN, Chin Chan HAN a Laly POTHEN A. *Natural Rubber Materials, Volume 2 - Composites and Nanocomposites*. B.m.: RSC Publishing, 2014. ISBN 9781628708769.

[36] TREIB, Caroline, Klara LOOS, Michael JOHLITZ a Alexander LION. Ozone ageing: experimental methods on pristine and protected natural rubber. *Continuum Mechanics and Thermodynamics* [online]. 2022, 34(6), 1563–1577 [vid. 2025-03-18]. ISSN 14320959. Dostupné z: doi:10.1007/S00161-022-01148-X/TABLES/3

[37] LEWIS, P. M. Effect of ozone on rubbers: Countermeasures and unsolved problems. *Polymer Degradation and Stability* [online]. 1986, 15(1), 33–66 [vid. 2025-03-18]. ISSN 0141-3910. Dostupné z: doi:10.1016/0141-3910(86)90004-2

[38] KELLER, Robert W. Oxidation and Ozonation of Rubber. *Rubber Chemistry and Technology* [online]. 1985, 58(3), 637–652 [vid. 2025-03-18]. ISSN 00359475. Dostupné z: doi:10.5254/1.3536082

[39] KAMARUDDIN, S. a A. H. MUHR. Investigation of Ozone Cracking on Natural Rubber. *Journal of Rubber Research 2018 21:2* [online]. 2018, 21(2), 73–93 [vid. 2025-03-19]. ISSN 25243993. Dostupné z: doi:10.1007/BF03449163

[40] Product details: NR SVR CV-60. *Güçlü Polimer Sanayi ve Ticaret A.Ş.* [online]. Dostupné z: https://www.rubbercompounding.net/product-detail/110/svr-cv-60/

[41] SUPPLE RUBBER CHEMICALS PRIVATE LIMITED. Yellow Natural Rubber SVR CV-60. *https://www.indiamart.com/proddetail/natural-rubber-svr-cv60-20387902112.html?srsltid=AfmBOorbfUXmdmDHvBJktp4LliwdZjFTF3lLSPlaA_SR87r1zvhchg5u* [online]. [vid. 2025-03-24]. Dostupné z: https://www.indiamart.com/proddetail/natural-rubber-svr-cv60-20387902112.html?srsltid=AfmBOorbfUXmdmDHvBJktp4LliwdZjFTF3lLSPlaA_SR87r1zvhchg5u

[42] Product details: VULCAN® 6 carbon black. *Cabot Corporation* [online]. Dostupné z: https://www.cabotcorp.com.br/~/media/files/product-datasheets/datasheet-vulcan-6pdf.pdf

[43] Product details: Tudalen oil. *H&R Group* [online]. Dostupné z: https://metakimya.com/uploads/tudalen%203909%20-%201927.pdf

[44] Product details: ZnO. *SlovZink, a.s.* [online]. Dostupné z: https://www.slovzink.sk/certificates.php

[45] Product details: Stearin TEFACIO RG Flocken. *Art-Restore* [online]. Dostupné z: https://art-restore.ch/p/stearin-tefacio-rg-flocken

[46] Product details: Sulfur CRYSTEXTM OT 33. *Eastman Chemical Company* [online]. Dostupné z: https://productcatalog.eastman.com/tds/ProdDatasheet.aspx?product=71093024&pn=crystex-ot-33

[47] SPECIALCHEM. Product details: TBBS. *Shandong Fine Chemical Technology* [online]. Dostupné z: https://polymer-additives.specialchem.com/product/a-shandong-fine-chemical-technology-tbbs

[48] SPECIALCHEM. Product details: MBTS. *Shandong Fine Chemical Technology* [online]. Dostupné z: https://polymer-additives.specialchem.com/product/a-shandong-fine-chemical-technology-mbts

[49] SPECIALCHEM. Product details: TMTD. *Shandong Fine Chemical Technology* [online]. Dostupné z: https://polymer-additives.specialchem.com/product/a-shandong-fine-chemical-technology-tmtd

[50] Product details: DUSANTOX® 6PPD. *Duslo, a.s.* [online]. Dostupné z: https://www.duslo.sk/userfiles/products/en_dusantox_6ppd.pdf

[51] Premier MDR 3D rheometer . *Alpha Technologies* [online]. Dostupné z: https://www.alpha-technologies.com/instruments/premier-mdr-moving-die-rheometer/

[52] MARKOVIĆ, Gordana, Blaga RADOVANOVIĆ, Milena MARINOVIĆ-CINCOVIĆ a Jaroslava BUDINSKI-SIMENDIĆ. The effect of accelerators on curing characteristics and properties of natural rubber/chlorosulphonated polyethylene rubber blend. *Materials and Manufacturing Processes* [online]. 2009, 24(10–11), 1224–1228 [vid. 2025-04-01]. ISSN 10426914. Dostupné z: doi:https://doi.org/10.1080/10426910902967087

[53] TEKER, Murat, Ayşe USLUOĞLU a Esra ÖZTÜRK. The Effect Of Accelerators On Vulcanization Of Natural Rubber Compounds. *Journal of the Turkish Chemical Society Section B: Chemical Engineering* [online]. 2024, 7(1), 1–12 [vid. 2025-03-18]. ISSN 2564-6907. Dostupné z: doi:10.58692/JOTCSB.1330292

[54] BOONKERD, Kanoktip, Chudej DEEPRASERTKUL a Kanyarat BOONSOMWONG. Effect of sulfur to accelerator ratio on crosslink structure, reversion, and strength in natural rubber. *Rubber Chemistry and Technology* [online]. 2016, 89(3), 450–464 [vid. 2025-04-01]. ISSN 0035-9475. Dostupné z: doi:10.5254/RCT.16.85963

[55] PÖSCHL, Marek, Radek STOČEK, Petr ZÁDRAPA, Martin STĚNIČKA a Gert HEINRICH. How is cut and chip wear influenced by the variation of the cross-link density within the conventional vulcanization system of natural rubber? *Express Polymer Letters* [online]. 2024, 18(12), 1178–1190 [vid. 2025-04-26]. ISSN 1788618X. Dostupné z: doi:10.3144/EXPRESSPOLYMLETT.2024.90

[56] MASA, Abdulhakim, Siriwat SOONTARANON a Nabil HAYEEMASAE. Influence of Sulfur/Accelerator Ratio on Tensile Properties and Structural Inhomogeneity of Natural Rubber. *Polymer(Korea)* [online]. 2020, 44(4), 519–526 [vid. 2025-04-01]. Dostupné z: doi:10.7317/pk.2020.44.4.519

LIST OF FIGURES

Figure 1 A structural formula of NR....13
Figure 2 Flow line diagram for the production of different grades of NR....14
Figure 3 The presentation of rubber chains before and after the vulcanization process....25
Figure 4 Effect of vulcanization on physical properties of the final product 28
Figure 5 Effect of temperature on rubber breakdown in conventional mixing....30
Figure 6 Schematic representation of open mill mixer (A), internal mixer (B), compression molding (C)....33
Figure 7 Structural molecule of ozone....34
Figure 8 Chemical formulae of the most used antiozonants....36
Figure 9 The changes in molecular structure of NR sample exposed under strain to ozone 37
Figure 10 A Criegee's three-step mechanism of ozonolysis with basic NR monomer 38
Figure 11 Ozonation mechanism with 6PPD antiozonant 41
Figure 12 An example of a vulcanization curve 44
Figure 13 A representative stress-strain curve....47
Figure 14 A Banbury mixer by Pomini Farrel, model Midget....55
Figure 15 A kneader from Everplast Machinery Co., Ltd., model SYD–2L....56
Figure 16 A mixing mill Farrel G-2603, 150×330 mm 57
Figure 17 A Brabender kneader, model F-10572 58
Figure 18 Polymer Process Analyzer PPA-1 (left) and Premier MDR 3D (right) from Alpha Technologies 59
Figure 19 Vulcanization curves from the first round of experiments: (A) – TBBS-1, (B) – TBPD-1, (C) – TBBS-2, (D) – MBTS-1....61
Figure 20 Vulcanization curves from the second round of experiments: (A) – TBBS-3, (B) – MBTS-2, (C) – TMTD-1 62
Figure 21 A compressing machine P–11E from Blanické strojírny 66
Figure 22 A manual hydraulic press from Polymertest 66
Figure 23 A punching knife 67
Figure 24 A hydraulic punching machine ZPS 06102 P1....67
Figure 25 A rubber holder with a fixated rubber sample (left) and an ozone cabinet Ozone Check - UV by Gibitre Instruments S.r.l. (right) 68
Figure 26 A representative graph of the tests on the example of TBBS-2 69
Figure 27 A digital microscope model DVM2500 from Leica Microsystems GmbH 70
Figure 28 An example of highlighting the cracks in Matlab software....71
Figure 29 A visual representation of crack growth in TBBS-3 72

Figure 30 A visual representation of crack growth in MBTS-2 72
Figure 31 A visual representation of crack growth in TMTD-1 73
Figure 32 A Bareiss model BS 61 II durometer 77
Figure 33 A representation of a hardness Shore A test for non-ozonized samples 78
Figure 34 A tensometer T10D by Alpha Technologies 79
Figure 35 Breaking stress results between non-ozonated and ozonated samples 81
Figure 36 Elongation at break results between non-ozonated and ozonated samples 82
Figure 37 Breaking stress comparison between ozonated and non-ozonated samples respectively 83
Figure 38 Elongation at break comparison between ozonated and non-ozonated samples respectively 84

LIST OF TABLES

Table 1 Classification of main ingredients by their functions in a rubber compound 15
Table 2 Classification of additional ingredients by their functions in a rubber compound .16
Table 3 A formulation sample for a rubber compound.....16
Table 4 Comparison and classification of different accelerators 18
Table 5 Characterization of vulcanization systems.....27
Table 6 Compositions from the second round of experiments 50
Table 7 Characteristics of NR SVR-CV60 51
Table 8 Characteristics of CB VULCAN® 6 type N220.....52
Table 9 Characteristics of Tudalen oil type 11 52
Table 10 Characteristics of TEFACID® RG stearic acid.....53
Table 11 Characteristics of sulfur CRYSTEX™ OT 33.....53
Table 12 Characteristics of TBBS, MBTS and TMTD 54
Table 13 Characteristics of DUSANTOX® 6PPD 54
Table 14 A procedure of rubber compounding.....58
Table 15 Vulcanization characteristics from the first round of experiments.....61
Table 16 Vulcanization characteristics from the second round of experiments 63
Table 17 The average values of vulcanization characteristics among compositions.....64
Table 18 Evaluation of surface area of TBBS-3 composition in “%” 72
Table 19 Evaluation of surface area of MBTS-2 composition in “%” 73
Table 20 Evaluation of surface area of TMTD-1 composition in “%”.....74
Table 21 Median results of the hardness test 78
Table 22 Results obtained from the tensile strength test 80

LIST OF ABBREVIATIONS

6PPD	N-(1,3-Dimethylbutyl)-N'-Phenyl-P-Phenylenediamine
ADS	Air-Dried Sheet
ASTM	American Society For Testing And Materials
BET	Brunauer-Emmett-Teller
BHT	Butylated Hydroxytoluene
BS	Breaking Stress
CB	Carbon Black
CBS	N-Cyclohexyl-2-Benzothiazole Sulfenamide
CGR	Crack Growth Ratio
COAN	OAN After Crushing
CV	Conventional
DCBS	N,N-Dicyclohexyl-2-Benzothiazole Sulfenamide
DOTG	Diorthotolyl Guanidine
DPG	Diphenyl Guanidine
EB	Elongation At Break
EPDM	Ethylene Propylene Diene Monomer
EV	Efficient
EVA	Ethylene-Vinyl Acetate
FCM	Farrel Continuous Mixer
IRHD	International Rubber Hardness Degrees
ISO	International Organization For Standardization
LOI	Loss On Ignition Test
MBT	Mercaptobenzothiazole
MBTS	Dibenzothiazyl Disulfide
MDR	Moving Die Rheometer
MMT	Million Metric Tons
MPa	Megapascal
NR	Natural Rubber
OAN	Oil Absorption Number
ODR	Oscillating Disk Rheometer
PHR	Parts Per Hundred
PPA	Polymer Process Analyzer

PPD	Para-Phenylenediamine
PPHM	Parts Per Hundred Million
PPM	Parts Per Million
RPA	Rubber Process Analyzer
RSS	Ribbed Smoked Sheet
SBR	Styrene Butadiene Rubber
SD	Standard Deviation
SEV	Semi-Efficient
SIR	Standard Indonesian Rubber
SLR	Sri Lanka Rubber
SMR	Standard Malaysian Rubber
SSR	Standard Singapore Rubber
STR	Standard Thai Rubber
STSA	Statistical Thickness Surface Area
SVR	Standard Vietnamese Rubber
TBBS	N-Tert-Butyl-2-Benzothiazole Sulfenamide
TBPD	TBBS + 6PPD
TBzTD	Tetrabenzylthiuram Disulfide
TETD	Tetraethylthiuram Disulfide
TMQ	1,2-Dihydro-2,2,4-Trimethylquinoline
TMTD	Tetramethylthiuram Disulfide
TMTM	Tetramethylthiuram Monosulfide
TPG	Triphenyl Guanidine
TSR	Technically Specified Rubber
VGC	Viscosity Gravity Constant
VOC	Volatile Organic Compounds
ZDBC	Zinc Dibutyl Dithiocarbamate
ZDEC	Zinc Diethyldithiocarbamate
ZDMC	Zinc Dimethyl Dithiocarbamate
ZMBT	Zinc Mercaptobenzothiazole

APPENDICES

Appendix 1 Tables of compositions for the first round of experiments 100

Appendix 2 The photos from the first round 101

Appendix 3 The photos from the second round 110

Appendix 4 The tables of modules from tensile strength experiment 116

Appendix 5 The graphs representing modules at varying elongations, comparing ozonated and non-ozonated samples with the same accelerator 117

Appendix 6 The graphs representing modules at same elongations, comparing ozonated and non-ozonated samples with different accelerators 118

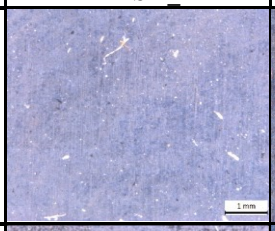
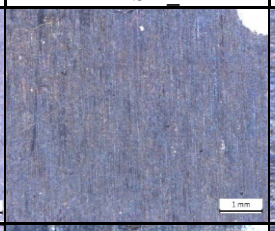
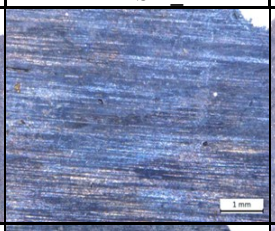
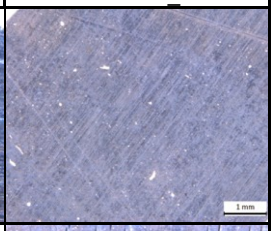
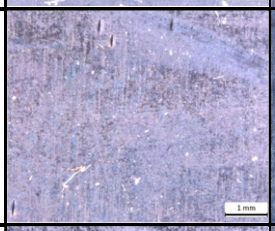
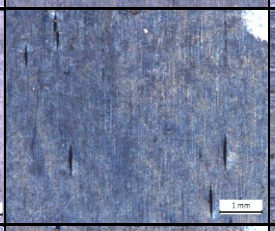
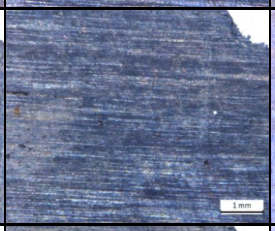
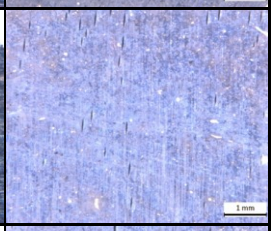
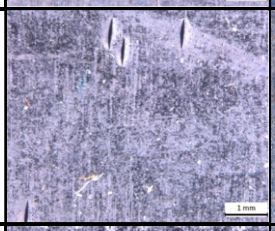
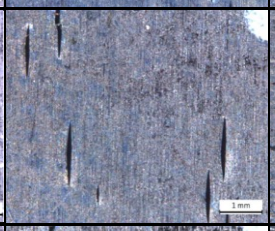
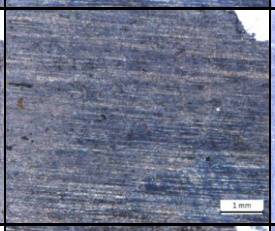
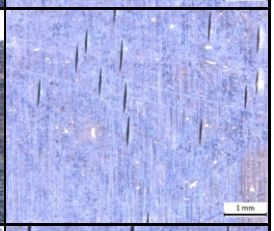
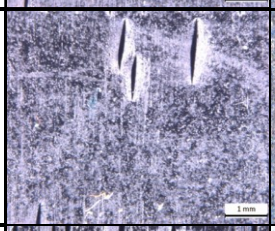
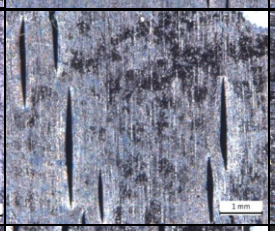
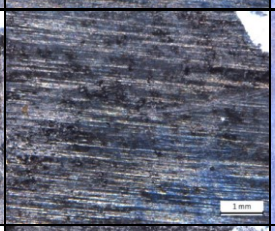
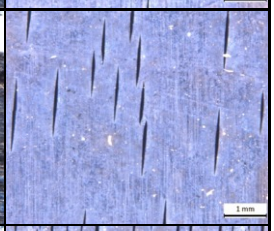
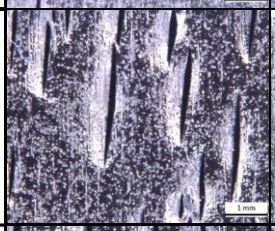
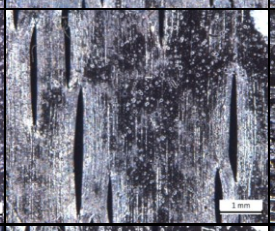
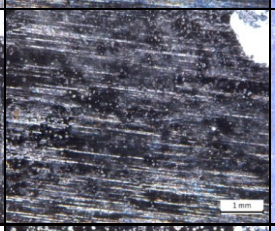
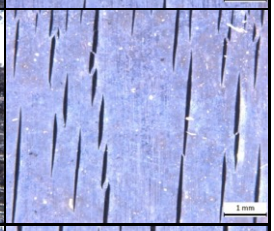
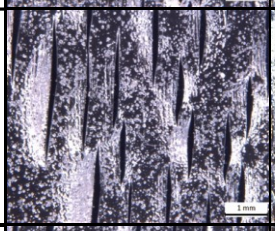
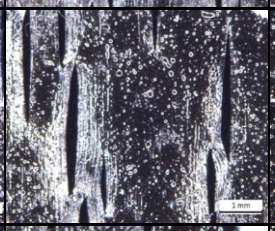
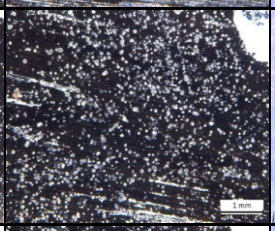
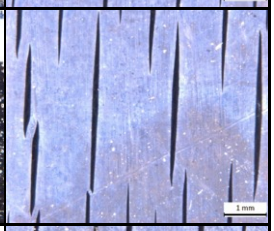
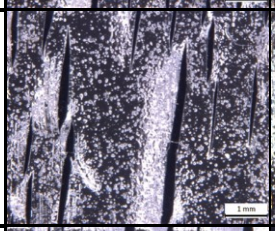
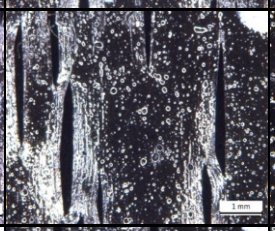
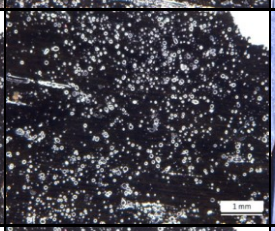
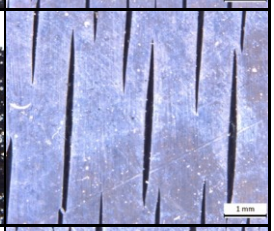
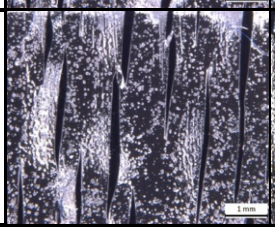
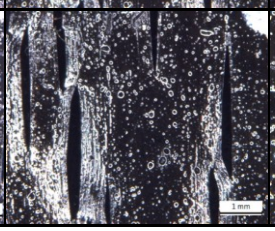
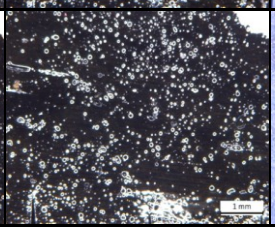
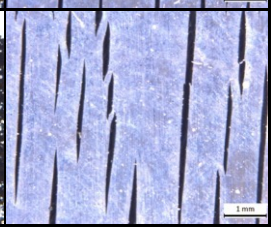
APPENDIX 1 TABLES OF COMPOSITIONS FOR THE FIRST ROUND OF EXPERIMENTS

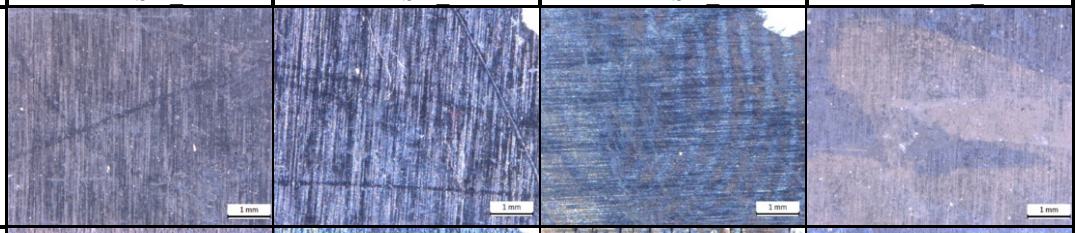
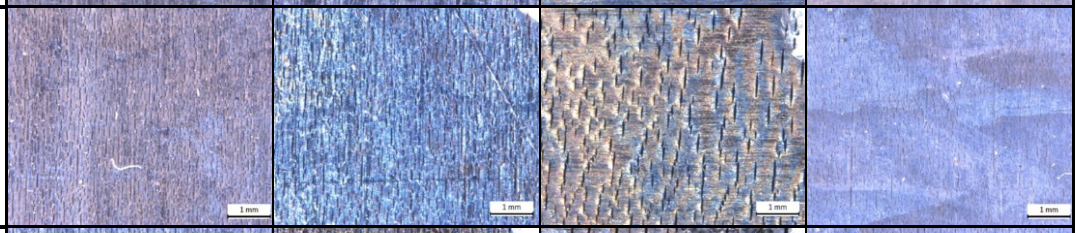
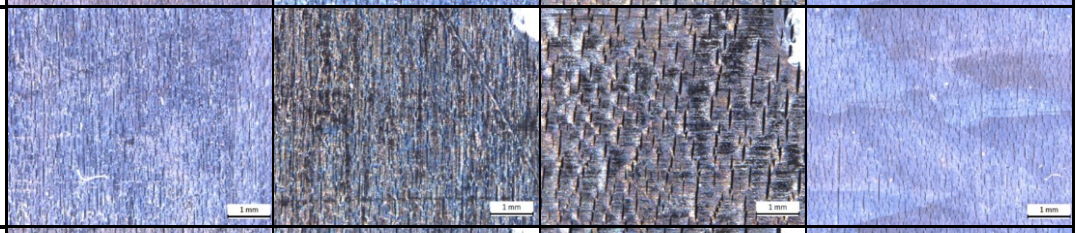
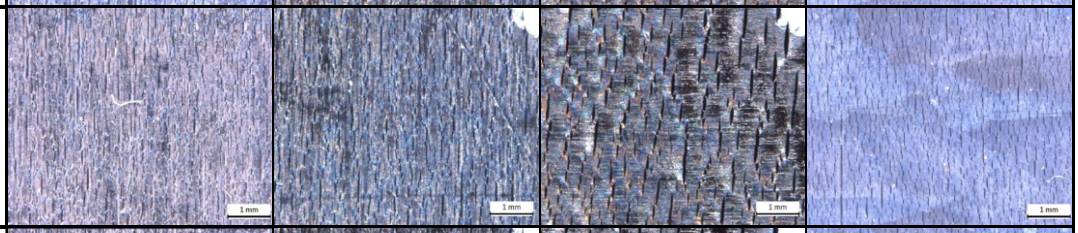
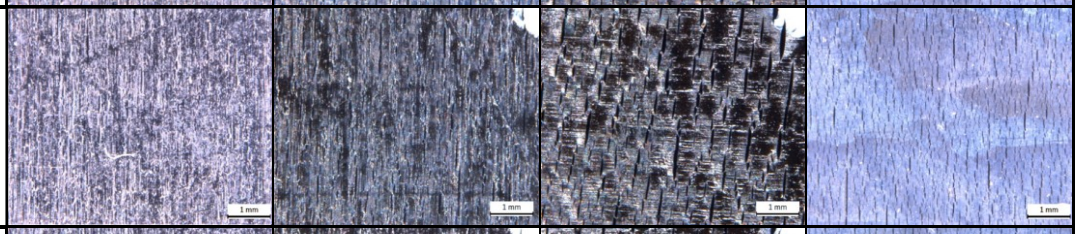
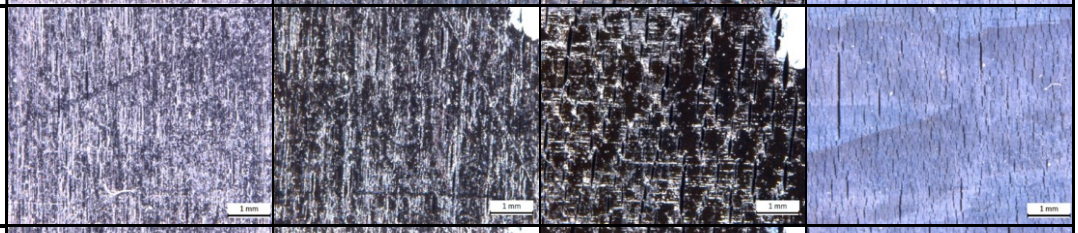
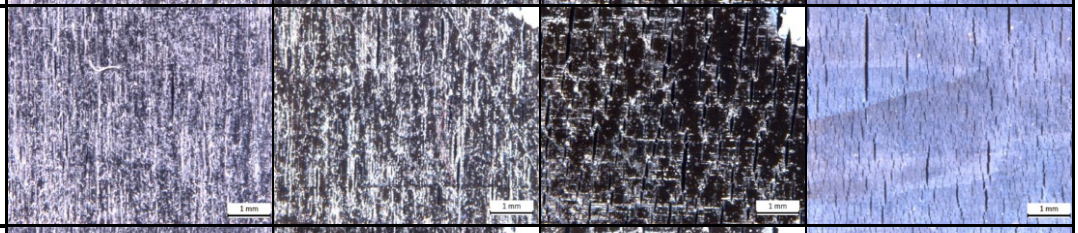
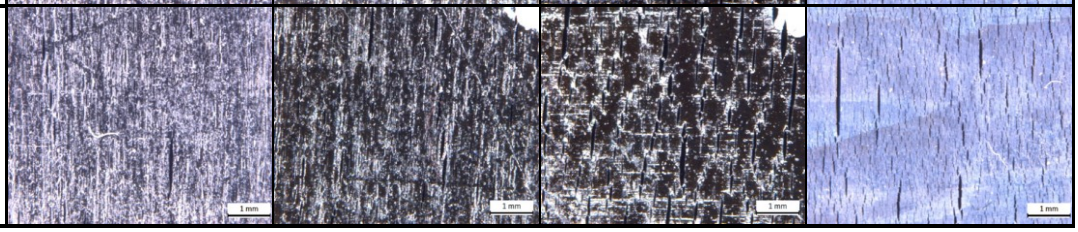
The left table shows a composition without an antiozonant, while the right one contains it.

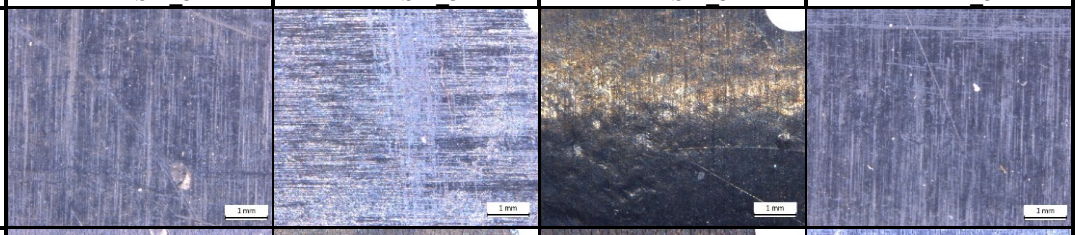
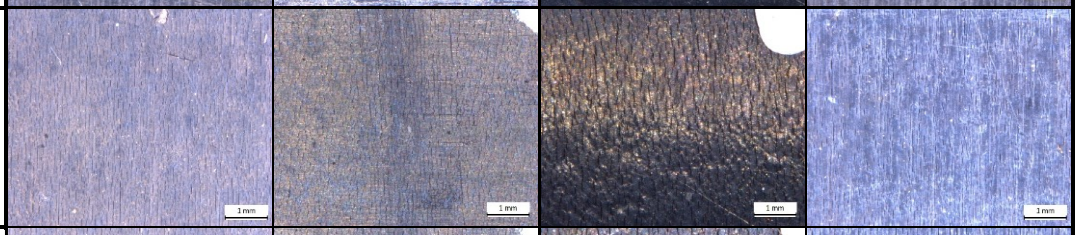
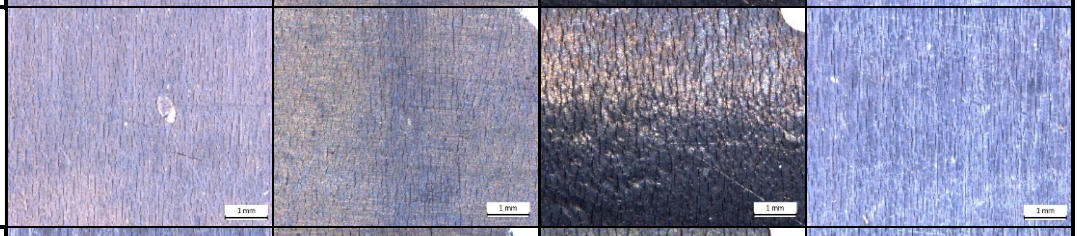
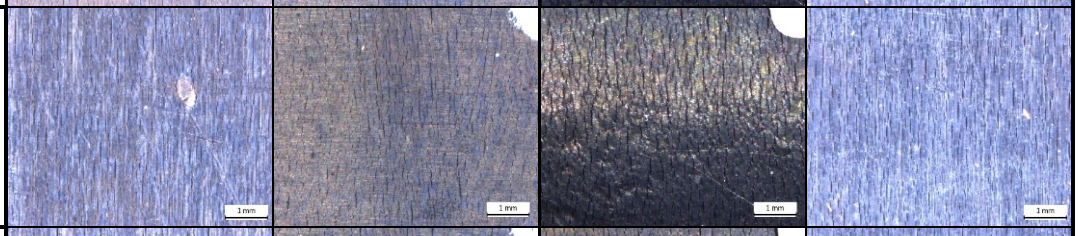
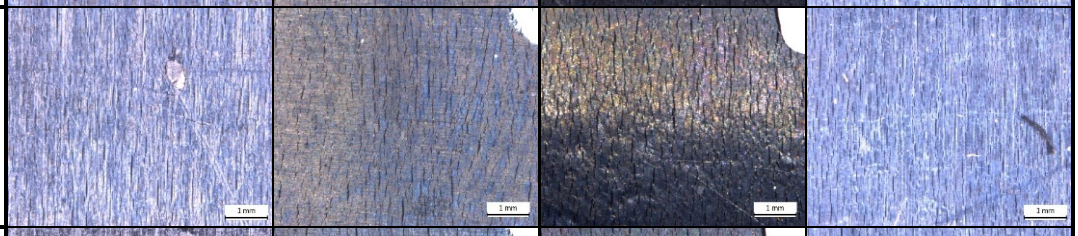
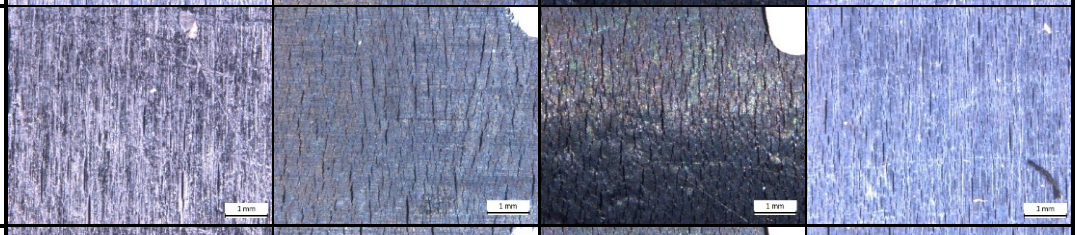
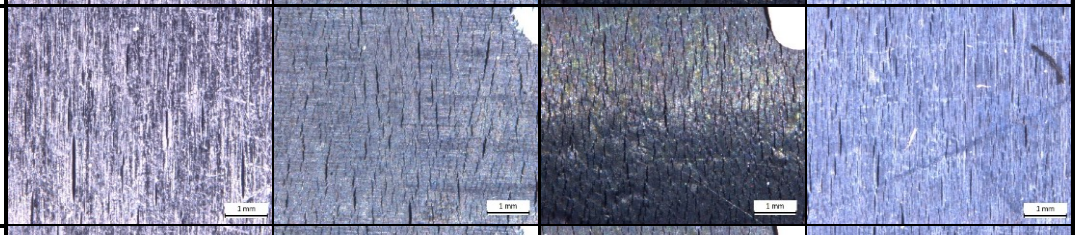
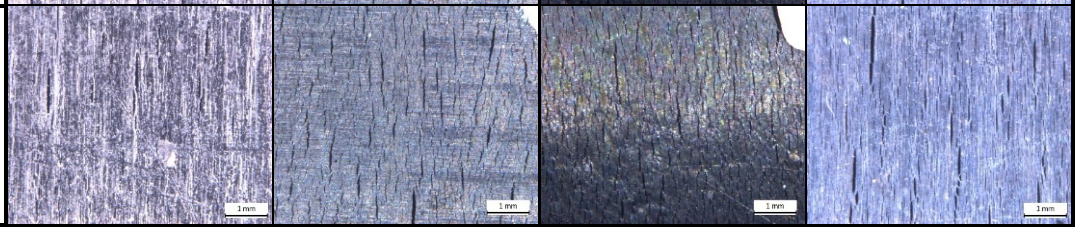
	Loading in phr								
A/S ratio	**0.1 CV**	**0.3 CV**	**0.6 SEV**	**0.7 SEV**	**1.0 SEV**	**1.5 SEV**	**2.0 SEV**	**2.5 EV**	**3.0 EV**
Ingredients / Samples	**1**	**2**	**3**	**4**	**5**	**6**	**7**	**8**	**9**
NR SVR-CV60	100.00	100.00	100.00	100.00	100.00	100.00	100.00	100.00	100.00
N220	58.00	58.00	58.00	58.00	58.00	58.00	58.00	58.00	58.00
Tudalen oil 11	6.00	6.00	6.00	6.00	6.00	6.00	6.00	6.00	6.00
ZnO	5.00	5.00	5.00	5.00	5.00	5.00	5.00	5.00	5.00
Stearic acid	3.00	3.00	3.00	3.00	3.00	3.00	3.00	3.00	3.00
Accelerator	**0.25**	**0.75**	**1.50**	**1.75**	**2.50**	**3.75**	**5.00**	**6.25**	**7.50**
Sulphur OT33	2.50	2.50	2.50	2.50	2.50	2.50	2.50	2.50	2.50
Sum	**174.75**	**175.25**	**176.00**	**176.25**	**177.00**	**178.25**	**179.50**	**180.75**	**182.00**

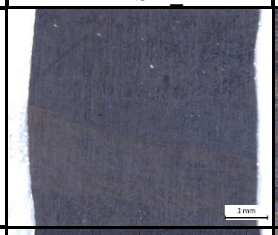
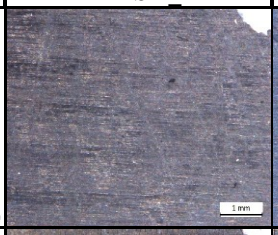
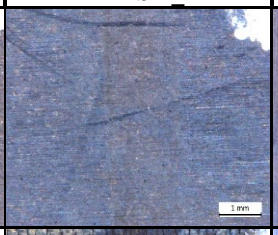
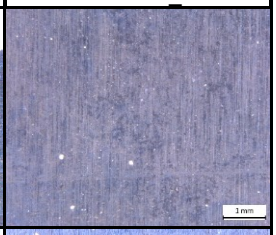
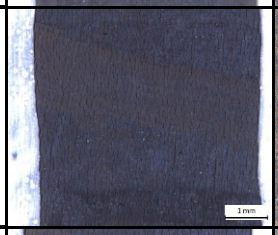
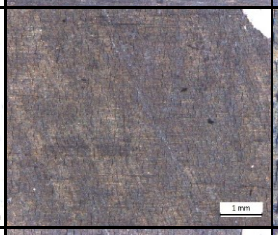
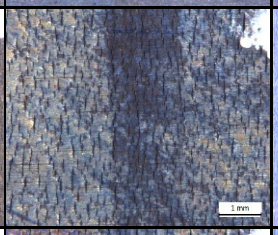
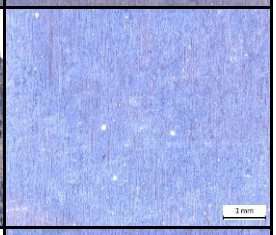
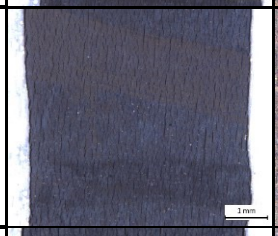
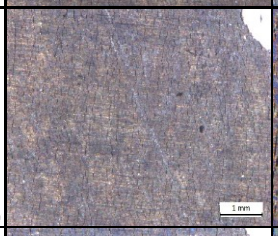
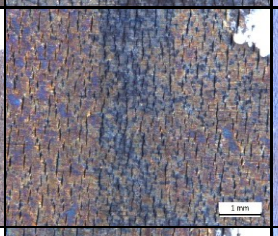
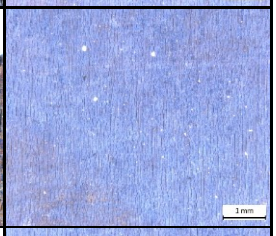
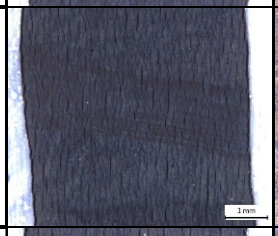
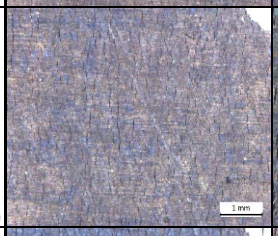
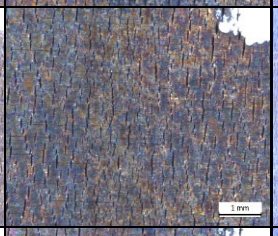
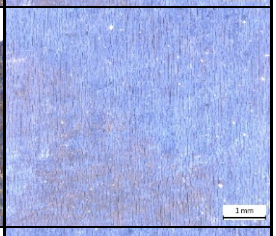
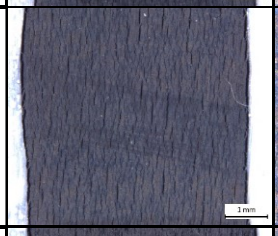
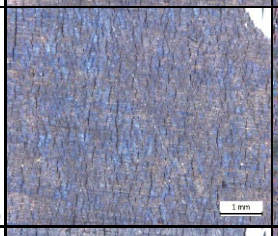
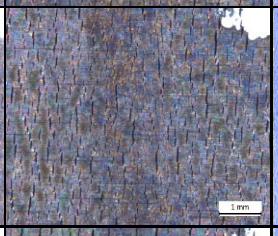
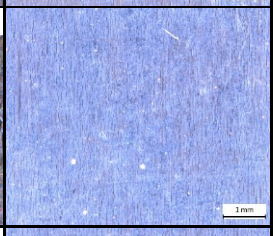
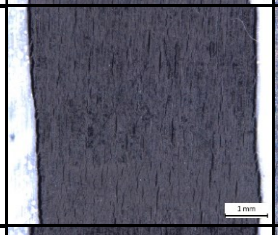
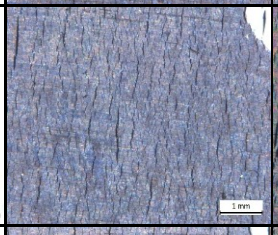
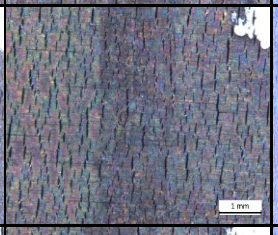
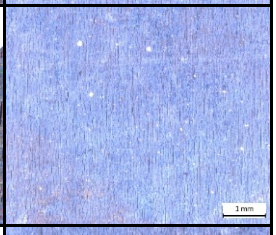
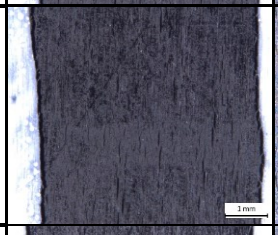
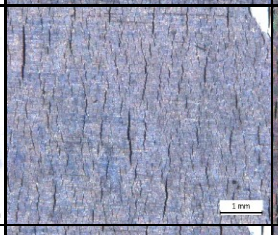
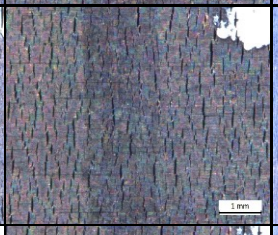
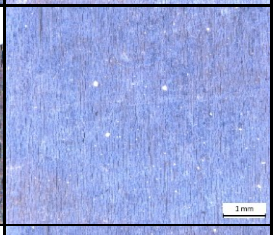
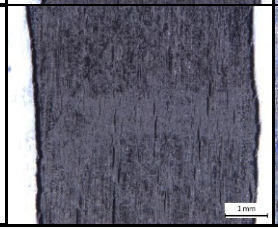
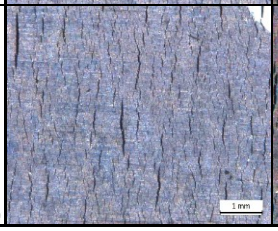
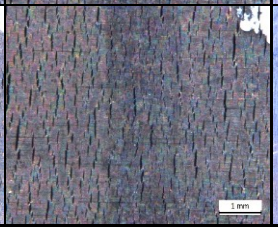
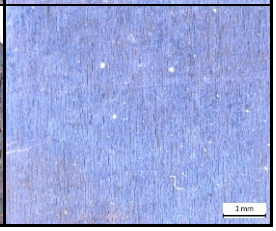
	Loading in phr								
A/S ratio	**0.1 CV**	**0.3 CV**	**0.6 SEV**	**0.7 SEV**	**1.0 SEV**	**1.5 SEV**	**2.0 SEV**	**2.5 EV**	**3.0 EV**
Ingredients / Samples	**1**	**2**	**3**	**4**	**5**	**6**	**7**	**8**	**9**
NR SVR-CV60	100.00	100.00	100.00	100.00	100.00	100.00	100.00	100.00	100.00
N220	58.00	58.00	58.00	58.00	58.00	58.00	58.00	58.00	58.00
6PPD	**1.00**	**1.00**	**1.00**	**1.00**	**1.00**	**1.00**	**1.00**	**1.00**	**1.00**
Tudalen oil 11	6.00	6.00	6.00	6.00	6.00	6.00	6.00	6.00	6.00
ZnO	5.00	5.00	5.00	5.00	5.00	5.00	5.00	5.00	5.00
Stearic acid	3.00	3.00	3.00	3.00	3.00	3.00	3.00	3.00	3.00
Accelerator	**0.25**	**0.75**	**1.50**	**1.75**	**2.50**	**3.75**	**5.00**	**6.25**	**7.50**
Sulphur OT33	2.50	2.50	2.50	2.50	2.50	2.50	2.50	2.50	2.50
Sum	**175.75**	**176.25**	**177.00**	**177.25**	**178.00**	**179.25**	**180.50**	**181.75**	**183.00**

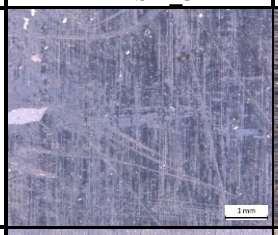
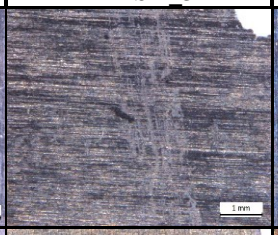
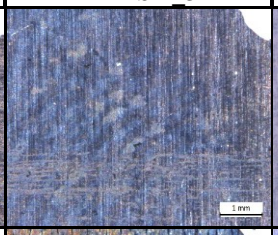
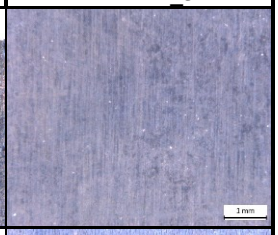
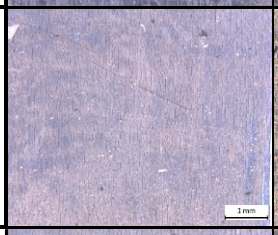
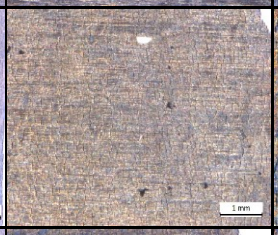
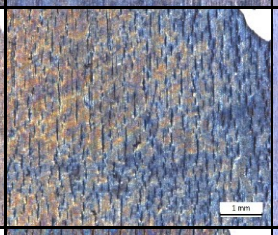
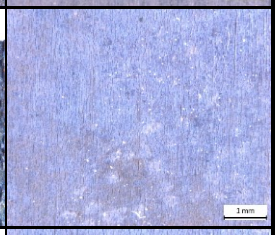
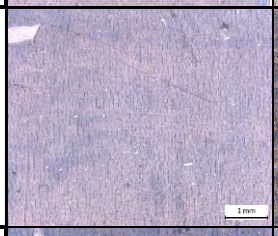
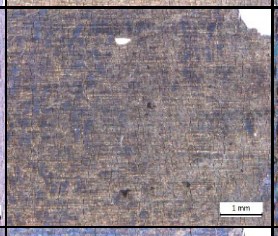
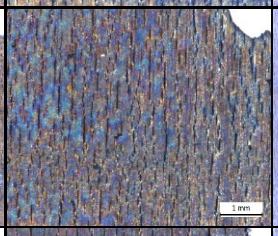
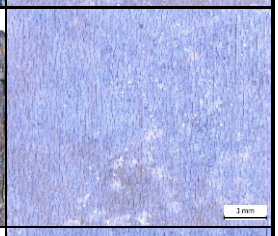
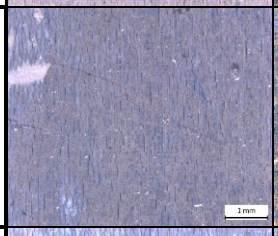
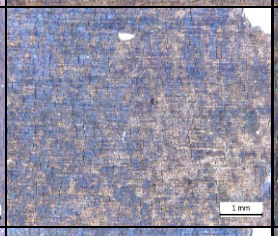
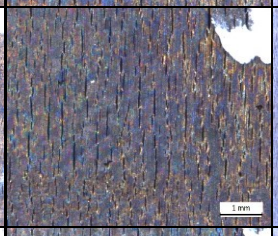
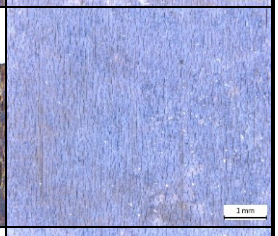
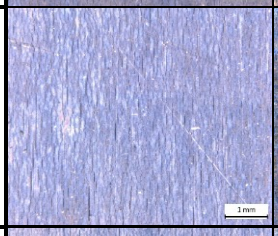
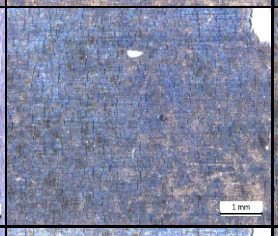
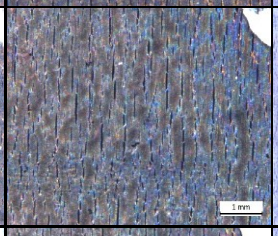
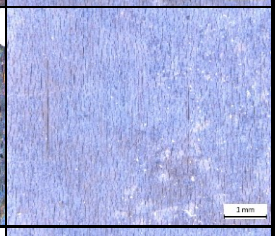
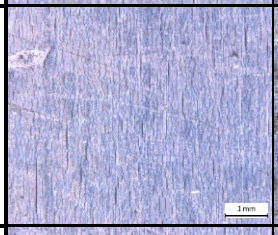
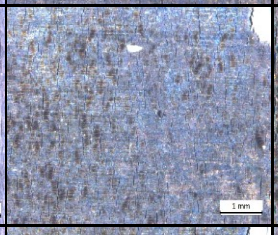
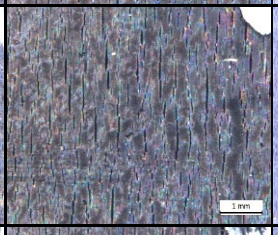
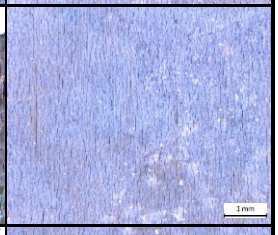
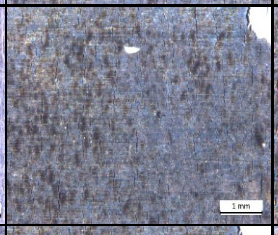
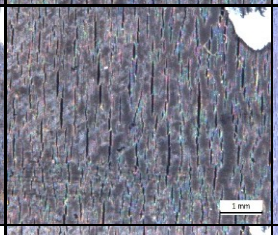
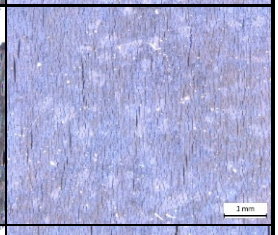
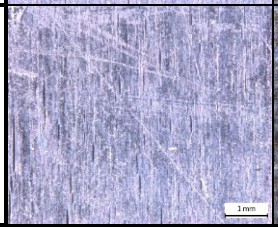
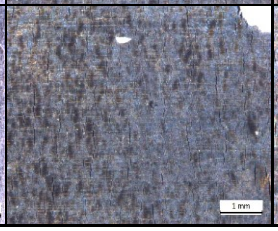
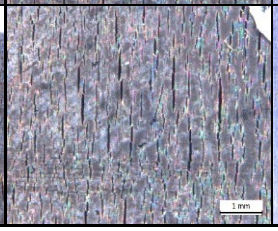
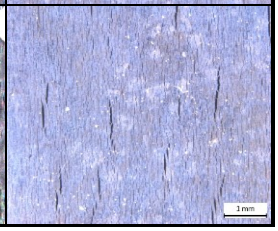
APPENDIX 2 THE PHOTOS FROM THE FIRST ROUND

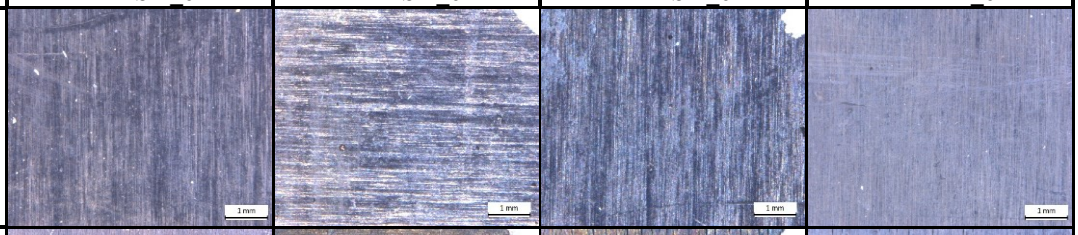
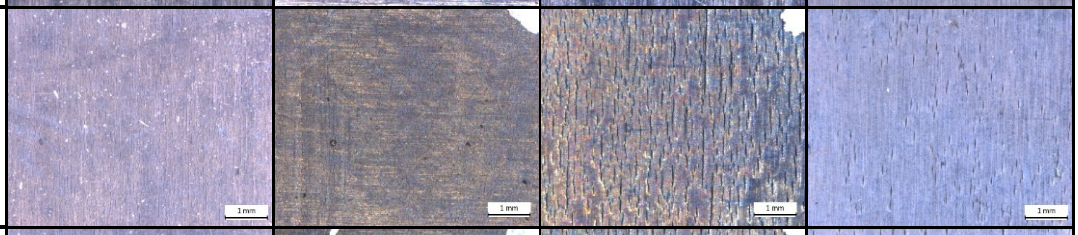
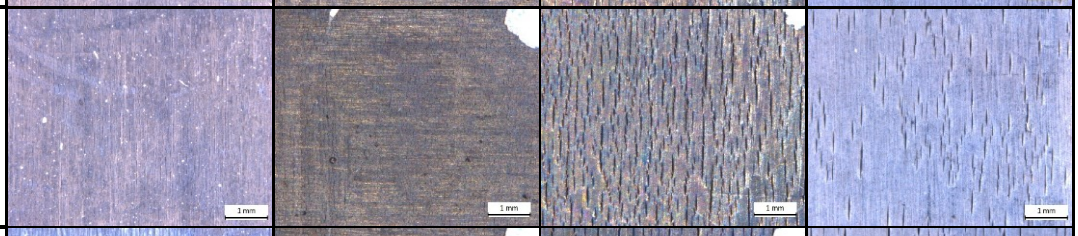
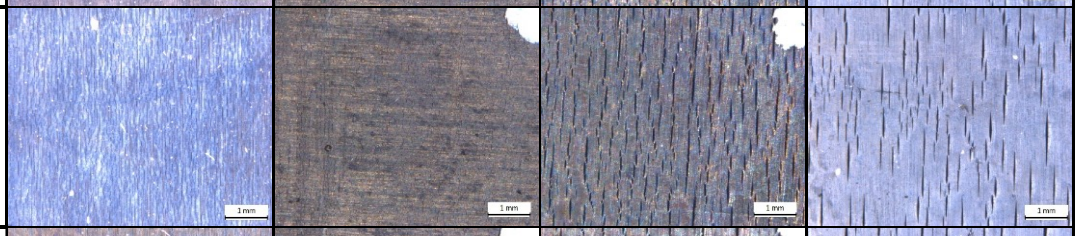
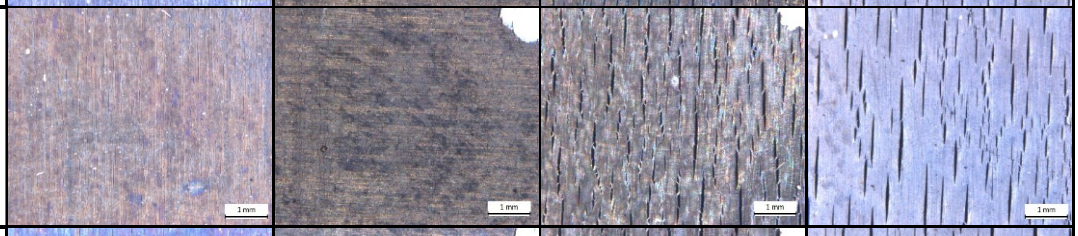
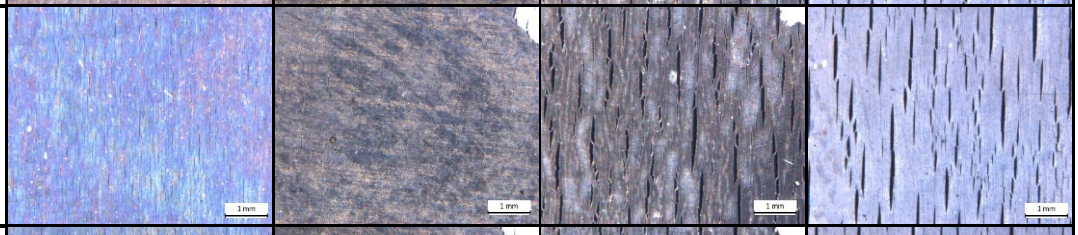
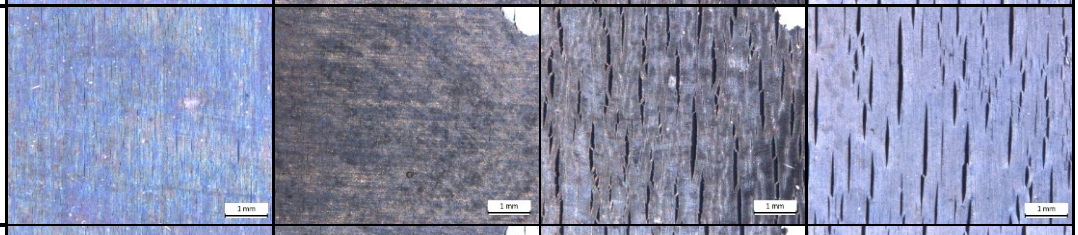
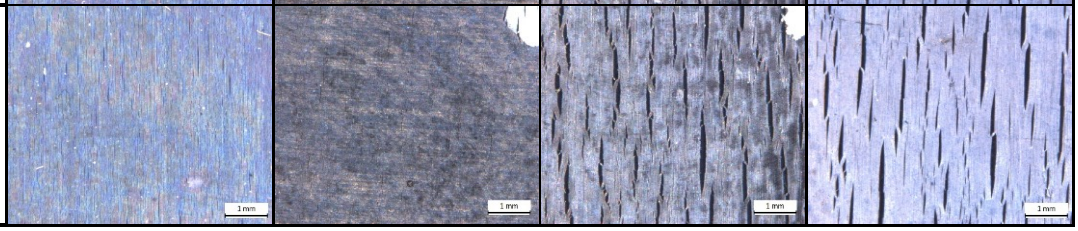
	TBBS-1_1	TBBS-2_1	MBTS-1_1	TBPD-1_1
0				
3				
6				
12				
24				
48				
72				
96				

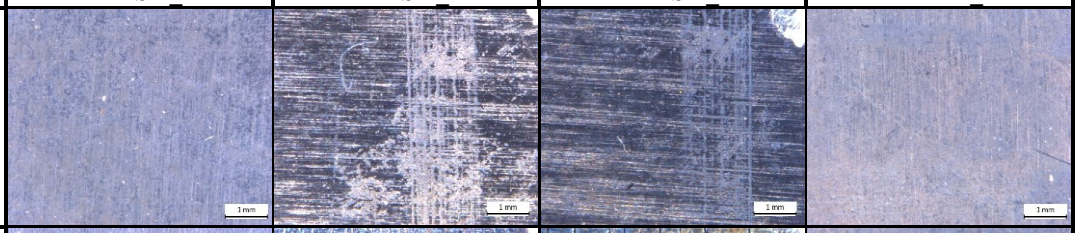
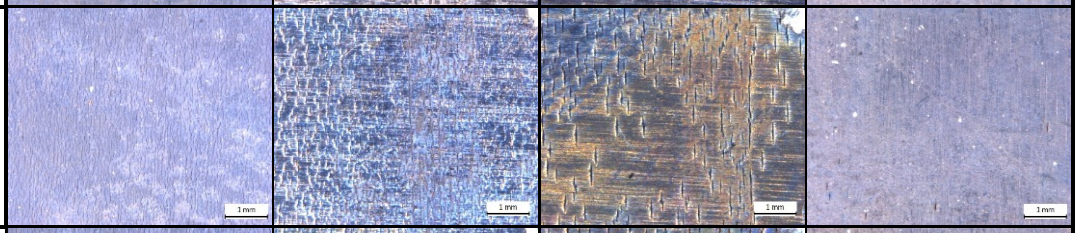
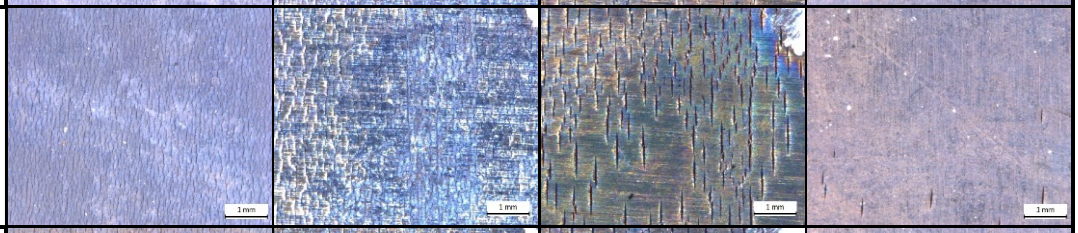
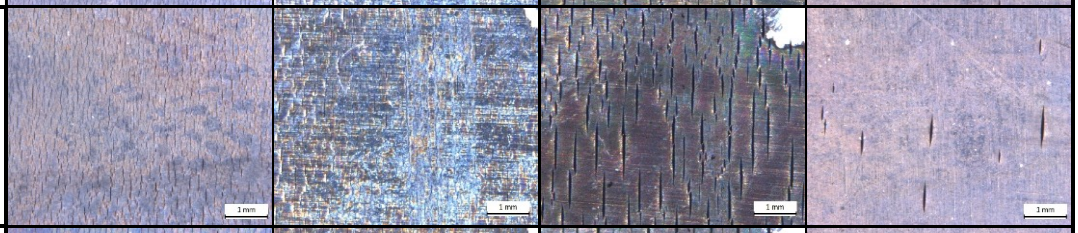
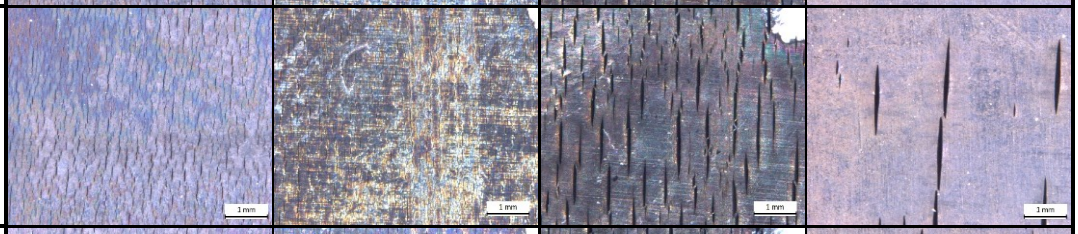
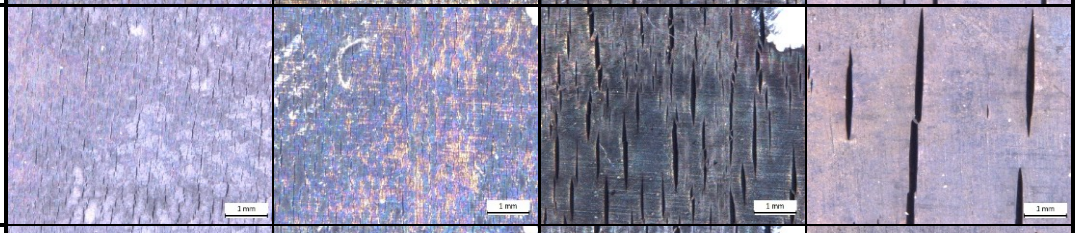
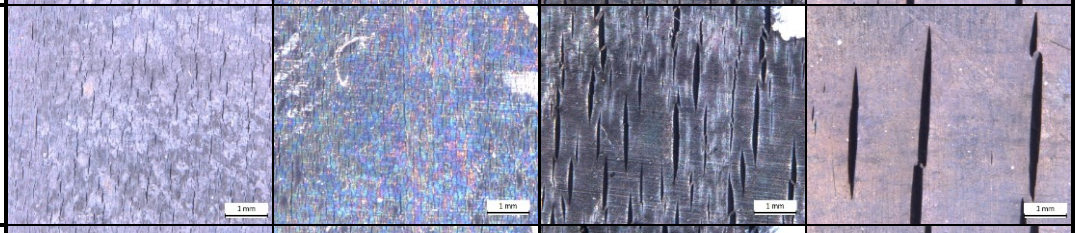
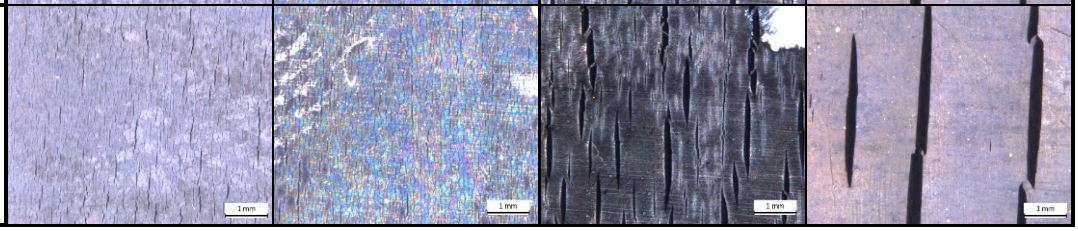
	TBBS-1_2	TBBS-2_2	MBTS-1_2	TBPD-1_2
0				
3				
6				
12				
24				
48				
72				
96				

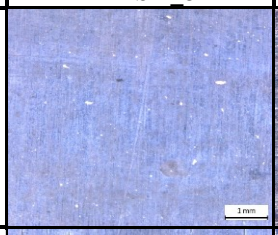
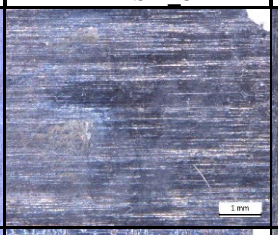
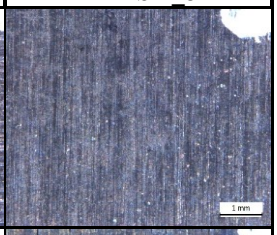
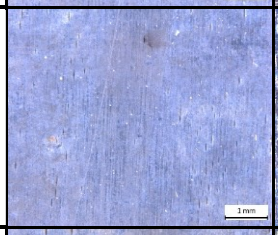
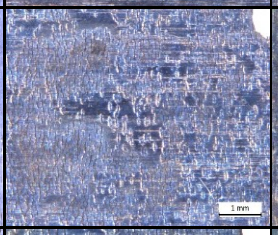
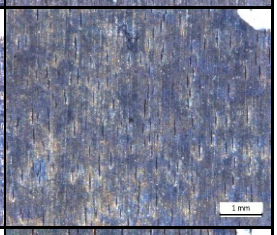
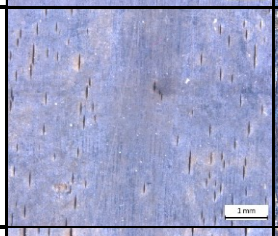
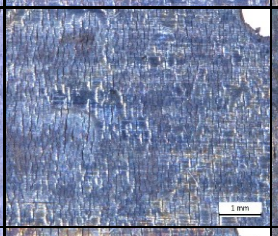
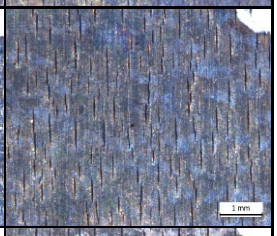
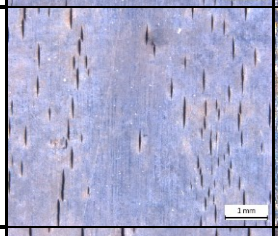
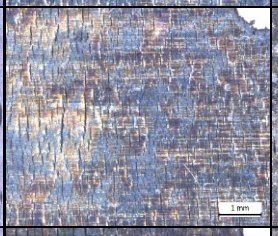
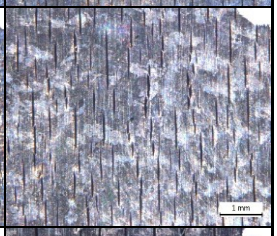
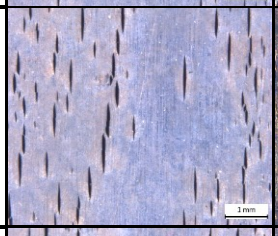
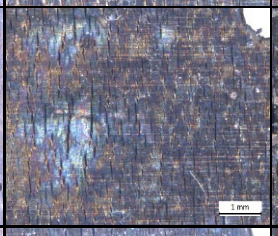
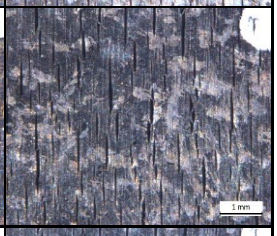
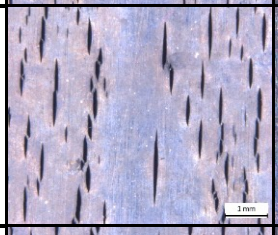
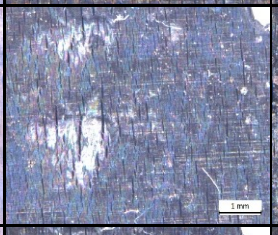
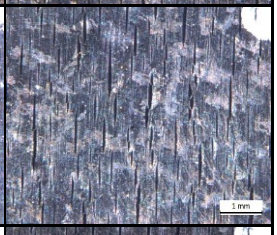
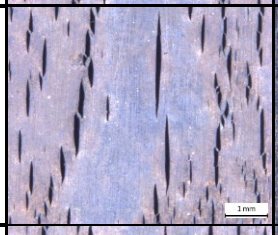
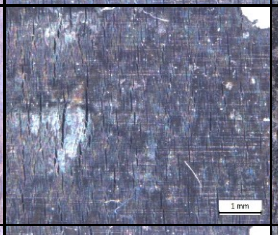
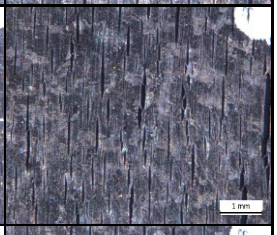
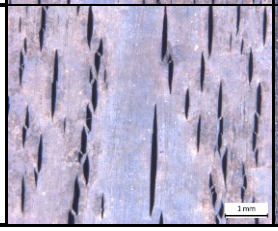
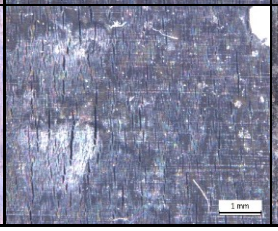
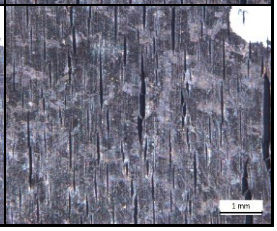
	TBBS-1_3	TBBS-2_3	MBTS-1_3	TBPD-1_3
0				
3				
6				
12				
24				
48				
72				
96				

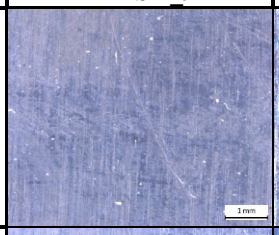
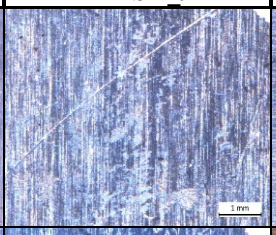
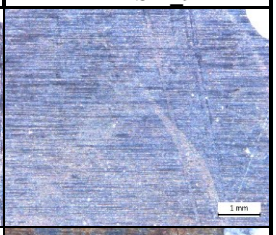
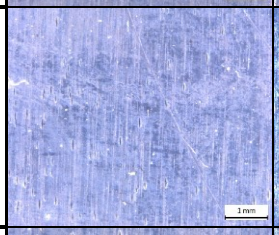
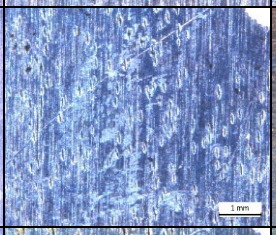
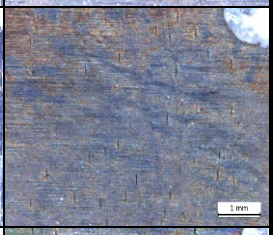
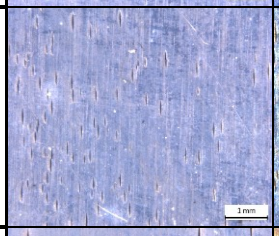
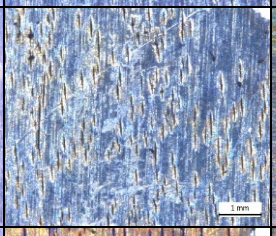
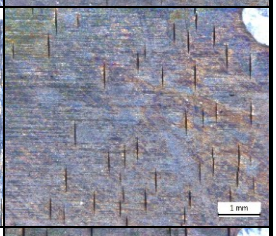
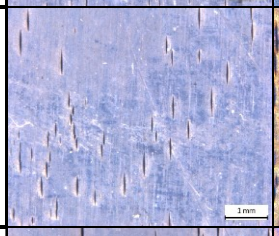
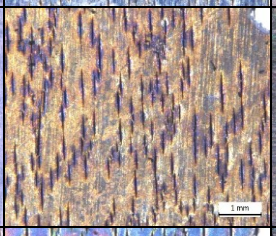
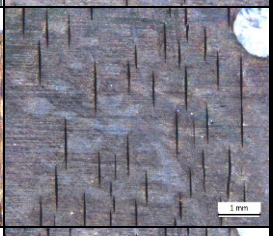
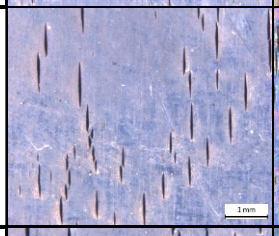
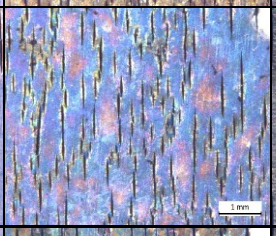
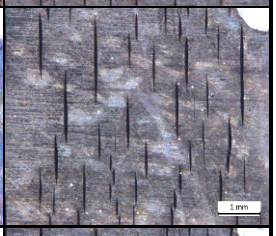
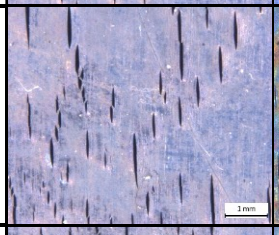
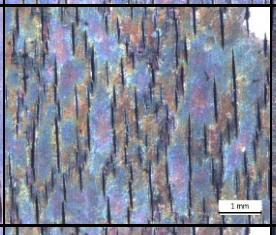
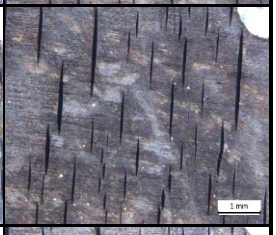
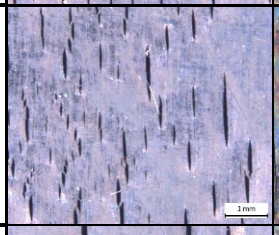
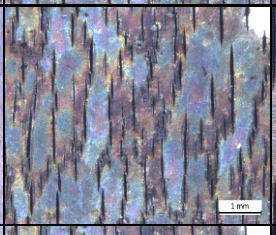
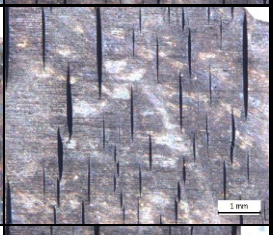
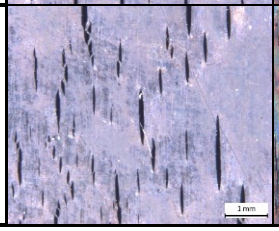
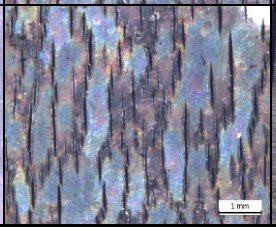
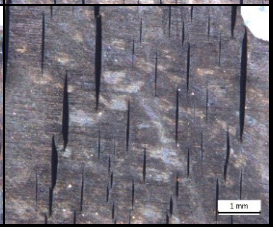
	TBBS-1_4	TBBS-2_4	MBTS-1_4	TBPD-1_4
0				
3				
6				
12				
24				
48				
72				
96				

	TBBS-1_5	TBBS-2_5	MBTS-1_5	TBPD-1_5
0				
3				
6				
12				
24				
48				
72				
96				

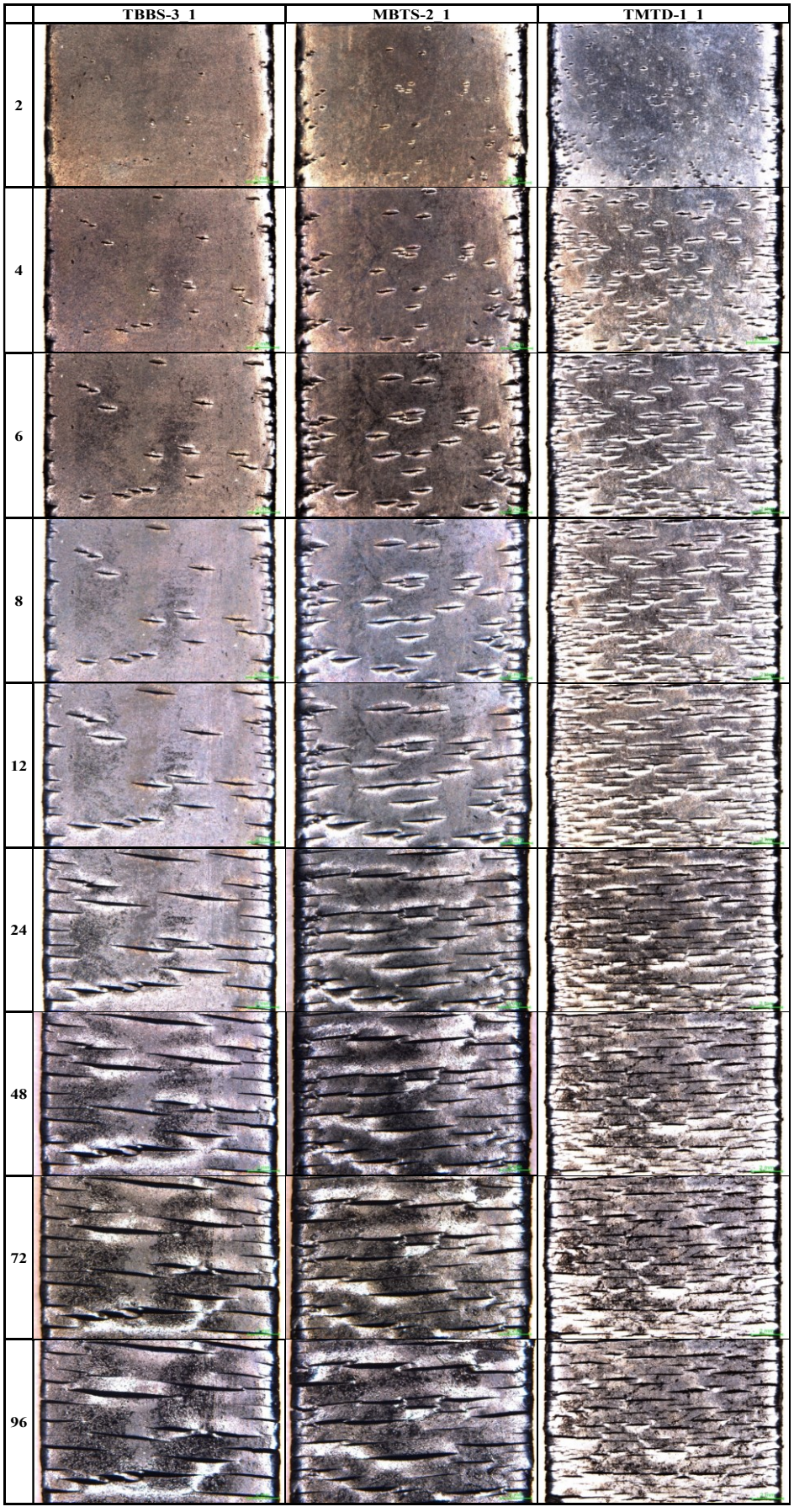
	TBBS-1_6	TBBS-2_6	MBTS-1_6	TBPD-1_6
0				
3				
6				
12				
24				
48				
72				
96				

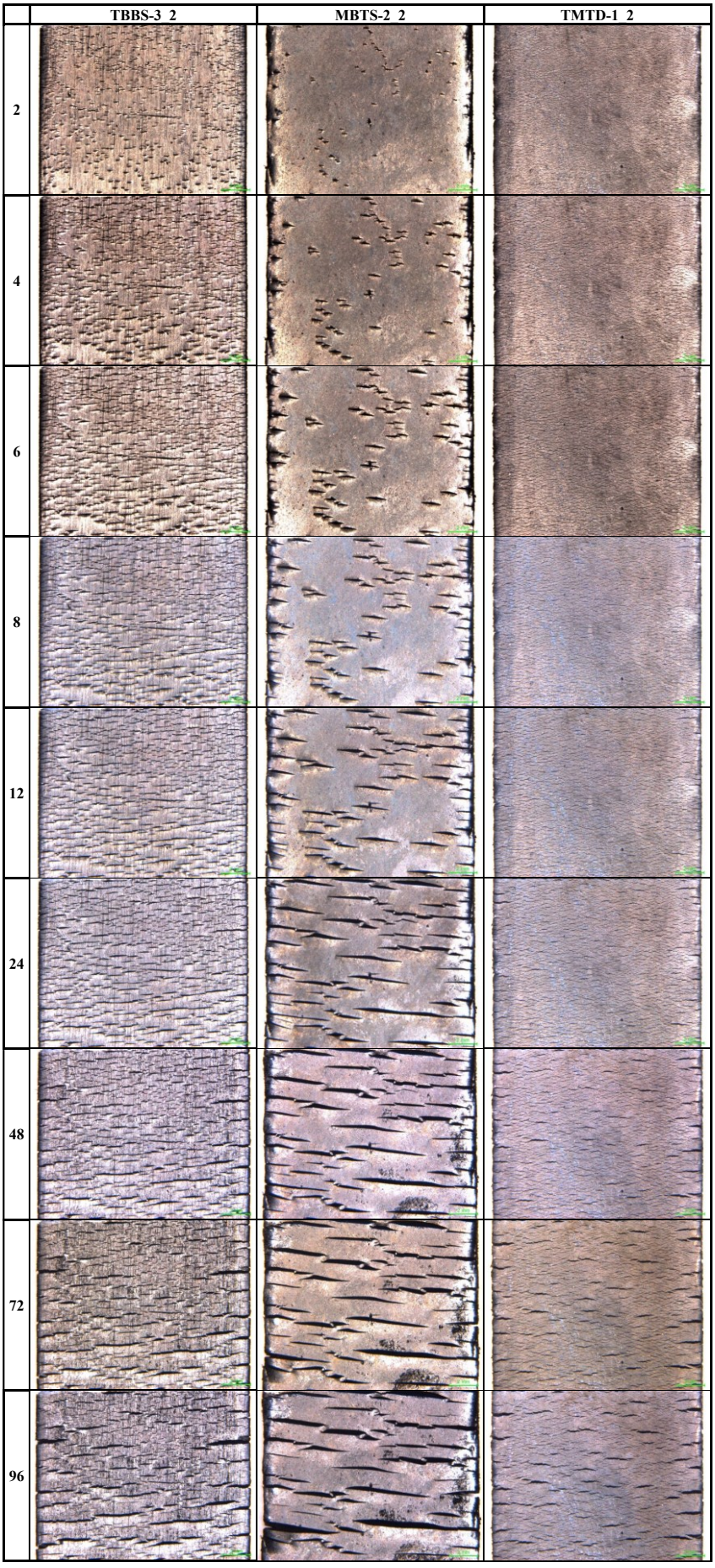
	TBBS-1_7	TBBS-2_7	MBTS-1_7	TBPD-1_7
0				
3				
6				
12				
24				
48				
72				
96				

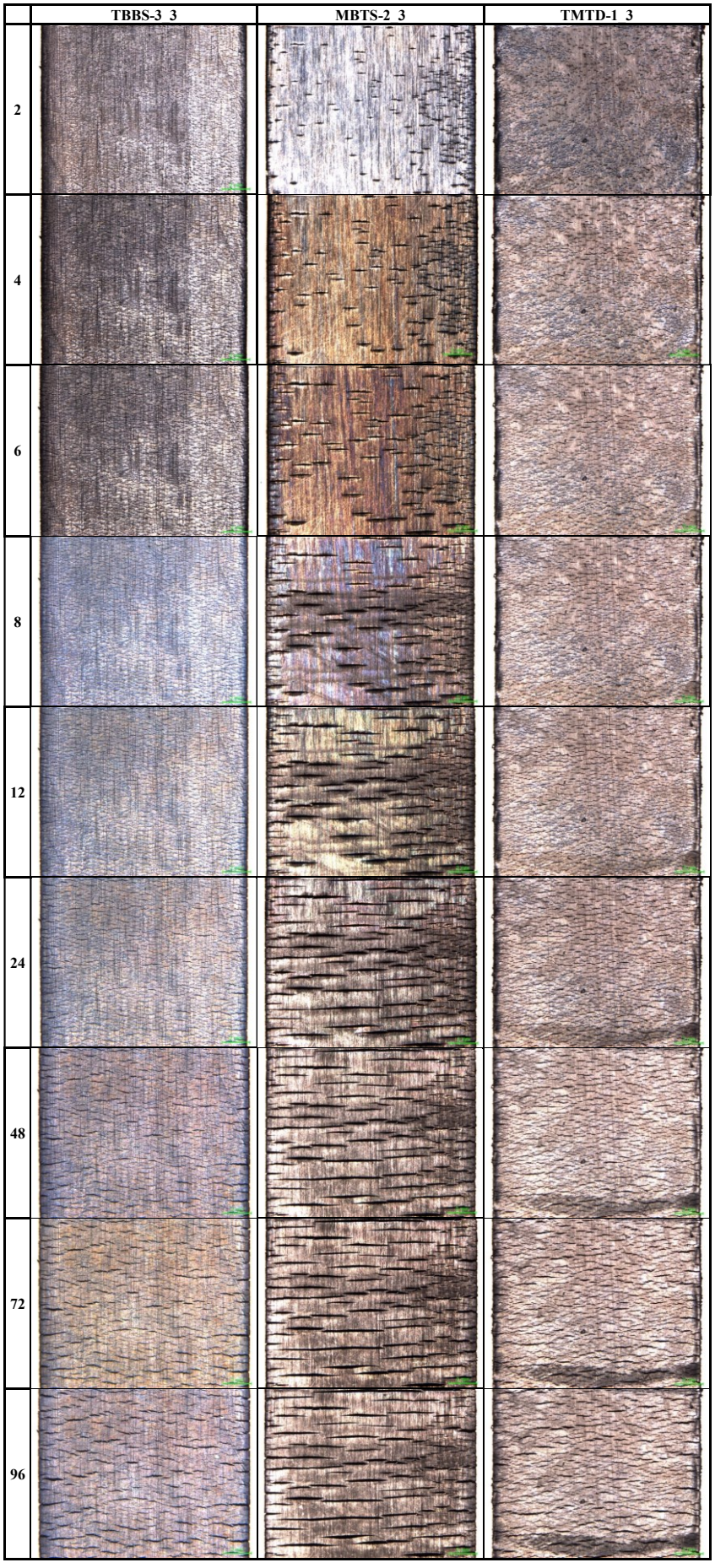
	TBBS-1_8	TBBS-2_8	MBTS-1_8
0			
3			
6			
12			
24			
48			
72			
96			

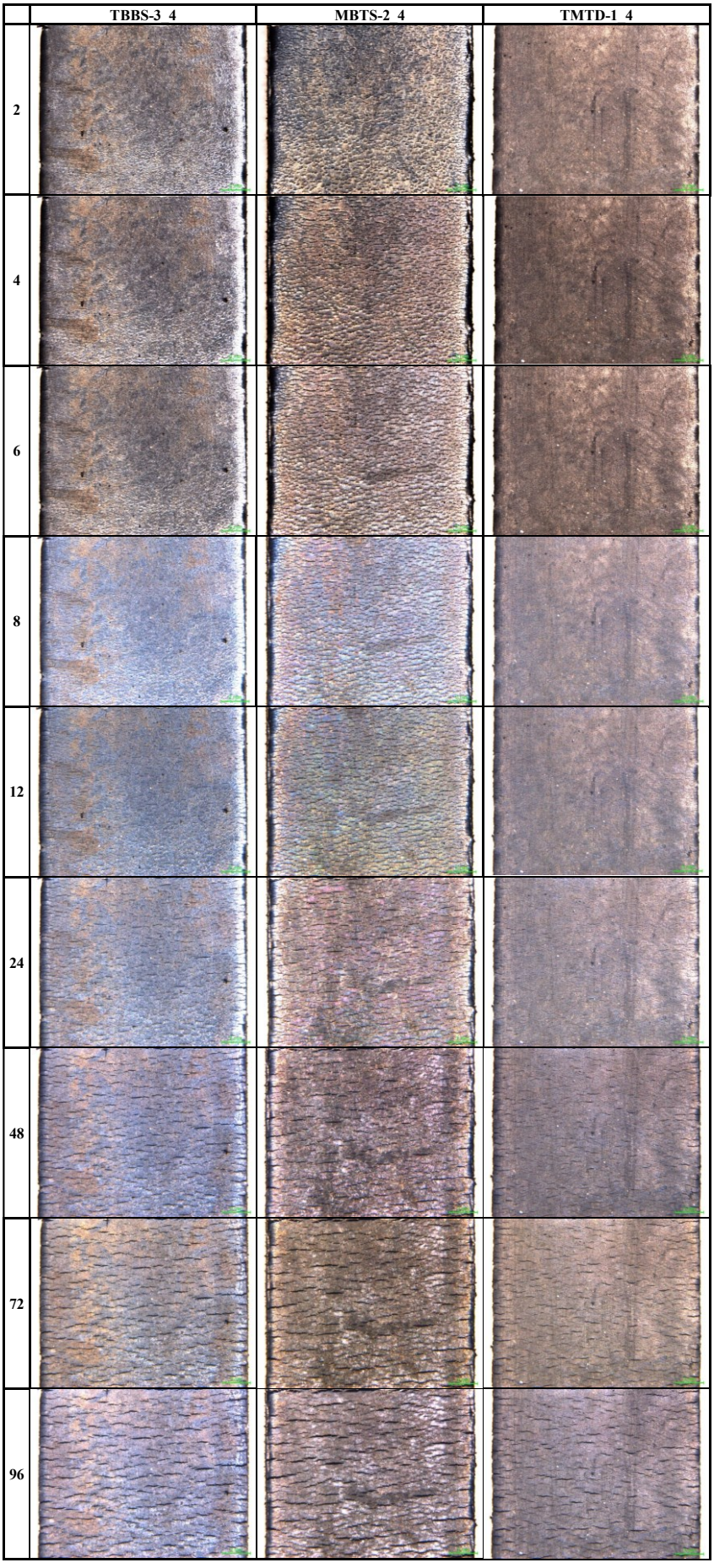
	TBBS-1_9	TBBS-2_9	MBTS-1_9
0			
3			
6			
12			
24			
48			
72			
96			

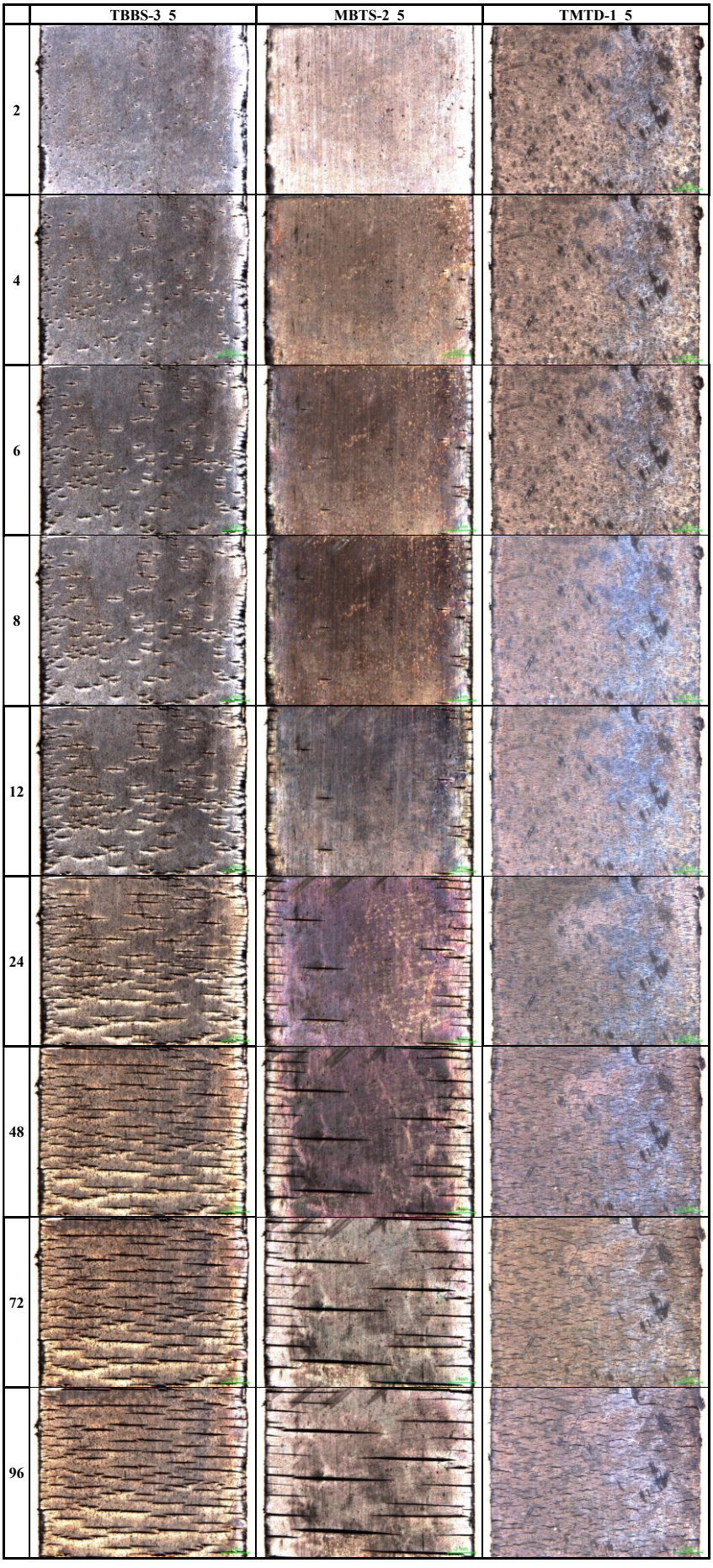
APPENDIX 3 THE PHOTOS FROM THE SECOND ROUND

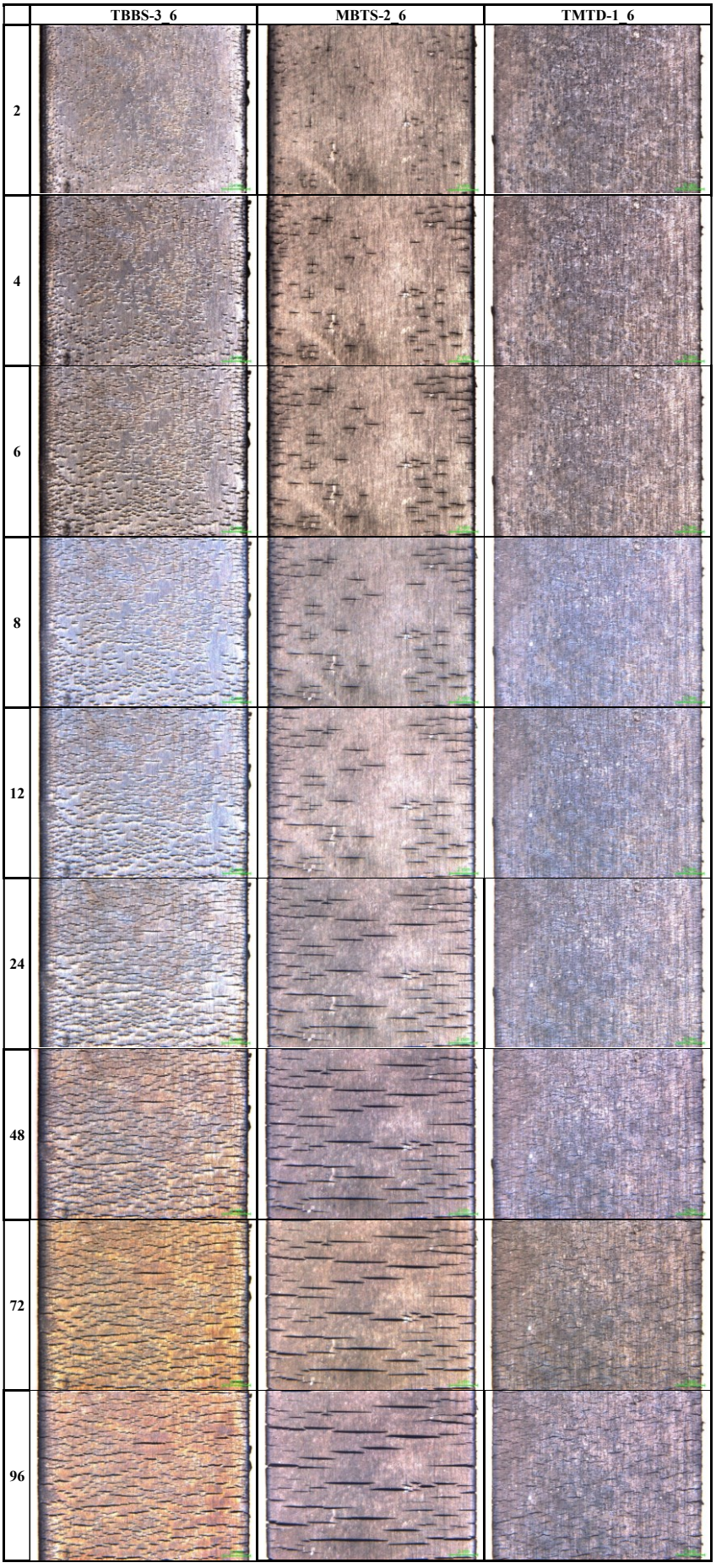



TBBS-3 2
MBTS-2 2
TMTD-1 2
2
4
6
8
12
24
48
72
96


TBBS-3 3
MBTS-2 3
TMTD-1 3
2
4
6
8
12
24
48
72
96


TBBS-3 4
MBTS-2 4
TMTD-1 4
2
4
6
8
12
24
48
72
96


TBBS-3 5
MBTS-2 5
TMTD-1 5
2
4
6
8
12
24
48
72
96


TBBS-3_6
MBTS-2_6
TMTD-1_6
2
4
6
8
12
24
48
72
96

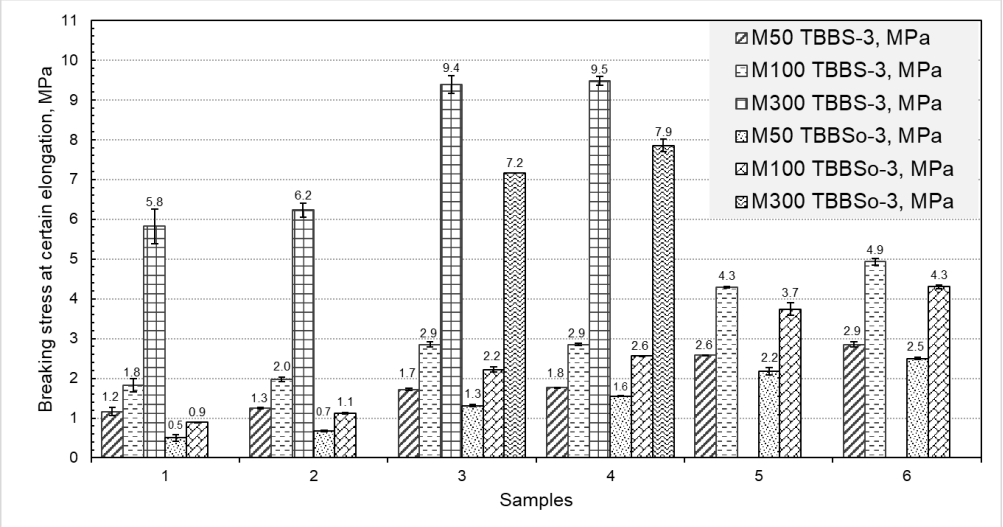
APPENDIX 4 THE TABLES OF MODULES FROM TENSILE STRENGTH EXPERIMENT

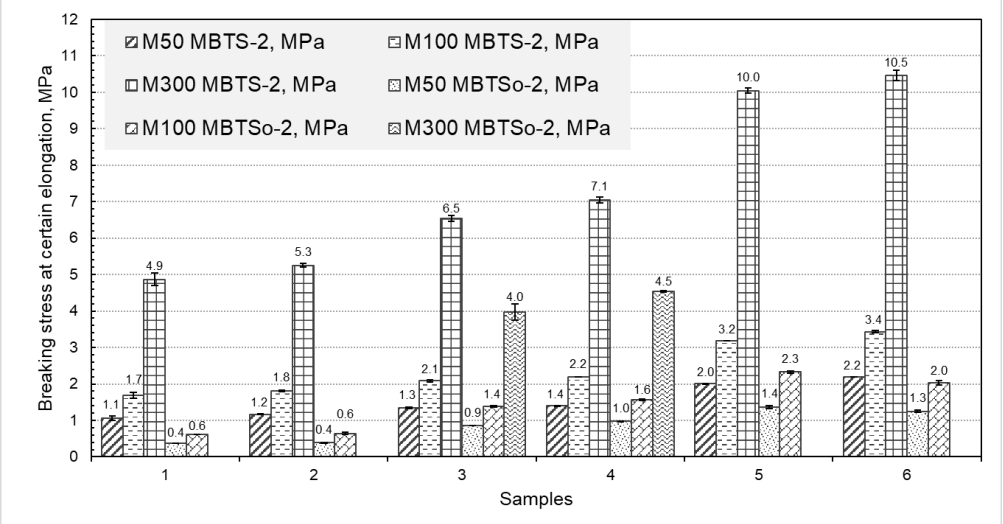
#	M50 TBBS-3	SD	M50 TBBSo-3	SD	M100 TBBS-3	SD	M100 TBBSo-3	SD	M300 TBBS-3	SD	M300 TBBSo-3	SD
1	1.16	0.1	0.5	0.09	1.82	0.17	0.89	0.01	5.82	0.43	0	0
2	1.25	0.02	0.68	0.02	1.97	0.05	1.12	0.02	6.23	0.18	0	0
3	1.72	0.03	1.31	0.03	2.85	0.06	2.22	0.06	9.39	0.22	7.16	0
4	1.76	0.01	1.55	0.01	2.85	0.03	2.56	0.01	9.48	0.11	7.85	0.16
5	2.58	0.01	2.18	0.09	4.29	0.02	3.74	0.16	0	0	0	0
6	2.85	0.07	2.5	0.03	4.93	0.09	4.3	0.05	0	0	0	0

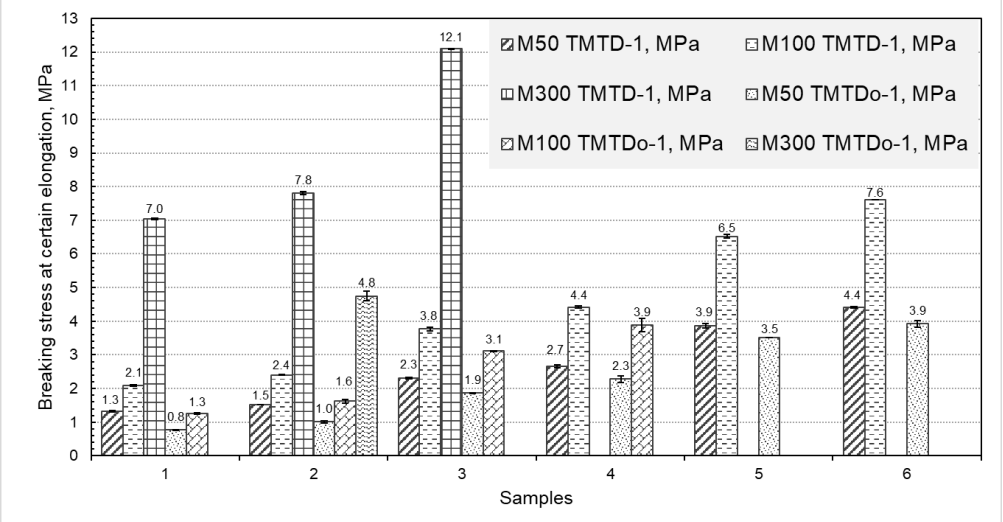
#	M50 MBTS-2	SD	M50 MBTSo-2	SD	M100 MBTS-2	SD	M100 MBTSo-2	SD	M300 MBTS-2	SD	M300 MBTSo-2	SD
1	1.07	0.06	0.38	0	1.68	0.08	0.61	0	4.87	0.17	0	0
2	1.17	0.01	0.39	0.01	1.81	0.02	0.64	0.03	5.25	0.05	0	0
3	1.34	0.02	0.85	0	2.09	0.03	1.39	0.02	6.54	0.08	3.97	0.22
4	1.4	0.01	0.97	0.01	2.19	0	1.56	0.02	7.05	0.08	4.54	0.02
5	2.01	0.01	1.37	0.04	3.18	0	2.33	0.03	10.04	0.07	0	0
6	2.19	0	1.25	0.03	3.43	0.03	2.04	0.06	10.46	0.14	0	0

#	M50 TMTD-1	SD	M50 TMTDo-1	SD	M100 TMTD-1	SD	M100 TMTDo-1	SD	M300 TMTD-1	SD	M300 TMTDo-1	SD
1	1.32	0.02	0.77	0.01	2.09	0.02	1.26	0.02	7.04	0.03	0	0
2	1.53	0	1.01	0.04	2.4	0.01	1.62	0.05	7.8	0.04	4.75	0.15
3	2.31	0.03	1.87	0.01	3.77	0.05	3.11	0.02	12.09	0.01	0	0
4	2.66	0.04	2.28	0.1	4.42	0.04	3.88	0.2	0	0	0	0
5	3.87	0.07	3.52	0	6.52	0.05	0	0	0	0	0	0
6	4.42	0.02	3.92	0.09	7.6	0	0	0	0	0	0	0

APPENDIX 5 THE GRAPHS REPRESENTING MODULES AT VARYING ELONGATIONS, COMPARING OZONATED AND NON-OZONATED SAMPLES WITH THE SAME ACCELERATOR







APPENDIX 6 THE GRAPHS REPRESENTING MODULES AT SAME ELONGATIONS, COMPARING OZONATED AND NON-OZONATED SAMPLES WITH DIFFERENT ACCELERATORS

